Master Thesis

# Investigation of Vapor-Liquid and Liquid-Liquid Equilibria by COSMO-RS

Submitted in satisfaction of the requirements for the degree of Diplom-Ingenieurin (Dipl.-Ing.) of the Vienna University of Technology, Faculty of Technical Chemistry

by

Perim Gezer Rollin, BSc

0527602

under the supervision of

Univ. Prof. Dipl.-Ing. Dr. Anton Friedl
Univ.Ass. Dipl.-Ing. Dr. techn. Martin Miltner
Univ.Ass. Dipl.-Ing. Dr. techn. Walter Wukovits

Institute of Chemical, Environmental and Biological Engineering
Thermal Process Engineering & Simulation
Vienna University of Technology
Getreidemarkt 9/166-21060, Vienna, Austria

01.2019

## Acknowledgements

I would like to express my gratitude to Prof. Anton Friedl, Dr. Martin Miltner and Dr. Walter Wukovits for the useful comments, remarks and engagement through the learning process of this master thesis and for the support on the way. Without your guidance and persistent help this master thesis would not have been possible.

Furthermore I would like to thank my family and friends, who have supported me throughout entire process. I will be forever grateful.

# Kurzfassung

Die Aceton-Butanol-Ethanol-Fermentation (ABE Fermentation) ist ein vielversprechendes Verfahren zur Produktion erneuerbarer Treibstoffe und Lösungsmittel aus vielfältigen Arten von Biomasse. Eine Herausforderung bei der Entwicklung eines effizienten und kontinuierlichen Produktionsverfahrens ist dabei die niedrige Produktkonzentration der Lösungsmittel nach der Fermentation, die eine Folge der Produktinhibierung der produzierenden Mikroorganismen ist. Daher ist eine kontinuierliche Abtrennung aus der Fermentationsmaische mit nachfolgender Aufkonzentrierung für ein kontinuierliches Verfahren erforderlich. Neben anderen ist die organophile Pervaporation ein aussichtsreicher Kandidat für eine energieeffiziente Trenntechnologie in diesem Umfeld.

Zur Auslegung und Optimierung des Trennverfahrens ist die genaue Kenntnis der Mischungseigenschaften wässriger Aceton-Butanol-Ethanol-Lösungen bei verschiedenen Zusammensetzungen, Temperaturen und Drücken ausschlaggebend. Die wesentlichsten Stoffdaten sind dabei Reinstoffdampfdrücke, Aktivitätskoeffizienten, Flüssig-Flüssig-Gleichgewichte (LLE) und Flüssig-Dampf-Gleichgewichte (VLE) in binären, ternären und quaternären Systemen. Diese Daten sind ansatzweise in der Literatur dokumentiert aber oft nicht in ausreichender Menge oder in fragwürdiger Konsistenz verfügbar.

Diese Stoffeigenschaften sind auf der anderen Seite aber auch über moderne ab-initio-Simulationsverfahren zugänglich. Eine vielversprechende und leistungsfähige Methode ist in diesem Zusammenhang COSMO-RS, die im Rahmen dieser Arbeit untersucht wurde. Zusätzlich wurden auch noch die Aktivitätskoeffizienten-Modelle wie NRTL und UNIQUAC, die über die Simulationsumgebung Aspen Plus verfügbar sind, für dieses Stoffsystem herangezogen und mit den Ergebnissen aus der Literatur und von COSMO-RS verglichen.

Der Vergleich von COSMO-RS und Aspen Plus mit den Literatur Daten ergab die TZVPD-Fine (COSMOtherm) und UNIQUAC LLE (Aspen Plus) Optionen als vielversprechend für die Berechnung des Phasengleichgewichts im ABE Prozess.

# Abstract

Acetone-Butanol-Ethanol fermentation (ABE Fermentation) is a very promising method for production of renewable liquid fuels and solvent from various sources of biomass. One of the problems that is hindering commercial development of the fermentation process is the fact that it suffers severely from product inhibition, caused principally by butanol. One way to overcome this problem would be to couple the fermentation process to a continuous product removal technique, so that inhibitory product concentrations are never reached. An organophilice pervaporation is a candidate for an energy efficient separation technology in this environment.

To design and optimize the separation method the exact knowledge of properties of aqueous acetone-butanol-ethanol mixture with different compositions, temperatures and pressures are determining. The most important property data are pure component vapor pressure, as well as activity coefficient, liquid-liquid-equilibrium (LLE) and vapor-liquid-equilibrium (VLE) in binary, ternary and quaternary systems. These data are documented to some extent in literature but often not in sufficient amount or only at questionable consistence available.

These substance data are on the other hand accessible via modern ab-initio-simulation method. A very promising and efficient method in this context is COSMO-RS, which was investigated in this work. Additionally, activity coefficient models like NRTL and UNIQUAC, available via simulations environment of Aspen Plus, were used describe this multicomponent system.

In this work calculations of vapor pressures, activity coefficients and phase equilibriums of binary, ternary and quaternary systems of the ABE fermentation products (acetone, 1-butanol, ethanol, water) are carried out with Aspen Plus and COSMOtherm. Results of these calculations are compared with the literature data. It is concluded that TZVPD-Fine parameterization within the COSMO-RS theory and UNIQUAC LLE option provided in Aspen Plus are promising to provide property data of aqueous acetone-butanol-ethanol mixtures.

# Contents

1. Introduction ..... 8
2. Biofuels ..... 10
2.1. Butanol & Biobutanol ..... 10
2.2. ABE Fermentation ..... 12
2.3. The Challenges for ABE Fermentation ..... 12
2.4. Advantages of Butanol vs. Ethanol as engine fuel ..... 13
3. Thermodynamics of Mixtures ..... 15
3.1. Equilibrium and Gibbs' Phase Rule ..... 15
3.2. Two-Phase Systems ..... 16
3.2.2. The Chemical Potential and Phase Equilibria ..... 18
3.3. Vapor-Liquid Equilibrium ..... 20
3.3.1. Raoult's law ..... 20
3.3.2. Henry's Law ..... 23
3.4. Liquid-Liquid Equilibrium ..... 24
3.5. Activity Coefficient Models ..... 28
3.5.1. Random-Mixing-Based Models ..... 29
3.5.2. Local-Composition Models ..... 31
3.5.3. Advantages and Limitations of LC Models ..... 35
4. COSMOtherm & COSMO-RS Theory ..... 40
5. Simulations ..... 50
5.1. COSMOtherm Calculations ..... 50
5.1.2. Activity Coefficient Calculation ..... 52
5.1.3. Phase Equilibrium Calculations ..... 52
5.2. Aspen Plus Calculations ..... 55
5.2.1. Vapor Pressure Calculation ..... 57
5.2.2. Activity Coefficient Calculation ..... 58
5.2.3. Phase Equilibrium Calculation ..... 58
5.3. Calculation Summary ..... 60
6. Results ..... 63
6.1. Vapor Pressures ..... 63
6.2. Activity Coefficients ..... 66
6.3. Vapor-Liquid Equilibrium of Binary System 1-Butanol-Water ..... 70
6.3.1. Vapor-Liquid Equilibrium of Binary System 1-Butanol-Water with COSMOtherm 70
6.3.2. Vapor-Liquid Equilibrium of Binary System 1-Butanol-Water with Aspen Plus ..... 71

6.3.3. Vapor-Liquid Equilibrium of Binary System 1-Butanol-Water with COSMOtherm and Aspen Plus ..... 72
6.3.4. Vapor-Liquid Equilibrium of Binary System 1-Butanol-Water with COSMOtherm and Aspen Plus at 1013.25, 1980 and 4920 mbar ..... 73
6.4. Liquid-Liquid Equilibrium of Binary System 1-Butanol-Water ..... 74
6.5. Liquid-Liquid Equilibrium of Ternary Systems ..... 75
6.5.1. Liquid-Liquid Equilibrium of Ternary System 1-Butanol-Acetone-Water ..... 76
6.5.2. Liquid-Liquid Equilibrium of Ternary System 1-Butanol-Ethanol-Water ..... 79
6.6. Liquid-Liquid Equilibrium of Quaternary System 1-Butanol-Acetone-Ethanol-Water ..... 83
7. Summary, Conclusion and Outlook ..... 86
8. Appendix ..... 92
9. References ..... 103
10. Abbreviations and Symbols ..... 106
10.1. Abbreviations ..... 106
10.2. Symbols ..... 107

# 1. Introduction

Global energy crisis and limited supply of petroleum fuels have brought the worldwide focus towards development of sustainable technologies for alternative fuel production. Utilization of renewable biomass offers an excellent opportunity for the development of an economical biofuel production process which can have an impact on sustainability and security of supply objectives [1]. Several environmental benefits have also been linked with the utilization of renewable biomass. Biofuels produced from renewable biomass are the sustainable energy resource with the greatest potential for $CO_2$ neutral production. They can easily be implemented gradually to supplement fossil fuels by processes like blending and can be produced fermentatively [2].

Biobutanol is an attractive renewable liquid transportation biofuel and can be produced from a wide variety of waste biomass feedstock which fits the existing fuel infrastructure. Butanol is considered to be superior to ethanol due to its higher energy content, less hygroscopy and use in conventional combustion engines without modification. This has led to an increased research interest in butanol production from renewable biomass [2]. Thus, biobutanol has the potential to substitute for both ethanol and biodiesel in the biofuelmarket [3].

Renewable 1-butanol is produced from the fermentation of carbohydrates in a process called ABE fermentation, after its major chemical products: acetone, butanol and ethanol. The production of acetone, butanol and ethanol (ABE) mixtures using the anaerobic bacterium Clostridium acetobutylicum has potential commercial significance. However, a barrier for the commercial development of the fermentation process is the fact that it suffers severely from product inhibition caused principally by butanol. In batch fermentation, product concentrations in excess of 20 g/litre are rarely observed because of this problem. One way to overcome this would be to couple the fermentation process to a continuous product removal technique, so that inhibitory product concentrations are never reached [4].

An economical biofuel/biobutanol production requires further investigation in separation processes. The classical distillation process for the removal of butanol is far too energy demanding, at a factor of 220% of the energy content of butanol. Alternative separation processes are hybrid processes of gas-stripping, liquid-liquid extraction, pervaporation with distillation and adsorption/drying/desorption hybrid process [5]. A promising method of biobutanol separation from the fermentation broth is the use of ionic liquids (IL) [6].

The capacity to describe the water solubility in biofuels is important to insure the fuel quality during production. Water affects biofuel calorific value, shelf life and composition and can cause engine problems. The design and optimization of the biofuel purification requires a model that can describe the phase equilibria of water-alcohol systems. The accurate knowledge of the vapor-liquid equilibria of the system is thus essential for the design of the separation and purification processes [7]. This information can be reached via experimental methods or process simulations.

Process simulation is very efficient and accessible method enabling the design, optimization and improvement of separation processes by predicting the behavior of a process, using basic engineering relationships and reliable thermodynamic data and models. The software tools COSMOtherm and Aspen Plus in this respect are very promising and used in this work to provide the essential data for vapor pressure, activity coefficient, VLE and LLE of ABE fermentation solvents acetone, 1-butanol, ethanol, water and mixtures thereof.

In the following chapters of the thesis, biofuels and the importance of ABE fermentation solvents, the problems of this process, thermodynamics of mixtures, simulations using COSMO-RS and, Aspen Plus will be discussed. The results of the calculations with COSMOtherm and Aspen Plus will be compared with the literature data and discussed.

# 2. Biofuels

Vegetable oils, biodiesels, bioalcohols and biogas are some of the biofuels evaluated for their suitability in compression-ignition (CI) engines. Bioalcohols and biogas can be produced from any kinds of biomass through fermentation. Therefore, bioalcohols can be considered as the next generation alternative fuels for automobiles. Investigations have been already initiated to determine the effects of bioalcohols, such as methanol and ethanol, in automobiles as fuel. However, they pose some problems like phase separation, low cetane and octane number and low calorific value. On the other side, the effects of higher alcohols, such as butanol, pentanol, octanol, are investigated very rarely. The addition of butanol to gasoline seems to an alternative fuel that can replace conventional fuel [8]. As an attractive renewable liquid transportation biofuel, biobutanol fits the existing fuel infrastructure, has a better energy density and performance than ethanol and can be made from more sustainable feedstocks than biodiesel [11].

## 2.1. Butanol & Biobutanol

1-Butanol (butyl alcohol or n-butanol) is a colorless substance and a four carbon straight chained alcohol, with a molecular formula of $C_4H_9OH$ (MW 74.12), boiling point of 117.7 °C and flash point of 29°C. Relative density of 1-butanol (water = 1) is 0.81. Butanol is very hydrophobic with a water solubility of 7.7 g/100 ml (at 20°C) [9].

The unmodified term butanol usually refers to the straight chain isomer with the alcohol functional group at the terminal carbon, which is also known as n-butanol or 1-butanol. Its isomers include isobutanol, 2-butanol, and tert-butanol. The butanol isomers have different melting and boiling points. n-butanol and isobutanol have limited solubility, sec-butanol has substantially greater solubility, while tert-butanol is fully miscible with water above tert-butanol's melting point. The hydroxyl group makes the molecule polar, promoting solubility in water, while the longer hydrocarbon chain mitigates the polarity and reduces solubility [10]. 1-Butanol can have the following conformers with a single bond rotation (fig. 2-1).

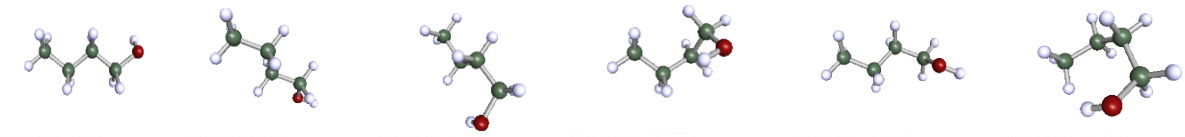

**Fig. 2-1. Conformers of 1-Butanol**

1-Butanol is an important chemical precursor for paints and polymers with a growing market value [11]. Most 1-butanol produced today is synthetic and derived from a petrochemical route based on propylene oxo synthesis in which aldehydes from propylene hydroformylation (fig. 2-2) are hydrogenated to yield 1-butanol (fig. 2-3).

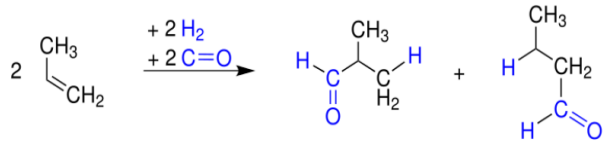

**Fig. 2-2. Propen reacts with hydrogen to butanal and 2-methylpropanal**

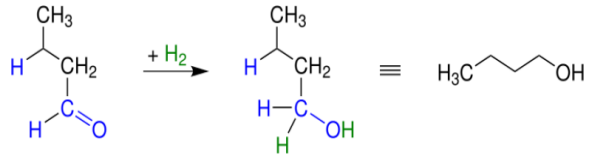

**Fig. 2-3. Butanal reacts with water to 1-butanol**

Butanol from biomass is called biobutanol [12]. Biobutanol is produced by fermentation of biomass by the ABE process with the bacterium Clostridium acetobutylicum, also known as the Weizmann organism, or Clostridium beijerinckii, which are anaerobic bacteria [13].

The process creates in addition to butanol a recoverable amount of $H_2$ and a number of other byproducts like acetic, lactic and propionic acid, isopropanol and ethanol. Metabolic pathways of ABE fermentation comprise two characteristic phases, acidogenesis, forming acetate, butyrate, hydrogen, and $CO_2$ and solventogenesis, forming butanol, acetone and ethanol [12]. Fig. 2-4 shows pathway of acetone-butanol-ethanol fermentation by clostridia [14].

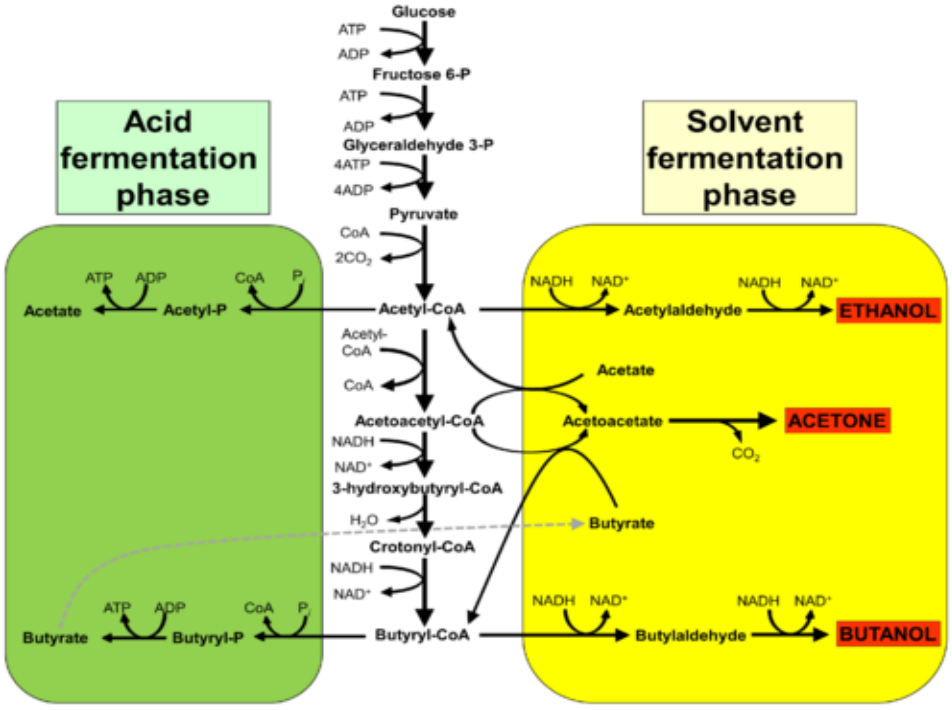


**Fig. 2-4. Acetone-Butanol-Ethanol (ABE) fermentation pathway by clostridia [14]**

## 2.2. ABE Fermentation

Renewable 1-butanol is produced from the fermentation of carbohydrates in an ABE fermentation process named after its major chemical products; acetone, butanol and ethanol. The ABE fermentation uses solventogenic clostridia to convert sugar or starch into solvents. The fermentation occurs in two stages; the first is a growth stage in which acetic and butyric acid are produced and the second stage is characterized by acid reassimilation into ABE solvents. During this stage, growth slows, the cells accumulate granulose and form endospores. The fermentation also produces carbon dioxide and hydrogen. Commercial solvent titres peak at about 20 g/L from 55 to 60 g/L of substrate giving solvent yields of around 0.35 g/g sugar. The butanol:solvent molar ratio is typically 0.6 with an A:B:E ratio of 3:6:1. Butanol is the preferred solvent since it attracts the highest price in the chemical market [11].

China has made efforts to recommercialize the ABE fermentation process investing over $200 million to install 0.21 million t/a of solvent capacity with plans to expand to 1 million t pa. Six major plants produce about 30.000 t/a of butanol from corn starch. Most plants operate in a semi-continuous fashion with each fermentation lasting up to 21 days. The plants typically house several trains of up to eight fermentation tanks (300–400 $m^3$ volumes) linked together in series. Fresh feedstock and periodic additions of seed culture, cascades through the fermentors in a process that provides sufficient residence time for reassimilation of acids to solvents. For the recovery of acetone, butanol and ethanol, conventional distillation is used. To reduce utility and operating costs, most plants are located next to ethanol plants and co-located operations tend to share effluent treatment facilities based on anaerobic digestion (AD). Biogas, produced from the AD process, is used to generate heat and power. Additional value can be gained from the recovery of hydrogen from the fermentation exhaust gas (typically 1/10th of mass of butanol produced) [11].

## 2.3. The Challenges for ABE Fermentation

The challenges for the conventional ABE fermentation are in general a need for cheaper feedstocks, improved fermentation performance and more sustainable process operations for solvent recovery and water recycle. Feedstocks contribute most to production cost. While energy for operations contributes 14% to the overall cost, corn starch accounts for up to 79% of the overall solvent production. Therefore, transition towards cheaper feedstocks offers a big opportunity for cost reduction and improved sustainability [11].

ABE fermentation process suffers severely from product inhibition, caused principally by butanol. This problem affects the commercial development of the process. Coupling the fermentation process to a continuous product removal technique could help avoiding the inhibitory product concentrations [4]. Integrating solvent recovery with fermentation is therefore an attractive process option. Solvent recovery using conventional distillation is robust and proven but energy intensive. For every 1 t of solvent, approximately 12 t of steam is required. Streams can be recycled to avoid product loss. But non-conventional methods are required to significantly reduce energy and cost. Gas stripping can minimize end product inhibition and improve both solvent titre and productivity. Other methods for solvent recovery include liquid–liquid extraction, adsorption, pervaporation, reverse osmosis and aqueous two phase separation [11].

Energy requirements for butanol separation with various recovery processes suggests that recovery of butanol from fermentation broth in adsorption-desorption process using silicalite

would require 0.008 MJ/kg recovered butanol. Butanol recovery by liquid–liquid extraction requires 0.009 MJ/kg butanol, followed by pervaporation 0.014 MJ/kg butanol, by gas stripping 0.022 MJ/kg butanol, and by steam stripping and distillation 0.024 MJ/kg butanol [15]. The energy demand of a hybrid process gas-stripping/distillation (from 0.78 wt% to pure) is 21 MJ/kg butanol. Also an energy demand in a range from 14 to 31 MJ/kg butanol for gas-stripping/distillation is reported. Another published gas-stripping/pervaporation/distillation hybrid process (1 wt% to > 99.5 wt%) requires 23 MJ/kg butanol. For liquid–liquid extraction a novel dual extraction/distillation (from 2.2 wt% ABE to 92 wt% ABE) process has been presented in which the energy consumption for the production of an ABE product mixture is as low as 4 MJ/kg. Other publications support this figure with a value of 5 to 6MJ/kg butanol for the separation of butanol from 0.8 wt% to 99.5 wt%. Experimental investigation and simulation of a novel adsorption/drying/desorption hybrid process show that the separation and concentration of butanol from 2 wt% to 98 wt% requires only 3.4 MJ/kg butanol for a silicalite sorbent. The pervaporation/distillation hybrid process is with 4 and 8.2 MJ/kg butanol (0.5 wt%– 99.9 wt%) [5].

The ABE fermentation process is economic on starch and sugar based feedstocks if 1-butanol is sold at a premium into the chemical market (GBL model data). In order to have an impact on a larger biofuel market, biobutanol needs to compete on cost with ethanol despite its superior fuel properties [11]. Significant cost reduction can be achieved using cheaper agricultural residues or wastes such as corn cobs, corn stover, sugar cane bagasse, wheat straw and municipal solid waste (MSW). Use of cellulosic and waste material is also more sustainable offering a lower carbon footprint and reduced green house gas (GHG) emissions. Reduction in feedstock cost offers the best opportunity especially since clostridia are well suited for sugars derived from cellulosic material. Clostridia have broad substrate ranges (including pentose sugars) and display superior tolerance to typical feedstock inhibitors [11]. Bacterial butanol fermentation could be more efficient due to gene modification of bacteria already used in butanol production or by utilization of another bacteria strain, more tolerant to produced product. The anaerobic bacterium, Clostridium acetobutylicum is being investigated to engineer recombinant strains with superior biobutanol-producing ability [2].

## 2.4. Advantages of Butanol vs. Ethanol as engine fuel

Processing corn products to create fuels like butanol and ethanol benefits the environment, reduces petrochemical dependence, and provides a potential new market for farmers. Butanol can be produced from a wide variety of biomass feedstock which does not compete with food. Although both fermentation products have benefits, butanol is superior to ethanol and has following advantages vs. ethanol [9, 16, 17, 58];

- Butanol has four more hydrogen and two more carbon atoms than ethanol, resulting in a higher energy output, which equates to a 25 percent increase in harvestable energy. Butanol is more similar to gasoline than ethanol. The similarity is a consequence of its longer hydrocarbon chain, which means there is more carbon in relation to the single oxygen and thus the molecule is less polar and also means that it can be used in a standard vehicle without the need for modifications with an energy density similar to that of gasoline.
- Butanol is less corrosive than ethanol.
- The energy content for butanol is higher than ethanol (table 2-1).

- Butanol is less hazardous to handle because of its lower vapor pressure and lower volatility. The higher boiling point 117.7°C and flash point 29°C make butanol safer than ethanol (boiling point 78.3°C, flash point 14°C), and other lower alcohols.
- Butanol is very hydrophobic, whereas lower alcohols (methanol, ethanol and n-propanol) are miscible in water.

The table 2-1 below summarizes energy densities and average octane numbers of fuels. Higher octane numbers are indicative of a fuel that burns slowly. Thus, a higher octane number reveals a more energy efficient fuel.

| Fuel | Energy density (MJ/L) | MJ/kg | Average Octane |
|---|---|---|---|
| Gasoline | ~33 | 44.4 | 85-96/90-105 |
| Methanol | ~16 | 17.9 | 98.65/108.7 |
| Ethanol | ~20 | 26.8 | 99.5/108.6 |
| Propanol | ~24 | 33.6 | 108/118 |
| Diesel | ~39 | 45.4 | 25 |
| Butanol | ~30 | 36.1 | 97/103 |
| Wood | 9 | ~15 | |
| Liquefied natural gas | 25.3 | ~55 | |
| Autogas (LPG) (60% propane+40% butane) | 26.8 | 50 | |
| Aviation gasoline (high-octane gasoline) | 33.5 | 46.8 | 100/130 |
| Gasohol (90% gasoline, 10% ethanol) | 33.7 | 47.1 | 93/94 |
| Charcoal, extruded | 50 | 23 | |

**Table 2-1. Differences in energy contents of fuels [58]**

# 3. Thermodynamics of Mixtures

Process simulations are used in this work to investigate and optimize processes to produce and separate alternative fuels. Simulation gives consistent mass and energy balances to compare processes with accurate physical and thermodynamic properties. In ABE fermentation the crucial step is solvent separation, thus reliable data on VLE, LLE and VLLE are necessary. The related basic engineering relationships, thermodynamic data and models will be explained in this part according to the following sources [18-26]. Some of the main topics of this part are equilibrium and Gibbs' phase rule, two-phase systems, phase equilibriums (VLE, LLE) and activity coefficient models.

## 3.1. Equilibrium and Gibbs' Phase Rule

Equilibrium is a word to express static condition and the absence of change on a macroscopic scale. A system at equilibrium exists when all forces are in exact balance [20].

$$T' = T''$$

$$p' = p''$$

$$\mu_1' = \mu_1''$$

$$\mu_2' = \mu_2''$$

Separation processes such as distillation, absorption and extraction bring phases of different composition into contact. When the phases are not in equilibrium, mass and energy transfer between phases changes their compositions and thermal state.

The state of a homogeneous fluid (phase) is fixed, when two intensive thermodynamic properties are set at specific values. The intensive state of the system at equilibrium is set when its temperature, pressure and the compositions of all phases are fixed. These are the phase-rule variables which must be specified in any order to fix all remaining phase-rule variables, and thus the intensive state of the system.

When a single property is specified, the state of the system is fixed and two phases are in equilibrium. For multi-phase systems at equilibrium, the number of independent variables that must be fixed in any order to set its intensive state is given by the phase rule of J. W. Gibbs, in an applicable form to nonreacting systems,

$$F = 2 - \pi + N \tag{3.1}$$

where $\pi$ is the number of phases, N the number of chemical species, and F degrees of freedom of the system. For phase rule to apply coexisting phases must be in equilibrium. When $F = 0$, the system is invariant, eq. (3.1) becomes $\pi = 2 + N$, e.g. if the number of independent variables required to identify the intensive state of the system is 4 and the number of phases present for binary systems of butanol and water 2, two degrees of freedom are available for

biphasic systems, and the independent variables ($T, p$) can be used to define the composition of the system. Degrees of freedom of a liquid-liquid system containing $N$ chemical species is,

$$F = 2 - \pi + N = 2 - 2 + N = N \tag{3.2}$$

The same result can be obtained for a vapor-liquid system, since the number of the phases do not change [20].

## 3.2. Two-Phase Systems

As explained above in Gibbs' phase rule, independent variables ($T, p$) can be used to define the composition of a two-phase system. A phase transition at constant $T$ and $p$ occurs whenever one of these curves is crossed in a phase diagram. For two phases $\alpha$ and $\beta$ of a pure species coexisting at equilibrium,

$$G^{\alpha} = G^{\beta} \tag{3.3}$$

where $G^{\alpha}$ and $G^{\beta}$ are the molar or specific Gibbs energies of the individual phases [20].

The Clapeyron equation, eq. (3.10), follows from this equality, eq. (3.3). When the temperature of a two-phase system is changed, the pressure must change accordantly with the relation between vapor pressure and temperature if the two phases continue to coexist in equilibrium. The eq. (3.3) applies throughout this change,

$$dG^{\alpha} = dG^{\beta} \tag{3.4}$$

and Gibbs energy is defined as,

$$dG = Vdp - SdT \tag{3.5}$$

Substituting expressions for $dG^{\alpha}$ and $dG^{\beta}$ by eq.(3.5) yields,

$$V^{\alpha}dp^{sat} - S^{\alpha}dT = V^{\beta}dp^{sat} - S^{\beta}dT \tag{3.6}$$

which becomes eq. (3.7) when rearranged,

$$\frac{dp^{sat}}{dT} = \frac{S^{\beta} - S^{\alpha}}{V^{\beta} - V^{\alpha}} = \frac{\Delta S^{\alpha\beta}}{\Delta V^{\alpha\beta}} \tag{3.7}$$

The entropy change $\Delta S^{\alpha\beta}$ and the volume change $\Delta V^{\alpha\beta}$ occur when a unit amount of a pure chemical species is transferred from phase $\alpha$ to phase $\beta$ at the equilibrium $T$ and $p$.

Differential change of enthalpy for a homogeneous fluid of constant composition is defined as,

$$dH = TdS + Vdp \tag{3.8}$$

Assuming pressure is constant $dp = 0$, integration of eq. (3.8) for this change gives the latent heat of phase transition,

$$\Delta H^{\alpha\beta} = T\Delta S^{\alpha\beta} \tag{3.9}$$

Thus $\Delta S^{\alpha\beta} = \Delta H^{\alpha\beta}/T$, and substitution in the previous eq. (3.7) gives,

$$\frac{dp^{sat}}{dT} = \frac{\Delta H^{\alpha\beta}}{T\Delta V^{\alpha\beta}} \tag{3.10}$$

which is the Clapeyron equation.

For the case of phase transition from liquid $l$ to vapor $v$, eq. (3.10) becomes,

$$\frac{dp^{sat}}{dT} = \frac{\Delta H^{lv}}{T\Delta V^{lv}} \tag{3.11}$$

as the Clapeyron equation for vaporization [20].

### 3.2.1. Temperature Dependence of the Vapor Pressure of Liquids, Antoine and Wagner equations

Antoine and Wagner equations are used to estimate vapor pressures of pure components in this work, the utilization of these equations will be discussed in the simulation part. The Antoine equation is a class of semi-empirical correlations describing the relation between vapor pressure and temperature for pure components, derived from the Clausius-Clapeyron relation. The Clapeyron equation provides a connection between the properties of different phases. When applied to the calculation of latent heats of vaporization, its use presumes knowledge of the vapor pressure vs. temperature relation. Such relations are empirical because thermodynamics do not impose model of material behavior. $lnp^{sat}$ vs. $1/T$ generally gives a nearly straight line, where A and B are constants for a given species [20]. The Antoine equation for general use,

$$lnp^{sat} = A - \frac{B}{T+C} \tag{3.12}$$

where A, B, C are the constants. A principle advantage of this equation is values of the constants are available for a large number of species. Each set constants is valid for a specified temperature range [20].

Vapor pressure data over a wide temperature range requires an equation of greater complexity. The Wagner equation denotes the reduced vapor pressure, $p_r$, as a function of reduced temperature, $T_r$, since the accurate representation of vapor pressure data over a wide temperature range requires a more complex equation,

$$ln{p_r}^{sat} = \frac{A\tau + B\tau^{1.5} + C\tau^3 + D\tau^6}{1-\tau} \quad (3.13)$$

where the parameter $\tau$ is defined as,

$$\tau \equiv 1 - T_r \quad (3.14)$$

and A, B, C and D are constants [20]. Values of the constants for this equation and for eq. (3.13) are given e.g. by Reid, Prausnitz, and Poling for many species [20], [24].

### 3.2.2. The Chemical Potential and Phase Equilibria

The chemical potential is a fundamental property, which facilitates treatment of phase equilibria and transfer of species from one phase to another in industrial processes like mixing and separation [20]. Relating the molar specific Gibbs energies of the individual phases coexisting in equilibrium, eq. (3.4), to its standard variables, $T$ and $p$ in a closed system yields,

$$d(nG) = (nV)dp - (nS)dT \quad (3.15)$$

where $n$ is the total number of moles of the system. A proper application is to a single-phase fluid in a closed system wherein no chemical reactions occur. For such a system the composition is necessarily constant and therefore,

$$\left[\frac{\partial(nG)}{\partial p}\right]_{T,n} = nV \quad (3.16) \quad \text{and} \quad \left[\frac{\partial(nG)}{\partial T}\right]_{p,n} = -nS \quad (3.17)$$

For the more general case in a single-phase, open system,

$$nG = g(p, T, n, n_2, \ldots, n_i) \quad (3.18)$$

where $n_i$ is the number of moles of species $i$. The total differential of $nG$ is then:

$$d(nG) = \left[\frac{\partial(nG)}{\partial p}\right]_{T,n} dp + \left[\frac{\partial(nG)}{\partial T}\right]_{p,n} dT + \sum_i \left[\frac{\partial(nG)}{\partial n_i}\right]_{p,T,n_j} dn_i \quad (3.19)$$

Definition of the chemical potential of species $i$ in the mixture is,

$$\mu_i \equiv \left[\frac{\partial(nG)}{\partial n_i}\right] \quad (3.20)$$

with this definition and with the first two partial derivatives replaced by $(nV)$ and $(-nS)$, the preceding equation becomes,

$$d(nG) = (nV)dp - (nS)dT + \sum_i \mu_i dn_i \quad (3.21)$$

Eq. (3.21) is the foundation upon which the structure of solution thermodynamics is built. For the special case of one mole of solution, $n = 1$ and $n_i = x_i$,

$$dG = Vdp - SdT + \sum_i \mu_i dx_i \quad (3.22)$$

$$G = G(T, p, x_1, x_2, \dots, x_i) \quad (3.23)$$

For a closed system consisting of two phases in equilibrium, each individual phase is open to the other and mass transfer between phases may occur. Eq. (3.22) applies separately to each phase,

$$d(nG)^\alpha = (nV)^\alpha dp - (nS)^\alpha dT + \sum_i \mu_i^\alpha dn_i^\alpha \quad (3.24)$$

$$d(nG)^\beta = (nV)^\beta dp - (nS)^\beta dT + \sum_i \mu_i^\beta dn_i^\beta \quad (3.25)$$

where superscripts $\alpha$ und $\beta$ identify the phases. The presumption here is that equilibrium implies uniformity of $T$ and $p$ throughout the entire system [20].

The change in the total Gibbs energy of the two–phase system is the sum of these equations. When each total-system property is expressed by an equation of the form,

$$nM = (nM)^\alpha + (nM)^\beta \quad (3.26)$$

the sum is,

$$d(nG) = (nV)dp - (nS)dT + \sum_i \mu_i^\alpha dn_i + \sum_i \mu_i^\beta dn_i^\beta \quad (3.27)$$

Because the two-phase system is closed eq. (3.4) is also valid. Comparison of the eq. (3.4) and eq. (3.27) show that at equilibrium,

$$\sum_i \mu_i^\alpha dn_i^\alpha + \sum_i \mu_i^\beta dn_i^\beta = 0 \quad (3.28)$$

The changes $dn_i^\alpha$ and $dn_i^\beta$ result from mass transfer between the phases; mass conservation therefore requires,

$$dn_i^\alpha = -dn_i^\beta \quad (3.29) \quad \text{and} \quad \sum_i \left(\mu_i^\alpha - \mu_i^\beta\right) dn_i^\alpha = 0 \quad (3.30)$$

Quantities $dn_i^\alpha$ are independent and arbitrary; therefore the only way the left side of the eq. (3.30) can in general be zero is for the term in parentheses to be zero. Hence,

$$\mu_i^{\alpha} = \mu_i^{\beta} \qquad (i = 1, 2, \dots, N) \tag{3.31}$$

where $N$ is the number of species present in the system. Succesive application of this result to pairs of phases allows its generalization to multiple phases; for $\pi$ phases,

$$\mu_i^{\alpha} = \mu_i^{\beta} = \cdots = \mu_i^{\pi} \qquad (i = 1, 2, \dots, N) \tag{3.32}$$

Thus, multiple phases at the same $T$ and $p$ are in equilibrium when the chemical potential of each species is the same in all phases [20].

## 3.3. Vapor-Liquid Equilibrium

Vapor-liquid equilibrium (VLE) is the state of coexistence of liquid and vapor phases. In this work VLE for binary system “1-butanol-water” is calculated by simulations.

The two simplest formulations that allow calculation of temperatures, pressures and phase compositions for systems in VLE are Raoult’s law and Henry’s law (chapters 3.3.1 and 3.3.2) [20].

### 3.3.1. Raoult’s law

The mathematical expression which reflects the two listed assumptions below and which therefore gives quantitative expression to Raoult’s law is,

$$y_i p = x_i p_i^{sat} \qquad i = 1, 2, \dots, N \tag{3.33}$$

where $x_i$ is a liquid-phase mole fraction, $y_i$ is a vapor phase mole fraction, and $p_i^{sat}$ is the vapor pressure of pure species $i$ at the temperature of the system. The product $y_i p$ in eq. (3.33) is the partial pressure of species $i$ [20].

The two major assumptions required to reduce VLE calculations to Raoult’s law are:

- The vapor is an ideal gas
- The liquid is an ideal solution

The first assumption means that Raoult’s law can apply for low to moderate pressures. The second implies that it can have approximate validity when the species that comprise the system are chemically similar at low concentration. Raoult’s law can therefore be applied just to a small group [20].

The simple model for VLE represented by eq. (3.33) provides a realistic description of actual behavior for a relatively small class of systems. Nevertheless, it is useful for displaying VLE calculations in their simplest form, and it also serves as a standard of comparison for more complex systems. A limitation of Raoult’s law is that it can be applied only to species of known vapor pressure, and this requires the species to be “subcritical” i.e., to be at a temperature below its critical temperature [20].

## Modified Raoult's Law and Excess Gibbs Free Energy:

A modification of Raoult's law can remove the restriction to chemically similar species [20]. Modified Raoult's law results when $\gamma_i$, activity coefficient, is inserted into Raoult's law,

$$y_i p = x_i \gamma_i p_i^{sat} \qquad (i = 1, 2, \dots, N) \tag{3.34}$$

Excess properties serve as a reference for real-solution behavior. The residual Gibbs energy and the fugacity coefficient are directly related to experimental $p, V, T$ data, where such data can be correlated by equations of state and thermodynamic property information which is provided by residual properties. Liquid solutions are often more easily dealt with through properties that measure their departures, not from ideal-gas behavior, but from ideal-solution behavior. The mathematical formalism of excess properties is analogous to that of the residual properties. The excess Gibbs free energy, $G^E$, is defined as the difference between the actual Gibbs free energy of a solution $G$ and the Gibbs free energy it would have as an ideal solution, $G^{id}$, at the same $T$, $p$ and composition. Thus, the excess Gibbs free energy is,

$$G^E = G - G^{id} \tag{3.35}$$

and the excess Gibbs energy is zero for an ideal solution [20].

$G^E$ models provide a combination of activity coefficients and other experimental data. When activity coefficient and excess Gibbs free energy are coupled,

$$G^E = RT \sum_i x_i ln(\gamma_i) \tag{3.36}$$

Activity coefficients as derivatives: $\left(\frac{\partial G^E}{\partial n_i}\right)_{T,p,n_{j\neq i}} = RTln(\gamma_i)$ (3.37)

### VLE by modified Raoult's Law:

For low to moderate pressures a much more realistic equation for VLE results when the second major Raoult's law assumption is abandoned, and account is taken of deviations from solution ideality in the liquid phase. Bubblepoint and dewpoint calculations made with the eq. (3.35) are only a bit more complex than the same calculations made with Raoult's law. Activity coefficients are functions of temperature and liquid phase composition, and ultimately are based on experiment. For present purposes, the necessary values are assumed known [20].

Because $\sum_i y_i = 1$ and modified Raoult's law, eq. (3.34), may be summed over all species to yield,

$$p = \sum_i x_i \gamma_i p_i^{sat} \tag{3.38}$$

Alternatively, eq. (3.38) may be solved for $x_i$, in which case summing over all species yields,

$$p = \frac{1}{\left(\sum_i y_i / \gamma_i p_i^{sat}\right)} \tag{3.39}$$

**Dew point and bubble point calculations with Raoult's law:**

Although VLE problems with other combinations of variables are possible, engineering interest centers on dewpoint and bubblepoint calculations. One must specify either the liquid-phase or the vapor phase composition and either $p$ or $T$, thus fixing $1 + (N - 1)$ or $N$-phase rule variables, exactly the number of degrees of freedom $F$ required by the phase rule eq. (3.1) for VLE [20].

Because $\sum_i y_i = 1$ eq. (3.34) may be summed over all species to yield,

$$p = \sum_i x_i \, p_i^{sat} \tag{3.40}$$

This equation finds application in bubblepoint calculations, where the vapor phase composition is unknown. For a binary system with $x_2 = 1 - x_1$,

$$p = p_2^{sat} + (p_1^{sat} - p_2^{sat})x_1 \tag{3.41}$$

and a plot of $p$ vs. $x_1$ at constant temperature is a straight line connecting $p_2^{sat}$ at $x_1 = 0$ with $p_1^{sat}$ at $x_1 = 1$.

Eq. (3.33) may also be solved for $x_i$ and summed over all species. With $\sum_i x_i = 1$, this yields,

$$p = \frac{1}{\sum_i \frac{y_i}{P_i^{sat}}} \tag{3.42}$$

an equation applied in dewpoint calculations, where liquid phase compositions are not known [20].

**The Gamma/Phi Formulation of VLE:**

The simplest models for VLE, based on Raoult's law is presented in chapter 3.3.1 and Henry's law in chapter 3.3.2 below. The calculations by modified Raoult's law are adequate for many purposes, but are limited to low pressures [20].

Multiple phases at the same $T$ and $p$ are in equilibrium when the fugacity of each constituent species is the same in all phases. For the specific case of multicomponent VLE,

$$f_i^v = f_i^l \qquad (i = 1,2, \dots, N) \tag{3.43}$$

where $f_i^v$ indicates the fugacity of the pure species $i$ in gas mixture, $f_i^l$ the fugacity of the pure species $i$ in solution.

Modified Raoult's law includes the activity coefficient to account for liquid phase nonidealities, but is limited by the assumption of vapor phase ideality. This is overcome by introduction of the vapor phase fugacity coefficient. For species $i$ in a vapor mixture,

$f_i^v = y_i \phi_i p$ (3.44) and for species $i$ in the liquid phase $f_i^l = x_i \gamma_i f_i$ (3.45)

where $\phi_i$ is the fugacity coefficient of species $i$ in the gas mixture and $f_i$ is the standard fugacity of component $i$ in the liquid phase [20].

The two equations eq. (3.44) and eq. (3.45) become,

$y_i \phi_i p = x_i \gamma_i f_i \ \ (i = 1, 2, \dots, N)$ (3.46) and $y_i \phi_i p = x_i \gamma_i p_i^{sat} \ \ (i = 1, 2, \dots, N)$ (3.47)

**Dewpoint and Bubblepoint Calculations with gamma/phi formulation:**

All such calculations made by the gamma/phi formulation require iteration because of its complex functionality,

$\phi_i = \phi(T, p, y_1, y_2, \dots, y_{N-1})$ (3.48)

$\gamma_i = \gamma(T, x_1, x_2, \dots, x_{N-1})$ (3.49)

$p_i^{sat} = f(T)$ (3.50)

At the moderate pressures where gamma/phi approach to VLE is appropriate, activity coefficients are assumed independent of pressure [20].

Equation for $y_i$ or $x_i$ : $y_i = \frac{x_i \gamma_i p_i^{sat}}{\phi_i p}$ (3.51) $x_i = \frac{y_i \phi_i p}{\gamma_i p_i^{sat}}$ (3.52)

### 3.3.2. Henry's Law

Henry's law is especially useful for dilute solutions. It is valid for any species present at low concentration, but also limited to systems at low to moderate pressures. Unlike Raoult's law, which requires the species to be "subcritical", Henry's law can be applied for the systems above the critical temperature. Application of Raoult's law to species $i$ requires a value for $p_i^{sat}$ at the temperature of application, and is not appropriate for species which are supercritical at the application temperature [20].

Henry's law states that the partial pressure of a species in the vapor phase is directly proportional to its liquid phase mole fraction for a very dilute solute in the liquid phase. Thus,

$y_i p = x_i H_i$ (3.53)

where $H_i$ is Henry's constant and values of $H_i$ come from experiment. Mole fraction of the gas component in liquid is proportional to the same component in gas. The solubility of the gases increases proportionally with the pressure [20].

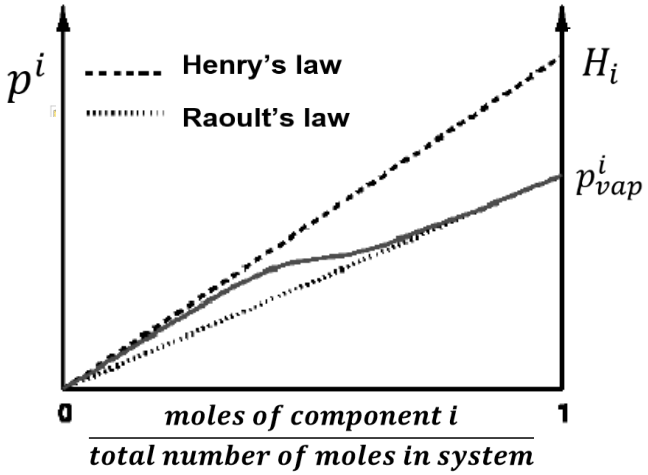


**Fig. 3-1. Henry's law and Raoult's law for a binary vapor-liquid system [22]**

Fig. 3-1 shows the applicability of Henry's law and Raoult's law, where $p^i$ is the partial vapor pressure of the solution, $H_i$ is the Henry constant for species $i$ and $p^i_{vap}$ is the vapor pressure of pure solvent $i$. The curve between Henry's law and Raoult's law shows the actual behavior of the vapor-liquid system. Henry's law shows here a positive deviation from Raoultian behavior.

## 3.4. Liquid-Liquid Equilibrium

Aqueous liquid-liquid equilibrium is the result of intermolecular forces, mainly of the hydrogen-bonding type. The equilibrium state of a closed system is the state for which the total Gibbs energy is a minimum with respect to all possible changes at the given $T$ and $p$ [18].

$$(dG)_{T,p} \leq 0 \tag{3.54}$$

Eq. (3.54) indicates that all irreversible processes occuring at constant $T$ and $p$ proceed in such a direction as to cause a decrease in the Gibbs energy of the system.

At the equilibrium state differential variations can occur in the system at constant $T$ and $p$ without producing any change in $G$. Thus, the form of this criterion of equilibrium is,

$$(dG)_{T,p} = 0 \tag{3.55}$$

Eq. (3.55) provides a criterion that must be satisfied by any single phase that is stable with respect to the alternative that it split into two phases. It requires that the Gibbs energy of an equilibrium state be the minimum value with respect to all possible changes at the given $T$ and $p$. Thus, e.g., when mixing of two liquids occurs at constant $T$ and $p$, the total Gibbs energy

must decrease, because the mixed state must be the one of lower Gibbs energy with respect to the unmixed state.

At constant temperature and pressure, $\Delta G$ and its first and second derivatives must be continuous functions of $x_1$, and the second derivative must be positive everywhere. Thus,

$$d^2\Delta G/dx_1^2 > 0 \quad (const.\, T, p) \qquad (3.56)$$

and

$$d^2(\frac{\Delta G}{RT})/dx_1^2 > 0 \quad (const.\, T, p) \qquad (3.57)$$

Many pairs of chemical species mixed to form a single liquid phase in a certain composition range, would not satisfy the stability criterion of eq. (3.57). Such systems therefore split in this composition into two liquid phases of different compositions. If the phases are at thermodynamic equilibrium, the phenomenon is an example of LLE, which is important for industrial operations such as solvent extraction.

LLE diagrams show two areas. Area I is called homogeneous area and area II is called heterogeneous area. Homogeneous area is the area over the liquid-liquid line where the liquids are miscible, and heterogeneous area, so called miscibility gap is the area under the liquid-liquid phase separation line, where liquids are immiscible and two liquid phase occur with different compositions.

In fig. 3-2, liquid-liquid phase equilibrium diagram is shown where the equilibrium line separates the homogeneous and heterogeneous phase areas [18]. The area above the binodal curve is the homogeneous area, and the area below is the heterogeneous area. The point over the equilibrium line at the temperature $T_1$ and the mole fraction $z_1$ is in homogeneous area. At the temperature $T_1$ there is homogeneous phase, at the temperature $T_2$ both homogeneous and heterogeneous phase areas exist. The line between $L_\alpha$ and $L_\beta$ at the temperature $T_2$ shows the heterogeneous area where component 1 exists in two phases with different compositions. At the point F and temperature $T_2$ the mole fraction of the two phase system is $z_1$.

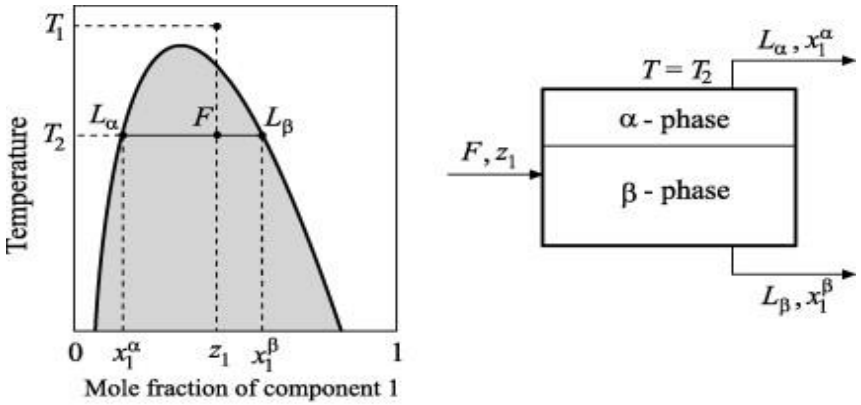


**Fig. 3-2. Temperature vs. mole fraction diagram of LLE of binary system $\alpha$ and $\beta$**

The equilibrium criteria for LLE is the same as for VLE, which is uniformity of $T, p$, and of the fugacity $f_i$ for each chemical species throughout both phases. For LLE in a system of $N$ species at uniform $T$ and $p$, denoting the liquid phases by $\alpha$ and $\beta$, the equilibrium criteria is,

$$\hat{f}_i^\alpha = \hat{f}_i^\beta \qquad (i = 1, 2, \dots, N) \qquad (3.58)$$

with the introduction of activity coefficients, this becomes,

$$x_i^\alpha \gamma_i^\alpha f_i^\alpha = x_i^\beta \gamma_i^\beta f_i^\beta \tag{3.59}$$

If each pure species exists as liquid at the system temperature, $f_i^\alpha = f_i^\beta = f_i$; whence,

$$x_i^\alpha \gamma_i^\alpha = x_i^\beta \gamma_i^\beta \qquad (i = 1, 2, \dots, N) \tag{3.60}$$

Activity coefficients $\gamma_i^\alpha$ and $\gamma_i^\beta$ derive from the same function $G^E/RT$; thus they are functionally identical, distinguished mathematically only by the mole fractions to which they apply. For a liquid-liquid system containing $N$ chemical species,

$$\gamma_i^\alpha = \gamma_i(x_1^\alpha, x_2^\alpha, \dots, x_{N-1}^\alpha, T, p) \tag{3.61}$$

$$\gamma_i^\beta = \gamma_i(x_1^\beta, x_2^\beta, \dots, x_{N-1}^\beta, T, p) \tag{3.62}$$

In the general description of LLE, any number of species may be considered, and pressure may be a significant variable. In this case here, binary LLE either at constant $p$ or at reduced $T$ low enough that the effect of pressure on the activity coefficients may be ignored. With one independent mole fraction per phase, eq. (3.60) gives,

$$x_1^\alpha \gamma_1^\alpha = x_1^\beta \gamma_1^\beta \tag{3.63}$$ and $$(1 - x_1^\alpha)\gamma_2^\alpha = \left(1 - x_1^\beta\right)\gamma_2^\beta \tag{3.64}$$

where,

$$\gamma_i^\alpha = \gamma_i(x_1^\alpha, T) \tag{3.65}$$ and $$\gamma_i^\beta = \gamma_i(x_1^\beta, T) \tag{3.66}$$

With two equations and three variables ($x_1^\alpha, x_1^\beta$, and $T$), fixing one of the variables allows solution of eqs. (3.65-3.66) for the remaining two. Because $ln\gamma_i$, rather than $\gamma_i$, is a more natural thermodynamic function, application of eqs. (3.65-3.66) often proceeds from the rearrangements,

$$\ln \frac{\gamma_1^\alpha}{\gamma_1^\beta} = \ln \frac{x_1^\beta}{x_1^\alpha} \tag{3.67}$$ and $$\ln \frac{\gamma_2^\alpha}{\gamma_2^\beta} = \ln \frac{1 - x_1^\beta}{1 - x_1^\alpha} \tag{3.68}$$

For conditions of constant $p$, or when pressure effects are negligible, binary LLE is conveniently displayed on a solubility diagram, a plot of $T$ vs. $x_1$. Binodal curves in a LLE diagram define an "island". They represent the compositions of coexisting phases: for the $\alpha$ phase (rich in species 2), and for the $\beta$ phase (rich in species 1). Equilibrium compositions $x_1^\alpha$ and $x_1^\beta$ at a particular $T$ are defined by the intersections of a horizontal tie line with the binodal curves. Temperature $T_L$ is a lower critical solution temperature (LCST); temperature $T_U$ is an upper consolute

temperature, or upper critical solution temperature (UCST), which can be seen in fig. 3-3. At temperatures between $T_L$ and $T_U$, LLE is possible; for $T < T_L$ and $T > T_U$, a single liquid phase is obtained for the full range of compositions. The consolute points are limiting states of two-phase equilibrium for which all properties of the two equilibrium phases are identical [18].

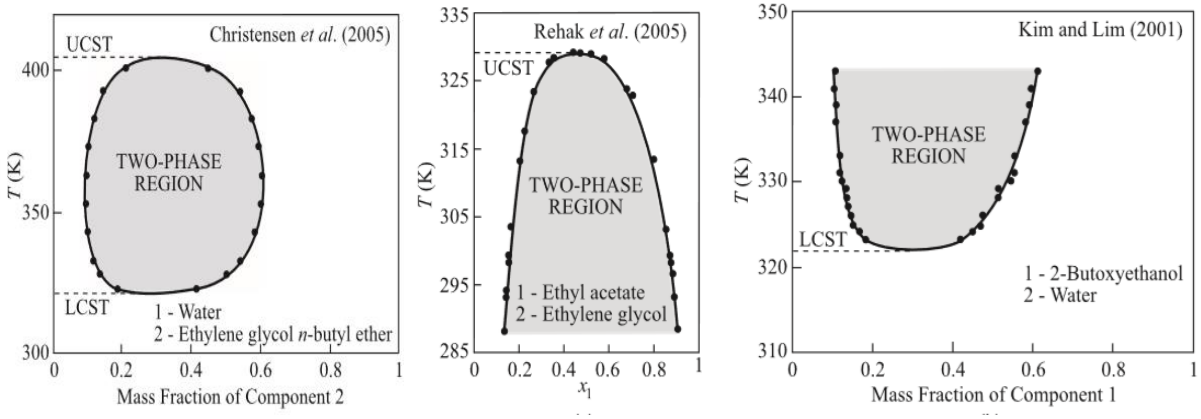


**Fig. 3-3. Three types of constant-pressure liquid-liquid solubility diagram for binary mixtures**

A typical liquid-liquid phase equilibrium diagram for a ternary mixture is shown in fig. 3-4. While components *S* and *C* are partially miscible, *A* dissolves completely in *C* or *S*.

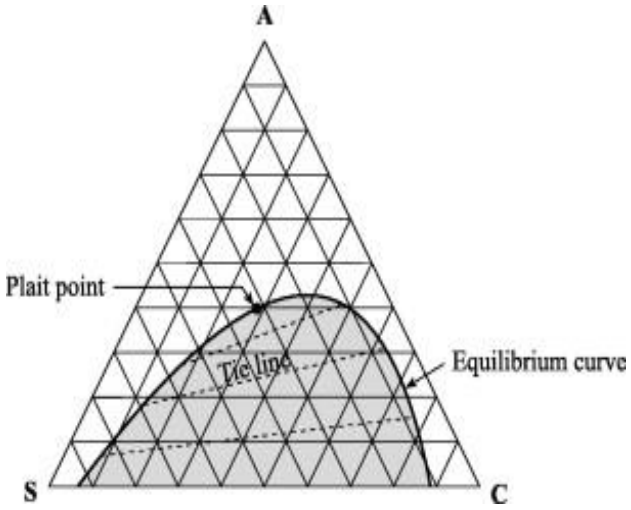


**Fig. 3-4. Concentration diagram of LLE of ternary system "A-C-S"**

The dome-shaped shaded region indicates the two-phase region, the boundary of which is determined from the equilibrium data, i.e. binodal curve. Within the two-phase region, the tie lines join the equilibrium compositions of the separate phases. The lengths of the tie lines decrease towards the apex of the dome-shaped region. At the *plait point*, the tie line shrinks to a point and, as a result, the two phases become identical. Outside the dome-shaped region all components are miscible in each other, i.e. one-phase region [18].

## 3.5. Activity Coefficient Models

LLE data for regression of interaction parameters and interaction parameters derived from the VLE data are to be used with activity coefficient models. Activity coefficient models are essential to estimate phase equilibriums (VLE, LLE). They are functions of $T$ and liquid phase composition, based on experiment as mentioned in chapter 3.3. Activity coefficient models can be divided into two groups; random-mixing-based models (Margules, Van Laar) and local composition (LC) models (Wilson, NRTL, UNIQUAC, UNIFAC). The activity coefficient models NRTL and UNIQUAC are of importance for this work because of their use in the phase equilibrium calculations (VLE, LLE) of ABE fermentation solvents with Aspen Plus simulation.

For non-ideal liquid solutions, the fugacity of the components in the solution deviates from that of the pure component. The ratio of the fugacity in solution to that of pure component is defined as the activity,

$$a_i = \frac{f_i}{f_i^\circ} \tag{3.69}$$

The activity coefficient $(\gamma)$ can be calculated as follows,

$$a_{i,L} = \gamma_{i,L} x_i \tag{3.70}$$

When the chemical potential of a component $i$, $\mu_i$, in an ideal mixture with activity $a_i$,

$$\mu_i(T, p, \{x_j\}) = \mu_{oi}^l(T, p) + RTlna_i \tag{3.71}$$

where $a_i = a_i(T, p, \{x_j\})$ is pressure, temperature and composition of liquid mixture dependent [20]. Activity is usually shown with activity coefficients $\gamma_i$,

$$\gamma_i(T, p, \{x_j\}) = a_i/x_i \tag{3.72}$$ and $$\mu_i(T, p, \{x_j\}) = \mu_{oi}^l(T, p) + RTlnx_i + RTln\gamma_i(T, p, \{x_j\}) \tag{3.73}$$

The activity coefficient $\gamma_i$ of component $i$ as correction of the ideal mixture model is,

$$RTln\gamma_i = \left(\frac{\partial G^E}{\partial n_i}\right)_{T,p,n_i} \tag{3.74}$$

where $G^E$ is the excess enthalpy of the mixture [20].

**Models for the Excess Gibbs Energy:**

In general $G^E/RT$ is a function of $T, p$ and composition, but for liquids at low to moderate pressures it is very weak function of $p$. Therefore, the pressure dependence of activity coefficients is usually neglected [20]. Thus, for data at constant $T$,

$$\frac{G^E}{RT} = g(x_1, x_2, \dots, x_N) \qquad (const\ T) \tag{3.75}$$

The various developments for activity coefficient models almost always start from an expression for the excess Gibbs energy [19].

### 3.5.1. Random-Mixing-Based Models

Traditional cubic EoS using the vdW mixing rules and activity coefficient models like the Margules and van Laar equations use 'average' or 'overall' compositions. They are models based on 'random mixing'. However due to intermolecular forces, the mixing of molecules is never entirely random and a way to account for the non-randomness can lead to improved models and better descriptions of phase behavior [19].

**Margules Equation**

The parameters of the Margules and other activity coefficient models are typically obtained by regressing activity coefficient or VLE $(p, T, x, y)$ data at constant $T$ or $p$. Alternatively, in the case of lack of data, they can be estimated from [19]:

- a single activity coefficient point at a specific concentration (for both components);
- infinite dilution activity coefficients (many databases are available, e.g. Reid et al.);
- azeotropic data ($\gamma = p/p^{sat}$).

**One-Parameter Margules Equation:**

The simplest expression for Gibbs excess energy function [19],

$$\frac{g^E}{RT} = Ax_1x_2 \tag{3.76}$$

One-parameter Margules equation for the activity coefficient (binary):

$$ln\gamma_i = A/RTx_j^2 \tag{3.77}$$

where A is a value from the chemical theory defined as,

$$A = z\left[\Gamma_{12} - \frac{\Gamma_{11}+\Gamma_{22}}{2}\right] \tag{3.78}$$

The parameter A is related to the intermolecular potentials of the compounds. An ideal solution is obtained in the case where the cross-potential is given by the arithmetic mean average of the potentials ($\Gamma_{12} = \frac{\Gamma_1+\Gamma_2}{2}$) [19].

**Two-parameters Margules Equation:**

The two parameter Margules model is developed in an empirical way. It has been observed for certain moderately non-ideal systems, and a relationship for the excess Gibbs energy has been established. The two-parameter Margules equation gives very good results in many cases, often even for highly non-ideal systems, and in the case of both positive and negative deviations from Raoult's law [19].

The expression for Gibbs excess energy function is,

$$\frac{g^E}{RT} = \left(A_{ji}x_i + A_{ij}x_j\right)x_i x_j \tag{3.79}$$

Two parameters Margules equation: $$ln\gamma_i = x_j^2\left[A_{ij} + 2\left(A_{ji} - A_{ij}\right)x_i\right] \tag{3.80}$$

For the limiting conditions of infinite dilution: $$ln\gamma_i^{\infty} = A_{ij}(x_i = 0)_) \tag{3.81}$$

$$ln\gamma_j^{\infty} = A_{ji}(x_j = 0) \tag{3.82}$$

$\gamma_i$ and $\gamma_j$ can be used to calculate VLE [19].

**Van Laar Equation**

Although it is possible to derive the van Laar equation empirically, similar to Margules, by noticing that $g^E/x_1x_2RT$ is inversely proportional to the composition, a better derivation which illustrates its physical meaning and the approach used by van Laar is based on the vdW EoS. Van Laar assumed that the volume can be approximated for liquids (far from the critical point) by their co-volume (i.e. $V_i = b_i$) and that the excess entropy and excess volume are zero [19].

$$\frac{g^E}{RT} = \frac{A_{12}x_1A_{21}x_2}{A_{12}x_1 + A_{21}x_2} \tag{3.83}$$

where $A_{12}$ and $A_{21}$ are the van Laar coefficients, which are obtained by regression of experimental vapor-liquid equilibrium data. The activity coefficient of component $i$ is derived by differentiation to $x_i$ [25]. Van Laar Equation for a binary mixture is,

$$ln\gamma_1 = \frac{A_{12}}{\left[1 + \frac{A_{12}x_1}{A_{21}x_2}\right]^2} \tag{3.84}$$

where,

$$A_{12} = \frac{b_1}{RT}(\delta_1 - \delta_2)^2 \tag{3.85}$$ and $$A_{21} = \frac{b_2}{RT}(\delta_1 - \delta_2)^2 \tag{3.86}$$

and $\delta$ is the solubility parameter [26]. Activity coefficients of compound 2 can be obtained by simply setting $A_{21}$ in place of $A_{12}$ and $A_{12}$ in place of $A_{21}$, as well as $x_2$ in place of $x_1$. As in the case of the two-parameter Margules equation, the two parameters of the van Laar equation are equal to the logarithms of the two activity coefficients (of component 1 and 2) at infinite dilution,

$$ln\gamma_i^{\infty} = A_{12} \quad (3.87) \quad \text{and} \quad ln\gamma_j^{\infty} = A_{21} \quad (3.88)$$

or rearranging to,

$$A_{12} = (ln\gamma_1)[1 + x_2 ln\gamma_2 / x_1 ln\gamma_1]^2 \quad (3.89)$$

Activity coefficient models based on rational functions, i.e., on equations for $g^E/x_1x_2RT$ like Margules and van Laar provide great flexibility in the fitting of VLE data for binary systems. However, they lack theoretical foundation and therefore fail to admit a rational basis for extension to multicomponent systems. Therefore, the molecular thermodynamics of liquid-solution behavior are often based on the concept of local composition (LC) models most notably NRTL and UNIQUAC equations [20].

### 3.5.2. Local-Composition Models

Reliable phase equilibrium data is essential for optimum separation process synthesis, design and operation. When experimental binary data is available, phase equilibrium behavior is easily modeled with the help of local composition (LC) models using activity coefficient data. When little or no experimental data are available, group contribution (GC) methods can be used to predict the phase equilibrium under specified conditions of temperature and pressure. LC models, Wilson, NRTL (Non-random-two-liquid) and UNIQUAC (Universal Quasi-chemical) can be extended to multicomponent systems, easier than the van Laar and Margules equations. In most cases two interaction parameters per binary mixture in LC activity coefficient models are sufficient for obtaining good VLE results [19].

NRTL and UNIQUAC models have been further developed into predictive GC versions Analytical Solution of Groups (ASOG) and Universal Quasi-chemical Functional Activity Coefficient (UNIFAC), suitable for preliminary design in the absence of experimental data [19].

#### Wilson's Equation

Wilson's equation like the Margules and van Laar equations, contains two parameters for a binary system ($\Lambda_{12}$, $\Lambda_{21}$) and is written [20],

$$\frac{G^E}{RT} = -x_1 ln(x_1 + x_2\Lambda_{12}) - x_2 \ln(x_2 + x_1\Lambda_{21}) \quad (3.90)$$

$$ln\gamma_1 = -\ln(x_1 + x_2\Lambda_{12}) + x_2\left(\frac{\Lambda_{12}}{x_1 + x_2\Lambda_{12}} - \frac{\Lambda_{21}}{(x_1\Lambda_{21} + x_2)}\right) \quad (3.91)$$

$$ln\gamma_2 = -\ln(x_1\Lambda_{21} + x_2) + x_1\left(\frac{\Lambda_{12}}{x_1+x_2\Lambda_{12}} - \frac{\Lambda_{21}}{(x_1\Lambda_{21}+x_2)}\right) \quad (3.92)$$

Wilson's equation for infinite dilution,

$$ln\gamma_1^{\infty} = -ln\Lambda_{12} + 1 - \Lambda_{21} \quad (3.93) \quad \text{and} \quad ln\gamma_2^{\infty} = -ln\Lambda_{21} + 1 - \Lambda_{12} \quad (3.94)$$

$$\Lambda_{12} = V_2/V_1 \exp\left(-\frac{A_{12}}{RT}\right) \quad (3.95) \quad \text{and} \quad \Lambda_{21} = V_1/V_2 \exp\left(-\frac{A_{21}}{RT}\right) \quad (3.96)$$

$V_i$, $V_j$: molar volume of pure liquid $i$, $j$, at temperature $T$ [23].

**NRTL Equation**

NRTL model is based on the local composition concept, and it is applicable for partially miscible systems. The NRTL equation containing three parameters for a binary system is [20]:

$$\frac{g^E}{x_1x_2RT} = \frac{G_{21}\tau_{21}}{x_1+x_2G_{21}} + \frac{G_{12}\tau_{12}}{x_2+x_1G_{12}} \quad (3.97)$$

$$ln\gamma_1 = x_2^2\left[\tau_{21}\left(\frac{G_{21}}{(x_1+x_2G_{21})^2} + \frac{G_{12}\tau_{12}}{(x_2+x_1G_{12})^2}\right]\right. \quad (3.98)$$

$$ln\gamma_2 = x_1^2\left[\tau_{12}\left(\frac{G_{12}}{(x_2+x_2G_{21})^2} + \frac{G_{21}\tau_{21}}{(x_1+x_2G_{21})^2}\right]\right. \quad (3.99)$$

The infinite dilution values of the activity coefficients are given by the equations,

$$ln\gamma_1^{\infty} = \tau_{21} + \tau_{12}\exp(-\alpha_{12}\tau_{12}) \quad (3.100) \quad \text{and} \quad ln\gamma_2^{\infty} = \tau_{12} + \tau_{21}\exp(-\alpha_{12}\tau_{21}) \quad (3.101)$$

with,

$$G_{12} = \exp(-\alpha_{12}\tau_{12}) \quad (3.102) \quad \text{and} \quad G_{21} = \exp(-\alpha_{21}\tau_{21}) \quad (3.103)$$

$$\tau_{12} = \frac{b_{12}}{RT} \quad (3.104) \quad \text{and} \quad \tau_{21} = \frac{b_{21}}{RT} \quad (3.105)$$

$\alpha_{12}$, $\alpha_{21}$ $b_{12}$, $b_{21}$ are parameters specific to a particular pair of species, and independent of composition and temperature [20]. The parameter $\alpha$ is a measure of the non-randomness of the mixture; when $\alpha$ is zero, the mixture is said to be completely random [19].

NRTL is utilized widely in phase equilibria calculations and employs three adjustable parameters (two interaction parameters and $\alpha_{12}$, the non-randomness factor) that are determined through regression of experimental data for a specific binary VLE system. The two interaction parameters account for the difference between the pure-component liquid interactions and mixed-component liquid interactions. $\alpha_{12}$, is often used as the third adjustable

parameter of the model. The main disadvantage of the NRTL model is the strong correlation between the two parameters of the model [19].

**UNIQUAC Equation**

The UNIQUAC equation is based on Guggenheim's quasi chemical lattice model. This model was restricted to describing only small molecules which were essentially the same size. Abrams and Prausnitz extended this theory to mixtures containing molecules of different size and shape by incorporating and adapting Wilson's local-composition model. The UNIQUAC equation is described in terms of the combinatorial and residual terms. Combinatorial term uses only pure component data and is determined only by the size, shape and composition of the molecules in the mixture [26].

For binary mixtures, the excess Gibbs energy of the combinatorial term is,

$$\left(\frac{g^E}{RT}\right)_C = x_1 ln\frac{\Phi_1}{x_1} + x_2 ln\frac{\Phi_2}{x_2} + \frac{z}{2}\left(q_1 x_1 ln\frac{\theta_1}{\Phi_1} + q_2 x_2 ln\frac{\theta_2}{\Phi_2}\right) \quad (3.106)$$

The residual term is used to describe the intermolecular forces responsible for enthalpy of mixing [26]. Thus the two adjustable binary interaction parameters appear only in the residual term. For binary mixtures the residual term is described in terms of excess energy as,

$$\left(\frac{g^E}{RT}\right)_R = -q_1 x_1 \ln(\theta_1 + \theta_2\tau_{21}) - q_2 x_2 \ln(\theta_2 + \theta_1\tau_{12}) \quad (3.107)$$

The UNIQUAC equation to calculate activity coefficients for a binary mixture,

$$ln\gamma_1 = x_1 ln\frac{\Phi_1}{x_1} + \frac{z}{2} q_1 ln\frac{\theta_1}{\Phi_1} + \Phi_2\left(l_1 - \frac{r_1}{r_2} l_2\right) - q_1 \ln(\theta_1 + \theta_2\tau_{21}) + \theta_2 q_1\left(\frac{\tau_{21}}{\theta_1 + \theta_2\tau_{21}} - \frac{\tau_{12}}{\theta_2 + \theta_1\tau_{12}}\right) \quad (3.108)$$

$$ln\gamma_2 = x_1 ln\frac{\Phi_2}{x_2} + \frac{z}{2} q_2 ln\frac{\theta_2}{\Phi_2} + \Phi_2\left(l_2 - \frac{r_2}{r_1} l_1\right) - q_2 \ln(\theta_2 + \theta_1\tau_{12}) + \theta_1 q_2\left(\frac{\tau_{12}}{\theta_2 + \theta_1\tau_{12}} - \frac{\tau_{21}}{\theta_1 + \theta_2\tau_{21}}\right) \quad (3.109)$$

The pure-component parameters ($l_1$) and ($l_2$) are determined as in,

$$l_1 = \frac{z}{2}(r_1 - q_1) - (r_1 - 1) \quad (3.110) \qquad \text{and} \qquad l_2 = \frac{z}{2}(r_2 - q_2) - (r_2 - 1) \quad (3.111)$$

The average segment (i.e. volume) fraction, $\Phi_i$, is only used in the calculation of the combinatorial term [26]. For a binary mixture, it is defined mathematically as,

$$\Phi_1 = \frac{x_1 r_1}{x_1 r_1 + x_2 r_2} \quad (3.112) \quad \text{and} \quad \Phi_2 = \frac{x_2 r_2}{x_1 r_1 + x_2 r_2} \quad (3.113)$$

The average area function, $\theta_i$, is used in both combinatorial and residual terms. For a binary mixture, the average area fraction, $\theta_i$, is defined as [26],

$$\theta_1 \equiv \frac{x_1 q_1}{x_1 q_1 + x_2 q_2} \quad (3.114) \quad \text{or} \quad \theta_1 \equiv \frac{x_1 q_1'}{x_1 q_1' + x_2 q_2'} \quad (3.115)$$

$$\theta_2 \equiv \frac{x_2 q_2}{x_1 q_1 + x_2 q_2} \quad (3.116) \quad \text{or} \quad \theta_2 \equiv \frac{x_2 q_2'}{x_1 q_1' + x_2 q_2'} \quad (3.117)$$

In terms of lattice theory, each molecule of component $i$ consists of a set of bonded segments occupying a set volume (parameter $r_i$). In terms of component $i$, parameter $r_i$ is the van der Waals molecular volume relative to that of a standard segment (1) and is expressed as,

$$r_i = {V_{wi}}/{V_{ws}} \quad (3.118)$$

where $V_{wi}$ is the van der Waals volume of molecule $i$ and $V_{ws}$ is the van der Waals volume of a standard segment [26]. The volume for a standard sphere in terms of its radius $R_{ws}$ is as in,

$$V_{ws} = {4}/{3}\, R_{ws}^3 \quad (3.119)$$

Parameter $q_i$ is referred to as the van der Waals molecular area relative to that of a standard segment (1) and is defined as,

$$q_i = {A_{wi}}/{A_{ws}} \quad (3.120)$$

where $A_{wi}$ is the van der Waals surface area of molecule $i$, $A_{ws}$ is the van der Waals surface area of a standard segment. The area of a standard sphere in terms of its radius $R_{ws}$ is provided as,

$$A_{ws} = 4\pi R_{ws}^2 \quad (3.121)$$

The binary adjustable parameters $\tau_{ij}$ contain the characteristic interaction energy parameters $u_{ij}$ which represent average intermolecular energies, since in a given molecule the segments are not necessarily chemically identical. These in turn relate to the UNIQUAC binary interaction parameters $a_{ij}$ as in

$$\tau_{12} = \exp\left(-\frac{\Delta u_{12}}{RT}\right) \equiv exp\left(-\frac{a_{12}}{T}\right) \quad (3.122) \quad \text{and} \quad \tau_{21} = \exp\left(-\frac{\Delta u_{21}}{RT}\right) \equiv exp\left(-\frac{a_{21}}{T}\right) \quad (3.123)$$

The parameters $a_{ij}$ are determined from binary experimental data, sourced mainly from VLE data $(p, y, x)$ at constant temperature, VLE data $(T, y, x)$ at constant pressure and total pressure data $(p, x \; or \; y)$ at constant temperature [26].

UNIQUAC equation can be extended to multicomponent systems [23],

$$\frac{G^E}{RT} = \sum_j x_j ln\left(\frac{\Phi_j}{x_j}\right) - 5\sum_j q_j x_j ln\left(\frac{\Phi_j}{\theta_j}\right) - \sum_j q_j x_j ln\left(\sum_i \theta_i \tau_{ij}\right) \quad (3.124)$$

$$ln\gamma_k = ln\gamma_k^{COMB} + ln\gamma_k^{RES} \quad (3.125)$$

$$ln\gamma_k^{COMB} = \ln\left(\frac{\Phi_k}{x_k}\right) + \left(1 - \frac{\Phi_k}{x_k}\right) - 5q_k\left[\ln\left(\frac{\Phi_k}{\theta_k}\right) + (1 - \frac{\Phi_k}{\theta_k})\right] \quad (3.126)$$

$$ln\gamma_k^{RES} = q_k\left[1 - ln(\sum_i \theta_i \tau_{ik}) - \sum_j \frac{\theta_j \tau_{kj}}{\sum_i \theta_i \tau_{ij}}\right] \quad (3.127)$$

**UNIFAC**

UNIFAC (Universal Quasi-chemical Functional Activity Coefficient) is used in predicting thermodynamic properties (especially activity coefficients) in non-electrolyte liquid mixtures. The model combines the solution of groups concept of Wilson with the UNIQUAC model [26].

In essence the UNIFAC model involves:

- suitable reduction of experimentally obtained activity coefficient data in order to obtain parameters which characterize the interactions between pairs of structural groups
- the use of these parameters in predicting activity coefficients for other systems for which no experimentally obtained data is available, but which contain the same functional groups.

The group interaction parameters can predict activity coefficients in a large number of binary and multicomponent mixtures with reasonably good accuracy. The UNIFAC model contains two adjustable parameters per pair of functional groups. The excess Gibbs energy differences due to molecular interactions is defined as in UNIQUAC model and UNIFAC model consists also of a combinatorial and a residual term [26].

### 3.5.3. Advantages and Limitations of LC Models

The local composition (LC) era began with Wilson equation using local composition fractions instead of the traditional segment or volume fractions. That was essentially a one-fluid derivation of a two-fluid model, but the most serious limitation of the Wilson equation was its inability to represent LLE. It is found that the Wilson equation cannot account for a system of limited miscibility. Wilson's LC model is suitable only for binary and multicomponent VLE [19].

J.M. Prausnitz has done major developments in the LC field: NRTL, UNIQUAC, UNIFAC. Unlike Wilson, all three models are suitable for both VLE and LLE. NRTL offered a solution to the LLE problem of Wilson, while maintaining good results for VLE, in some cases also for

heats of mixing. However, NRTL is essentially an $H^E$ rather than $G^E$ model, because of its lack of a combinatorial term. NRTL has three adjustable parameters and even though the non-randomness factor can sometimes be set to a constant value, experimental data may not be sufficient for adjusting all three parameters with good accuracy [19].

**Range of Applicability of LC Models [19]:**

1. Wilson, NRTL and UNIQUAC have parameters with a built-in temperature dependency and can be applied to multicomponent VLE, but only NRTL and UNIQUAC can be applied to LLE.

2. NRTL and UNIQUAC have some success in simultaneously representing VLE and LLE, the latter especially for binary mixtures, less so for multicomponent mixtures.

3. NRTL can be applied, in most cases, with some success also to excess enthalpies (at the cost of an extra parameter). UNIQUAC with temperature dependent parameters often yields good excess enthalpies.

LC models often correlate binary and multicomponent VLE much better than the random-mixing-based models (Margules and van Laar) for mixtures of non-polar and polar/complex compounds. Successful VLE representation is obtained at various temperatures, due to their built-in temperature dependency, but obtaining good results for heats of mixing typically requires temperature dependent interaction parameters [19].

The parameters of the LC models are strongly intercorrelated and often several sets of parameter pairs may represent VLE data equally well. Such intercorrelation may be eliminated if extensive data and also some ternary data are included in the parameter estimation [19].

LC models are easily extended to multicomponent systems and yield satisfactory multicomponent VLE in many cases, based only on binary data, which is of great importance in separation design, e.g. of distillation columns. LC models exhibit problems in representing LLE, for simultaneous descriptions of VLE and LLE with the same interaction parameters and multiphase equilibria (VLLE), and when highly polar and hydrogen bonding compounds (water, acids, etc.) are present. LLE prediction for ternary systems is improved when a few ternary LLE data are used in the parameter estimation [19].

Interaction parameters of LC models in table 3-1 have a built-in temperature dependency via the Boltzmann factors and they are not sensitive to the method used in the case of VLE. In many cases experimental data are not sufficient quantity and quality to justify use of more than two interaction parameters. Extensive data must be used to estimate temperature dependent parameters [19].

| Model | Interaction parameters |
|---|---|
| Wilson | $\Lambda'_{ij} = (\mathrm{V}_j/\mathrm{V}_i)\exp(-\Delta\lambda_{ji}/RT)$<br>$\Delta\lambda_{ij} = \lambda_{ij} - \lambda_{jj}$<br>$\Lambda_{ii} = \Lambda_{jj} = 1$ |
| NRTL | $G_{ij} = \exp(-a_{ij}\tau_{ij})$<br>$\tau_{ji} = (g_{ji} - g_{ij})/RT$<br>$G_{ii} = G_{jj} = 1$<br>$\tau_{ii} = \tau_{jj} = 0$ |
| UNIQUAC | $\tau_{ij} = exp\left(-\Delta U_{ij}/RT\right)$<br>$\Delta U_{ij} = U_{ij} - U_{jj}$ or $\Delta U_{ij} = Z/2(U_{ij} - U_{jj})$<br>$\tau_{ii} = \tau_{jj} = 1$ |

**Table 3-1. Interaction parameters of LC models**

### The Theoretical Limitations:

The parameter interrelation and its extension to multicomponent systems is not the only theoretical limitation of the LC models [19].

| Model | Entropic term | Problems with Z | Problems with R, Q | Interrelation of parameters |
|---|---|---|---|---|
| Wilson | Yes (hidden) | Yes | No | Yes |
| NRTL | No | Yes | No | Yes |
| UNIQUAC | Yes | Yes | Yes (many) | Yes |

**Table 3-2. Theoretical limitations of LC models**

In table 3-2 several problems of LC models due to the presence of the coordination number and the size parameters are summarized [19],

1. Division into an entropic and an energetic term: NRTL is an 'enthalpic' or $H^E$ model, while the other two models do have such an entropic contribution. Only UNIQUAC has two distinct contributions to the activity coefficient, one due to size and shape effects (combinatorial) and one due to energetic interactions (residual) [19].

2. The coordination number: All models have problems arising from the presence of the coordination number, $Z$, though of different type. For UNIQUAC, it is mostly related to the renormalization (scale) problem: if we change $Z$ (and $q$), e.q. via a new normalization way, we need to re-estimate the interaction parameters. The original derivation of UNIQUAC includes a term $Z/2$ in the exponential factor with the interaction parameters, which is a rather extreme correction to non-randomness, as verified by molecular simulation and quantum mechanics calculations. For NRTL, the $Z$ problem is mostly related to the fact that the non-randomness parameter, $\alpha_{12}$, is proportional to $2/Z$ according to theory, thus values of $\alpha_{12}$ are expected to be between 0.17 and 0.33, which are close to the values typically used. However, the $\alpha_{12}$ parameter is fitted to experimental data rather than being calculated from this expression. For

Wilson, if the model is derived from the two-fluid theory, $Z = 2$, which is a very low value for the liquid state [19].

3. UNIQUAC has more problems due to the presence of the normalized surface area, $Q$, parameter. The volume parameter $R$ and the group area parameter $Q$ are normalized to a specific value, where $Q$ is a multiplication factor to the residual term, thus they suffer from the same (normalization) problem as described above for UNIQUAC and $Z$. The best results for mixtures with water or alcohols require fitted (to VLE data) $R$ and $Q$ values, especially in the residual term. In the case of alcohols, often different $Q$ values are used in the residual and combinatorial terms. The same is true for one of the UNIFAC variants, the Dortmund modified UNIFAC, for which the interaction parameters as well as the $R$ and $Q$ values are fitted simultaneously to experimental mixture data. Naturally, the need to use fitted $R$ and $Q$ values is a limitation of the approach [19].

4. Molecular-dynamic calculations have shown that UNIQUAC often over-rectifies the deviations for random mixing because the magnitudes of the arguments of the Boltzmann factors are too large. Thus UNIQUAC is often not as accurate as NRTL for LLE calculations, and Wilson for VLE calculations [26].

5. For highly polar (hydrogen bonding) systems such as alcohol-alkanes LC models perform very well, where the interaction parameters were obtained from the azeotropic point. Lacking extensive experimental data, LC model parameters can be estimated from a single activity coefficient data. Such estimated parameters often yield good results over extensive concentrations. However, it is not always possible to describe satisfactorily phase equilibria with LC models over extensive temperature ranges [19].

**The following points summarize the conclusions for LC models [19]:**

1. For VLE of binary systems, Wilson and the other LC models perform as well as van Laar and Margules, and often better. For non-polar/slightly polar systems, there is little to gain by using the LC models over the random-mixing-based models.

2. For highly polar (hydrogen bonding) systems such as alcohol–alkanes LC models perform very well. Lacking extensive experimental data, LC model parameters can be estimated from a single point, e.g. from infinite dilution activity coefficient data. Such estimated parameters often yield good results over extensive concentrations.

3. NRTL can be successfully used for correlating both VLE and excess enthalpies for several mixtures. Excess enthalpies (heats of mixing) are usually difficult to describe satisfactorily with models having parameters based on phase equilibria (e.g. VLE) data because heats of mixing are often complex functions of temperature.

4. NRTL and UNIQUAC can successfully describe VLE and LLE with the same interaction parameters for several binary mixtures (not extremely non-ideal ones).

5. UNIQUAC is a very successful model, applicable to a variety of non-electrolyte liquid mixtures containing especially VLE of non-polar or polar and associating fluids such as hydrocarbons, nitriles, ketones, alcohols, aldehydes, acids, water, etc. Two examples are shown in fig. 3-5 with deviations from Raoult's law. Generally even for complex systems, it provides excellent correlation of binary VLE, including those having associating substances. In some cases, two parameters are not enough to represent high-quality data with good accuracy, but for most practical applications the representation is satisfactory. When organic acids are present, it is important to correct for the deviations from ideality also in the vapor phase.

7. UNIQUAC has been successfully used for hydrate formation calculations, in order to calculate activity coefficients of condensable components.

8. When Wilson equation is compared to UNIQUAC, the residual terms of the two models look similar, but the Wilson model is based on volume fractions, while the UNIQUAC model is based on surface area fractions. Both models have two interaction parameters that, have to be estimated from experimental phase equilibrium data. When the cross-interaction parameters are equal to those between like compounds or, when the exponential factors are equal to one in the two models, then the residual terms disappear. There are deviations from ideal solution behavior due to size and shape differences between the molecules, which are approximately accounted for via the combinatorial terms of the LC models. NRTL has no combinatorial term.

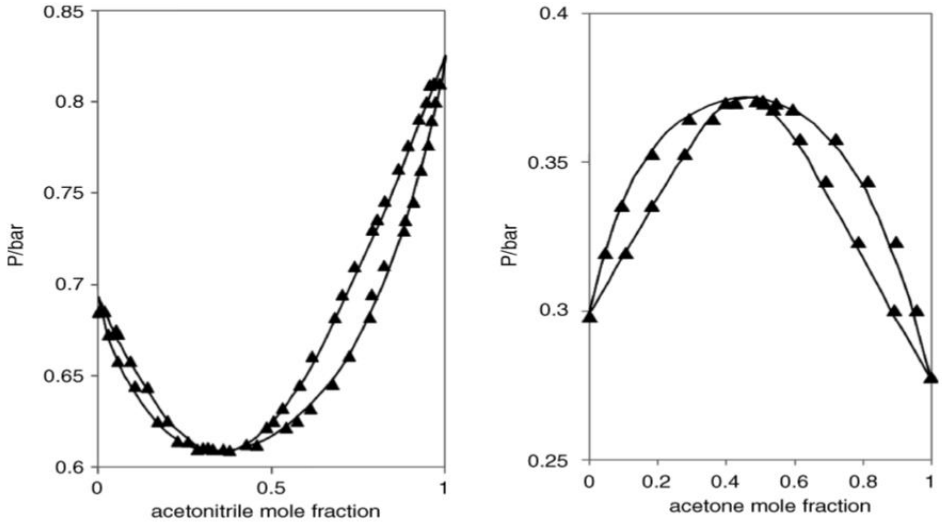


**Fig. 3-5. VLE correlation with UNIQUAC for one mixture with positive (right: acetonitrile(1)-benzene(2) at 45°C) and another one with negative deviations from Raoult's law (left: acetone(1)-chloroform(2) at 50°C) [19]**

All the LC models suffer from a number of deficiencies. The parameters used in the models come from regression of experimental data, which can be unreliable in some cases. Despite these limitations, the LC models are powerful tools, have found widespread use in engineering calculations, especially for low-pressure multicomponent VLE calculations using solely binary parameters estimated from binary mixture data and in addition their interaction parameters do possess a theoretical significance [19].

# 4. COSMOtherm & COSMO-RS Theory

COSMO-RS (COnductor-like Screening Model for Realistic Solvation) is an efficient variant of dielectric continuum solvation methods and a predictive method for thermodynamic equilibria of fluids and liquid mixtures that uses a statistical thermodynamic approach based on the results of QC calculations with the purpose of predicting chemical potentials in liquids. COSMO-RS combines an electrostatic theory of locally interacting molecular surface descriptors (which are available from QM calculations) with a statistical thermodynamics methodology. It processes the screening charge density on the surface of molecules to calculate the chemical potential of each species in solution. The resulting chemical potentials are the basis for other thermodynamic equilibrium properties. The main advantage of COSMO-RS is that it uses quantum chemically generated charge density surfaces to describe each molecule and its interactions with other molecules. It is therefore universally applicable without using group parameters or any system specific adjustments [27].

COSMOtherm is an implementation of an advanced variation of COSMO-RS, which computes thermophysical data of liquids based on COSMO-RS theory of interacting molecular surface charges computed by quantum chemical methods (QM). In this work, COSMOtherm is used to provide phase equilibriums (VLE, LLE), vapor pressure and activity coefficient data for the ABE fermentation solvents. The theory of this simulation will be presented according to the references [27-31].

COSMOtherm thermodynamic property computations only depend upon quantum chemical (QC) compound calculations, which are precalculated and stored in database. COSMOtherm uses the precalculated data from its database for its calculations to compute activity coefficients, solubility, phase diagrams, gas phase related data (Henry constant, $\Delta G$ solvation, vapor pressure, boiling point, flash point), ionic liquids properties, partition coefficients (logP/logD, liquid extraction, flatsurf, interfacial tension, COSMOmic (an additional module to calculate properties of molecules in micelles)), pure compound data (density, viscosity, pKa, ionic liquids properties, similarity, critical properties) and reaction constants. COSMOtherm also calculates the excess enthalpies along with the phase equilibrium data, which are experimentally hard to measure [27].

The 3D screening charge distribution on the surface of a molecule $i$ can be used to qualitatively describe the molecule. Polarity, hydrogen bonding and liphophilicity or hydrophilicity can be visualised on the molecular surface. The surface screening charges can be converted into a distribution function, the $\sigma$-profile $p^i(\sigma)$, which gives the relative amount of surface with polarity $\sigma$ on the surface of the molecule [27]. The surface of the molecule shaped cavity is called molecular surface, and the volume of the molecule shaped cavity is called molecular volume.

In fig. 4-1, the molecular surface of water coded by the polarization charge density, $\sigma$, is to be seen. The strongly negative polar regions of the electron ion-pairs of the oxygen atom are red (indicating a strongly positive screening charge $\sigma$) and hence the strongly positively polar hydrogen atoms are shown with deep blue (strongly negative $\sigma$) and green areas denote nonpolar surface.

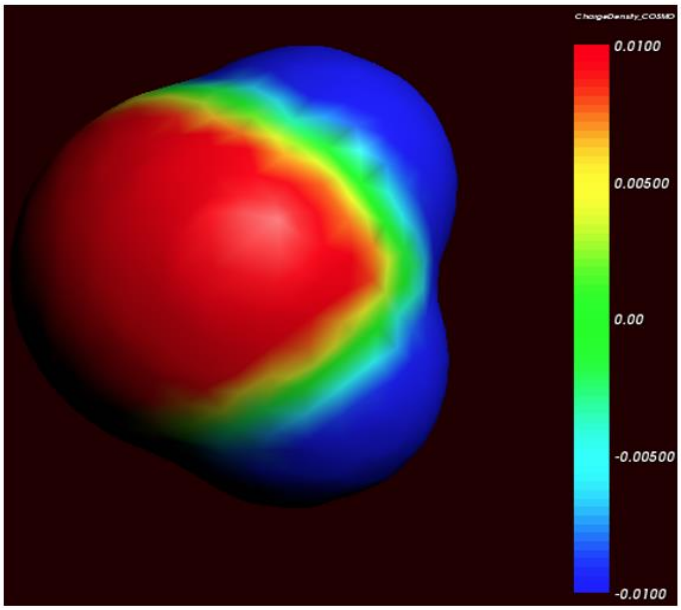


**Fig. 4-1. COSMO charge density on the COSMO surface of water [31]**

In COSMO calculations, the solute molecules are calculated in a virtual conductor environment. The solute molecule induces a $\sigma$ on the molecular surface. These charges act back on the solute and generate a polarized electron density. During the QC self-consistency algorithm, the solute molecule is converged to its energetically optimal state in a conductor with respect to electron density. The interactions of molecular surfaces can be described fully by $\sigma$ alone, i.e., by just one descriptor for each molecular surface segment. Since the interaction energies of the surfaces depend only on the local polarization charge-densities, only the net composition of the surface of a molecule $i$ with respect to $\sigma$ is of importance for the statistical thermodynamics of local pairwise surface interactions [27].

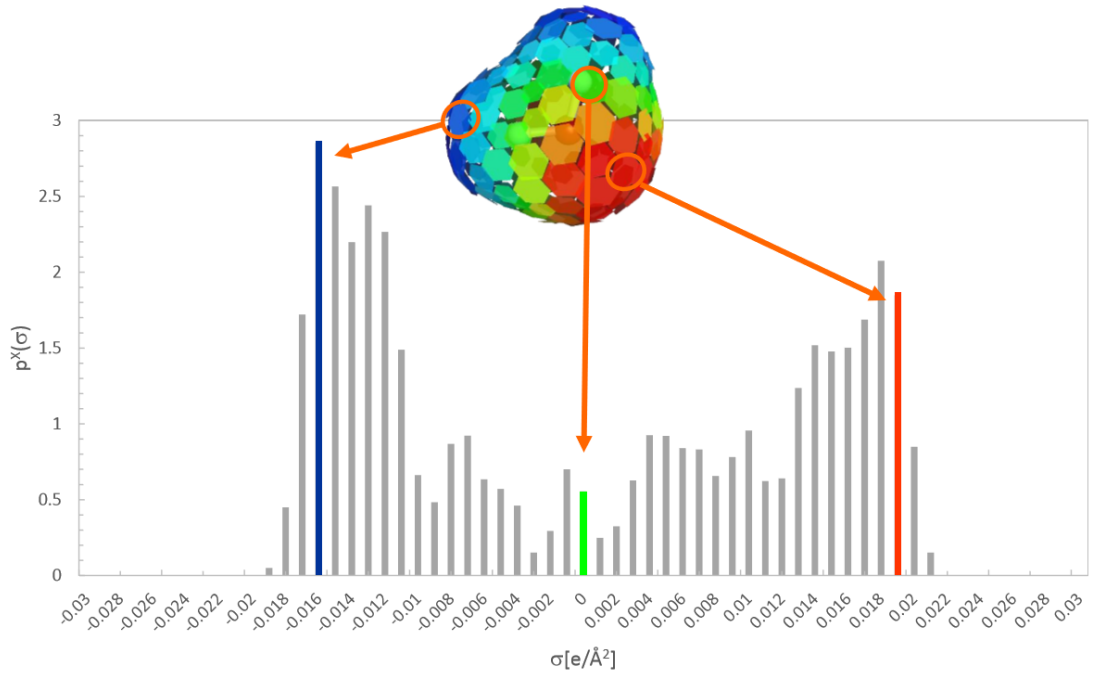


**Fig. 4-2. $\sigma$-profile of water, a histogram (distribution function) of charged surface segments of a molecule [57]**

COSMOtherm reads the compound information from the stored QM calculations and transforms the surface polarity into a polarization charge distribution, called $\sigma$-profile. Each molecule and mixture can be represented by distribution function $p(\sigma)$, the so-called $\sigma$-profile. $\sigma$-profiles for conformers of one compound may differ depending on the molecular structure, conformers have to be calculated individually. If COSMO files of several conformers exist for a compound, they will be combined into a single compound. The $\sigma$-profile of a mixture is the weighted sum of the profiles of all its components. Using the interaction energy $E_{int}(\sigma, \sigma')$ and the $\sigma$-profile of the solvent $p(\sigma')$, the chemical potential $\mu_S(\sigma)$ of a surface piece with polarization charge $\sigma$ is determined [27, 28].

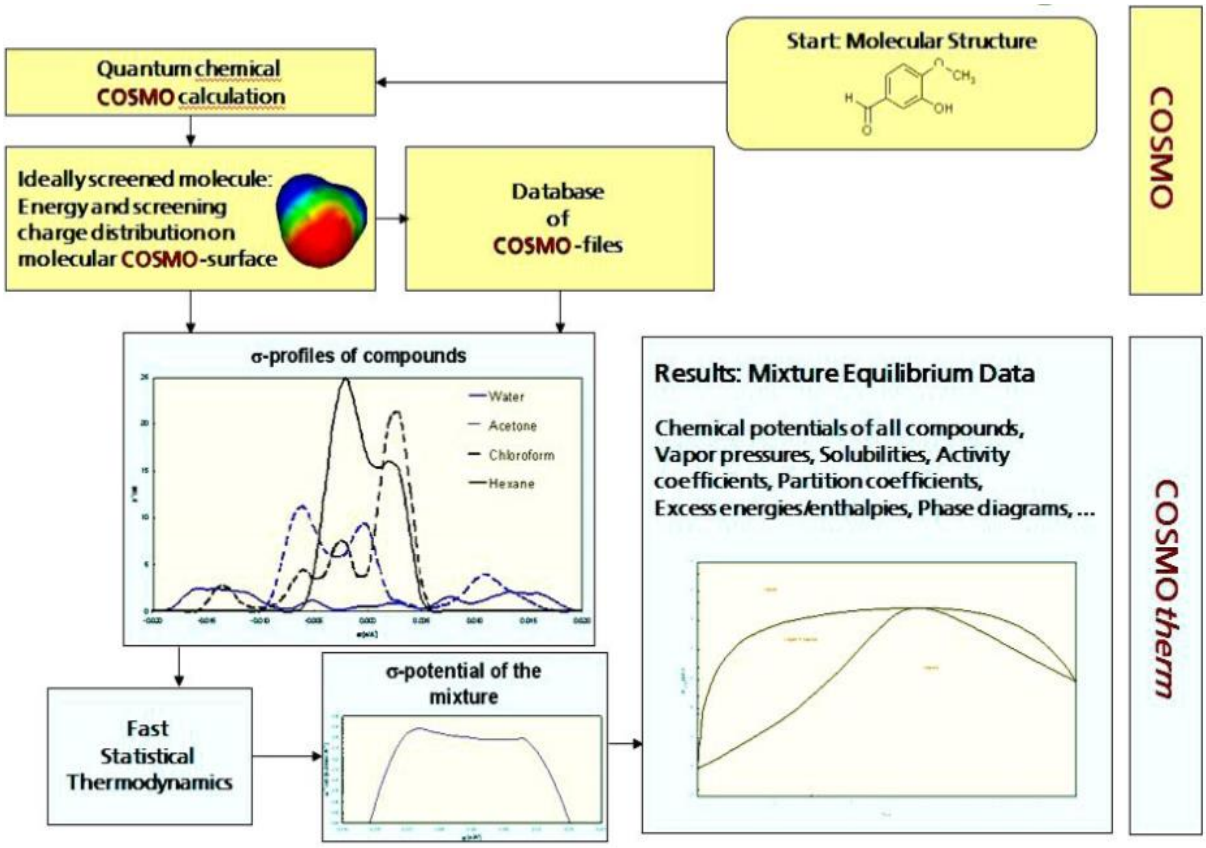


**Fig. 4-3. Flow chart of a COSMO calculation**

In fig. 4-3, the two steps of COSMO calculation are shown [27];

1. COSMO/DFT (Density functional theory); QM calculations are performed for each pure component $i$, a molecule of species $i$ is embedded in a virtual conductor. Through DFT calculations, $\sigma$ for molecule $i$ is calculated and the molecule is iteratively converged to its energetically optimal COSMO state. The resulting pure component $\sigma$-surface is stored in the COSMO file and thus re-useable for calculating mixture properties.

2. COSMOtherm; The statistical thermodynamics of the molecular interactions; $\sigma$ of the COSMO calculation is used to extent the model towards “Real Solvents” (COSMO-RS). This polarization charge density is used for the quantification of the interaction energy of pairs of surface segments. As most important molecular interaction modes, electrostatics and hydrogen bonding is taken into account in this way. Based on the $\sigma$-surface, a distribution function ($\sigma$-profile) is used to calculate the chemical potential ($\sigma$-potential) of a surface

segment. From this $\sigma$-potential, thermodynamic properties and phase equilibrium data are computed.

**COSMO-RS Theory:**

The polarization charge density of the COSMO calculation (also called screening charge density), which is a good local descriptor of the molecular surface polarity, is used to extent to model towards “Real Solvents” (COSMO-RS). The 3D polarization charge density distribution on the surface of each molecule $i$ is converted into a distribution function, the so-called $\sigma$-profile $p^i(\sigma)$, which gives the relative amount of surface with polarity $\sigma$ on the surface of the molecule. The $\sigma$-profile of the entire solvent of interest S, which might be a mixture of several compounds, $p_s(\sigma)$ can be built by adding the $p^i(\sigma)$ of the components weighted by their mole fraction $x_i$ in the mixture [27].

$$p_s(\sigma) = \sum_{i \epsilon S} x_i \, p^i(\sigma) \tag{4.1}$$

In addition to the liquid phase terms a chemical potential estimate for the ideal gas phase enables the prediction of vapor pressure, free energy of solvation and related quantities [28]. The chemical potential in solution can be calculated from the interaction energies. The interaction energies are defined in terms of the surface charge densities $\sigma$ and $\sigma$’ of the respective surface segments [27]. In analogy to activity coefficient models such as NRTL, UNIQUAC or UNIFAC, the final chemical potential can be split into a combinatorial and a residual (non-ideal) contribution, the residual term $\mu_s$ and combinatorial term, $\mu^i_{c,s}$ accounting for size and shape differences of the molecules in the system.

The interaction energy $E_{int}$ is the sum of three different contributions; electrostatic interaction $E_{misfit}$, hydrogen bonding energy $E_{hb}$ and van der Waals energy $E_{vdw}$.

$$E_{int} = E_{misfit} + E_{hb} + E_{vdw} \tag{4.2}$$

The most important molecular interaction energy modes, $E_{misfit}$ and $E_{hb}$ are described as functions of the polarization charges of two interacting surface segments $\sigma$ and $\sigma'$ or $\sigma_{acceptor}$ and $\sigma_{donor}$, if the segments are located on a hydrogen bond donor or acceptor atom [27]. Electrostatic energy arises from the misfit of screening charge densities $\sigma$ and $\sigma'$, as illustrated in fig. 4-4, where the grey lines indicate the residual thin film of conductor separating cavities.

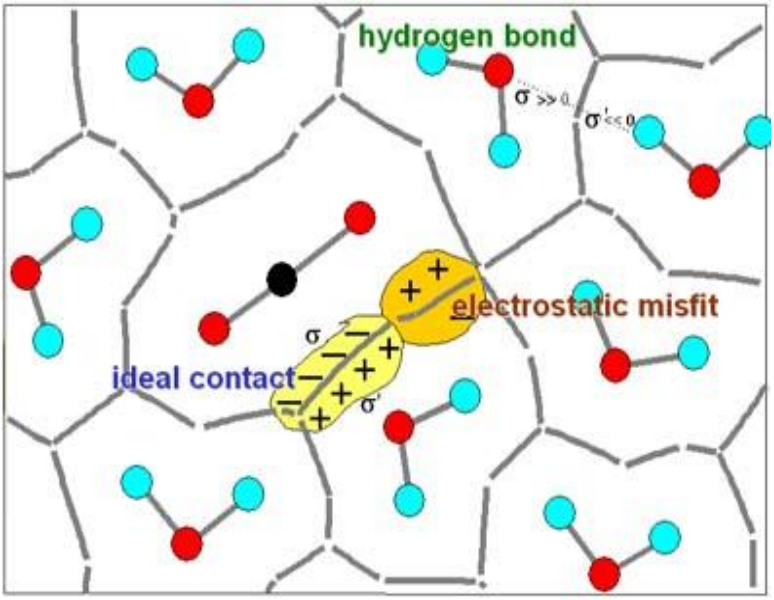


**Fig. 4-4. Schematic picture of an ensemble of molecules with COSMO cavities [29]**

The term $E_{misfit}$ has been labeled “misfit” energy, because it results from the mismatch of the charged pieces in contact. It represents the Coulomb interaction relative to the state in a perfect conductor. A molecule in a perfect conductor (COSMO state) is perfectly shielded electronically; each charge on the molecular surface is shielded by a charge of the same size but of opposite sign. If the conductor is replaced by surface pieces of contacting molecules the screening of the surface will not be perfect anymore [28].

$$E_{misfit}\,(\sigma, \sigma') \;=\; a_{eff}\;\frac{\alpha'}{2}\,(\sigma \;+\; \sigma')^2 \tag{4.3}$$

where $\alpha'$ an adjustable interaction parameter, $a_{eff}$ the effective contact area and $\sigma$ and $\sigma'$ refer to the screening charge densities of the two surface patches in contact [28].

$$E_{hb} \;=\; a_{eff}\; c_{hb}\; min\,(0;\; min\,(0;\; \sigma_{donor} \;+\; \sigma_{hb})\; max\,(0;\; \sigma_{acceptor} - \sigma_{hb})) \tag{4.4}$$

In the $E_{hb}$ expression $\sigma_{acceptor}$ and $\sigma_{donor}$ are the screening charge densities of the hydrogen bond acceptor and donor respectively. The hydrogen bonding threshold $\sigma_{hb}$ and the prefactor (hydrogen bond strength) $c_{hb}$ are adjustable parameters. The max[] and min[] construction ensures that the screening charge densities of the acceptor and donor exceeds the threshold for hydrogen bonding [28].

The less specific van der Waals ($E_{vdw}$) interactions are taken into account in a slightly more approximate way,

$$E_{vdW} \;=\; a_{eff}\;(\tau_{vdw} \;+\; \tau'_{vdw}) \tag{4.5}$$

where $\tau_{vdW}$ is the element specific $vdW$ interaction parameter [27].

Eqs. (4.3-4.5) contain five adjustable parameters, $\alpha'$, $a_{eff}$, $c_{hb}$, $\sigma_{hb}$, and $\tau_{vdW}$. In order to take the temperature dependancy of $E_{hb}$ and $E_{vdW}$ into account, temperature dependent factors are applied, each with one adjustable parameter [27]. Although the use of quantum chemistry reduces the need for adjustable parameters, some fitting to experimental data is inevitable. All parameters either are general or element specific, which is distinctive feature of COSMO-RS as compared to group contribution methods like UNIFAC [28].

The transition from microscopic molecular surface charge interactions to macroscopic thermodynamic properties of mixtures is possible with a statistical thermodynamic procedure. The molecular interactions in the solvent are fully described by $p_S(\sigma)$ to find a certain polarity inside the solvent, and the chemical potential of the surface segments can be calculated solving a coupled set of non-linear equations [27].

$$\mu_S(\sigma) = -\frac{RT}{a_{eff}} ln \left[\int p_s(\sigma') exp\left(\frac{a_{eff}}{RT}\left(\mu_s(\sigma') - E_{misfit}(\sigma,\sigma') - E_{hb}(\sigma,\sigma')\right)\right) d\sigma'\right] \quad (4.6)$$

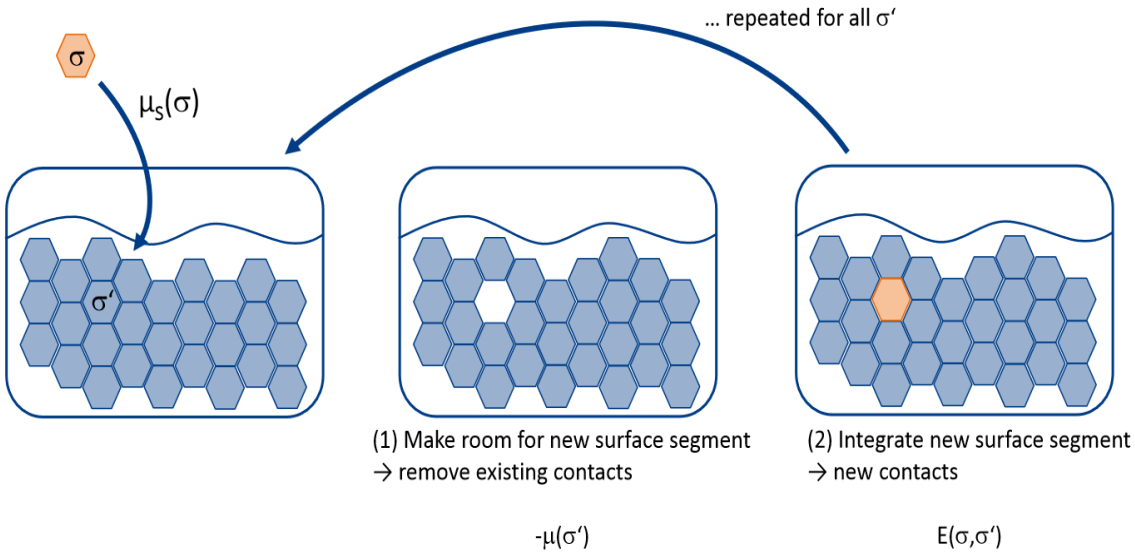


**Fig. 4-5. Statistical thermodynamics [57]**

The $\sigma$-potential $\mu_s(\sigma)$ is a measure for the affinity of the system S (solvent) to a surface of polarity $\sigma$.

The COSMO-RS dispersion energy of a solute depends on an element ($i$) specific prefactor $\gamma$ and the amount of exposed surface $A$ of this element. It is not part of the interaction energy but enters the chemical potential directly [28]. Dispersion (van der Waals energy) is defined as,

$$\mu_{disp} = \sum_i \gamma_i A_i \quad (4.7)$$

The $vdW$ energy, which does not appear in eq. (4.6), is added to the reference energy in solution (energy of the COSMO calculation). The chemical potential of compound $i$ in the system $S$ can be calculated by integration of $\mu_S(\sigma)$ over the surface of the compound,

$$\mu_s^i = \mu_{c,s}^i + \int p^i(\sigma).\mu_s(\sigma)\, d\sigma \quad (4.8)$$

To take into account size and shape differences of the molecules in the system an additional combinatorial term, $\mu_{c,s}^i$, which depends on the area and volume of all compounds in the mixture and three adjustable parameters is added [28]. The chemical potential can be used to calculate a wide variety of thermodynamic properties, e.g. the activity coefficient,

$$\gamma_s^i = exp\left\{\frac{\mu_s^i - \mu_i^i}{RT}\right\} \quad (4.9)$$

where $\mu_s^i$ is the chemical potential of compound $i$ in the solvent $S$, and $\mu_i^i$ the chemical potential of the pure compound $i$.

## From chemical potential to properties by COSMOtherm:

By calculating the chemical potentials in various phases, the required properties can be derived, some of which are summarized in table 4-1.

| **PROPERTY** | | $\boldsymbol{\mu_1}$ | $\boldsymbol{\mu_2}$ |
|---|---|---|---|
| ACTIVITY COEFFICIENT | $\gamma_S^i = exp\{(\mu_S^i - \mu_X^i)/RT\}$ | Infinite dilution | Pure compound |
| VAPOR PRESSURE | $p_{S,vap}^i = exp\{(\mu_{gas}^i - \mu_S^i)/RT\}$ | Gas phase | Pure bulk compound |
| LIQUID-LIQUID PHASE EQUILIBRIUM | $\mu_S^{x_i^1} + RTlnx_i^1 = \mu_S^{x_i^2} + RTlnx_i^2$ | Phase 1 | Phase 2 |

**Table 4-1. Properties calculated with chemical potential [57]**

COSMOtherm gamma option computes the chemical potentials of all pure compounds $i$ and subsequently the chemical potentials at infinite dilution in a given solvent compound $S$ by default as explained in COSMO-RS Theory [27].

$$\gamma_S^i = exp\left[\frac{\mu_S^i - \mu_X^i}{RT}\right] \quad (4.10)$$

The pvap option of COSMOtherm allows for the calculation of vapor pressures over a given temperature range (and fixed mixture composition) [30]. The energy of the gas phase $E_{int}$ is required for the calculation of the chemical potential in the gas phase. $E_{int}$ can be taken from a gas phase QC calculation or empirically estimated by COSMOtherm [27]. For a given pure compound or mixture composition $S$, the total vapor pressure of the system is computed from the partial vapor pressures of each compound $i$.

$$p_{S,vap}^i = \exp[\frac{\mu_{gas}^i - \mu_S^i}{RT}] \quad (4.11)$$

At each temperature, for each compound or mixture composition $S$, the partial vapor pressures $p^i_{S,vap}$, the chemical potential of the compound in the gas phase $\mu^i_{gas}$, and the enthalpy of vaporization $\Delta H^i_{vap}$ can be found in COSMOtherm output file [30].

If three or more temperature points are calculated in a vapor pressure curve, the total vapor pressure additionally will be fitted to Antoine's vapor pressure equation, eq. (3.13). If tabulated experimental vapor pressure data are available from a .vap file, they will be printed to the last column of the table file for comparison. Optional: Wagner equation, eq. (3.14). Wagner equation coefficients for many substances are tabulated in databases [27].

COSMOtherm allows the computation of phase diagrams (VLE, LLE) of binary, ternary or higher dimensional (multinary) mixtures. For the phase equilibrium calculations, at each point the following properties will be calculated; the excess properties $H^E$ and $G^E$, the chemical potentials $\mu_i + RTln(x_i)$, the activity coefficient $\gamma_i$, the total vapor pressure of the system $p^{(tot)}$ and the concentrations of the compounds in the gas phase $y_i$ [27].

The total pressures used in the computation of a phase diagram for a given temperature are obtained from,

$$p^{(tot)} = \sum_i p^i_{S,vap} x_i \gamma_i \tag{4.12}$$

Vapor mole fractions $y_i$ for an ideal gas are obtained from the ratio of $p^{(tot)}$ and a partial vapor pressure $p_i$,

$$p_i = p^i_{s,vap} x_i \gamma_i \tag{4.13}$$

$$y_i = \frac{p^i_{s,vap} x_i \gamma_i}{p^{(tot)}} \tag{4.14}$$

It is possible to calculate phase diagrams isobaric or isothermal. In an isobaric calculation, COSMOtherm will compute the mixture properties and vapor pressure for each concentration at different starting temperatures and iteratively converge to the temperature corresponding to the given pressure. The concentrations of VLE default grid are defined in mole fractions, which are unevenly spaced. Thus being uneven the default VLE grid tries to cover the phase space of the computed properties as comprehensive and as effective as possible. When the "search LLE point" suboptions are used, the default grid values are modified automatically. The default grid can be also modified with the 'change concentration grid' suboptions in the VLE/LLE panel. The concentration steps in the grid become smaller if a compound approaches infinite dilution. This specific grid accounts for the fact that properties such as activity coefficients or concentrations in the vapor phase $y_i$ typically show their strongest changes at low $x_i$ concentrations. Thus, being uneven the default grid tries to cover the phase space of the compound properties as comprehensive and effective as possible. When the "search LLE point" option is used, the default grid modifies the values automatically in order to locate LLE points more accurately [27].

The LLE properties are calculated from the liquid phase equilibrium condition eq. (4.15), where indices $x''$ and $x'$ denote the two liquid phases mole fractions, $\gamma_i'$ and $\gamma_i''$ activity coefficient of the two liquid phases and $i$ denotes the compound,

$$x_i' \gamma_i' = x_i'' \gamma_i'' \quad (4.15)$$

LLE renormalization is based upon the LLE miscibility gap width w:

$$w_R = max\left[0; w_z - e^{(6.16-13.095 w_z - e^{(145.26-260 w_z)})}\right] \quad (4.15)$$

In COSMOtherm “renormalized LLE” suboption can be used for the symmetrisation of the values and renormalization of the LLE phase diagram. The renormalized LLE loop is considerably closer to the measured one [30].

This description has the advantage that it depends only on the width of symmetrized miscibility gap $w_z = 1 - 2z(\tilde{x}_1)$. I.e. no data of the actual critical point has to be known in advance. Not even the temperature is included. Moreover, the parameters of the renormalization are fixed, as they result from a simple exponential fit of the symmetrized miscibility gap width of COSMO-RS to the one of the cubic lattice Ising model. This implies that eq. (4.15) can be applied not only to COSMOtherm LLE predictions, but to any LLE($T$) prediction computed from a “mean-field” activity coefficient or $G^E$-model. Thus the Ising model derived renormalization model, eq. (4.14) is completely general and does not include any adjustable parameters. The only adjustable parameter that enters the model indirectly, is the symmetrisation exponent of the LLE($T$) curves, which is required to scale the experimental (non-symmetric) Ising model [30].

**Limitations of COSMOtherm [27]:**

Due to the approximations made within COSMO-RS and the limits of quantum chemistry, predictions are not perfect. The standard error resulting from the COSMOtherm validation applies to a broad range of organic chemistry, but some compound classes are generally described better than others. Some of the limitations to property prediction with COSMOtherm come from COSMO-RS theory. In COSMOtherm however these limitations are not as pronounced as in less advanced implementations of COSMO-RS.

- COSMO-RS is an equilibrium theory. Non-equilibrium properties such as viscosity or excess volume can’t be predicted directly.
- COSMO-RS is a theory of incompressible liquids. Systems which cannot be treated with this approximation have to be treated with additional information. The gas phase is treated as ideal for the version used in this work (COSMOthermX17) but COSMOthermX18 allows also for non-ideal gases. COSMO-RS cannot predict fugacity.
- After the QM calculations are done, COSMO-RS neglects the 3D geometry (except in extensions as Flatsurf and COSMOmic). Larger systems with internal cavities are therefore beyond COSMO-RS. Effects like cooperative binding cannot be taken into account.
- Long range Coulomb interaction is not described by COSMO-RS. While this is not a problem for $pK_A$ prediction or ionic liquids, treatment of diluted electrolytes requires an additional Debye-Hückel contribution. While salt-in or salt-out effects can be predicted to a certain extent, activity coefficients of small ions in water are beyond the theory.
- The properties of strong (hydrogen) bonds (e.g. formed by $OH^-$ or atomic metal-ions in solvent water) are not fully taken into account. This may lead to problems in systems that

are near the Brönsted-limit of high ionic strength, e.g. resulting in physically wrong behavior such as “salting in”.

- Also systems near or beyond critical point cannot be treated well.

# 5. Simulations

In chapter 4, the theory of the simulation program COSMOtherm has been introduced as it is the main part of this work. COSMOtherm and Aspen Plus simulations are used for the calculations of activity coefficients, vapor pressures and phase equilibria (VLE, LLE) of the ABE fermentation solvents in this work. In addition to the calculations with COSMOtherm and, Aspen Plus, literature data will serve for the comparison of the results. In this chapter the simulation steps for the related calculations to this work with COSMOtherm and Aspen Plus will be presented.

## 5.1. COSMOtherm Calculations

The simulation program COSMOthermX17, version C30_1705 is used for vapor pressure, activity coefficient and phase equilibrium (VLE, LLE) calculation of the ABE fermentation solvents (1-butanol, acetone, ethanol, water and their mixtures). Every calculation is done with the pre-calculated $\sigma$-profiles of the conformers of acetone, 1-butanol, ethanol and water molecule from the COSMO Database (DB) using different QC levels.

Fig. 5-1 shows properties area of COSMOtherm, where the required calculation can be selected.

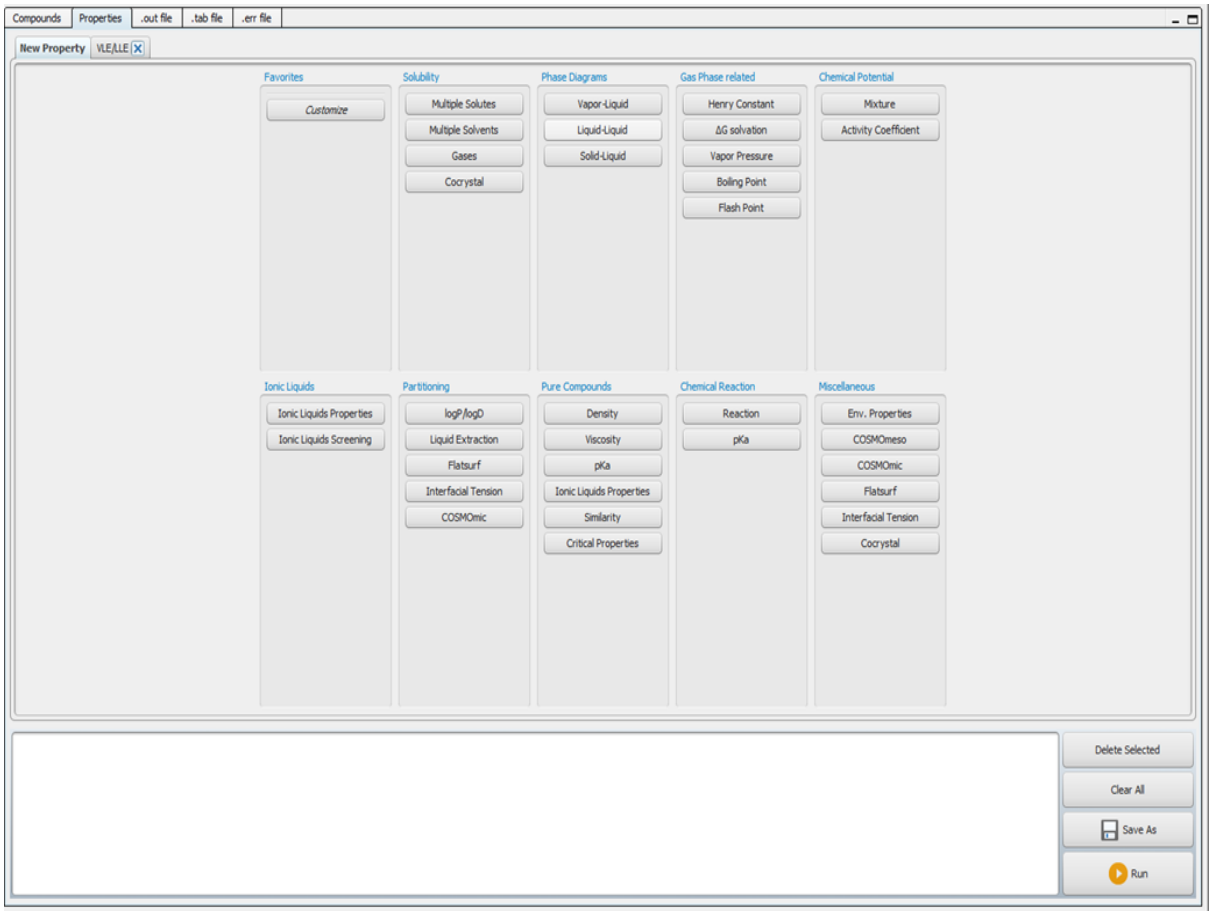


**Fig. 5-1. COSMOtherm properties area**

In general, for each calculation a QC level (SVP, DMOL3, TZVPD-FINE), then the required molecules and its conformers in the DB of this QC level are selected in the compounds tab. Clicking 'get selection' gives a list of chosen molecules and their conformers. After choosing compounds of interest, the required calculation type is selected in 'properties' and 'new property' tab. Selected calculation parameters are specified in the following step (temperature, pressure, composition etc.) and the so called 'job' is saved and run. More than one job can be specified and added in the calculation list by saving each job in a COMOtherm input file. When the calculation is finished the results window appears with the tabs showing the graphics and tables of calculated points. Calculations with COSMOtherm are very fast for more simple jobs like vapor pressure and activity coefficient calculations of binary systems but in the case of phase equilibrium calculations of ternary or quaternary systems calculations they can take hours depending on the computer power. Results are saved and diagrams are displayed in the results chapter of this thesis.

**Conformers:**

COSMO includes the conformers of the molecules to define $\sigma$. Molecules often can adopt more than one conformation. For COSMO-RS, only conformers with different $\sigma$-profiles are relevant. For each of these conformers, an individual COSMO file is required for the compound input. In the conformer options individual conformers can be set. Compounds for which options are to be set can be selected from the menu. If compounds are selected from the databases and the checkbox in the Use Conf. column is checked, all existing conformer COSMO files will be selected automatically. If the Activate Conformer Treatment checkbox in the compound section is checked, the conformers will be weighted internally by COSMOtherm using their COSMO energies and their chemical potentials [27].

**Parameterization of COSMOtherm:**

In principle, COSMO files can be generated on almost any QC level. If COSMO data is not available in the databases, it is possible to perform individual QC calculations. The quality, accuracy and systematic errors of the electrostatics resulting from the underlying quantum chemical COSMO calculations depend on the QC method (e.g. DFT-functional) as well as on the basis set (based on different QC level). The choice of the appropriate QC method and basis set level generally depends upon the required quality and the later application of the predictions. Based on quantum chemical COSMO calculations, the best quality of the COSMOtherm prediction can be achieved with TZVPD parameterization. TZVP is short for triple zeta valence polarized set. TZVPD or the TZVPD-FINE levels are based on molecular structures retrieved from DFT calculations, but the TZVPD-FINE level involves additional QM energy calculations with the TZVPD basis set. A similar quality can be reached with DMOL3. Depending on the number of compounds involved, the computer power available, and the accuracy required, other levels can be better suited for other purposes, e.g. SVP level [30]. More of this topic is found in literature.

### 5.1.1. Vapor Pressure Calculation

COSMO-RS allows for the estimation of pure compound vapor pressures. The energy of the gas phase $E_{gas}^{i}$ is required for the calculation of the chemical potential in the gas phase, $\mu_{gas}^{i}$.

$E_{gas}^{i}$ can be taken from a gas phase QC calculation or empirically estimated by COSMOtherm [27].

The vapor pressure option '*pvap*' enables the computation of vapor pressures for a given temperature or a temperature range. By default, the vapor pressure will be calculated at 10 temperature values (evenly spaced between $T_1$ and $T_2$). The number of temperature points to be calculated in the temperature range can be changed. Alternatively, the temperature points in the interval of $T_1$ and $T_2$ can be determined by a given temperature [27].

COSMOtherm also uses vapor pressure equations such as Antoine and Wagner equations in addition to its QC calculations. The vapor pressure equation coefficients required for these equations either can be given directly in the compound input section of the input file or they can be read from a vapor pressure/property file (vap-file) [30].

Calculations of the pure compound vapor pressures are done via the 'pvap' option of COSMOtherm. First compounds of interest (1-Butanol, Acetone, Ethanol, Water) in DB of TZVPD-FINE QC level and then the 'vapor pressure' in the properties workplace window are selected. The required component for the calculation is marked as pure and the temperature range is set. The 'job' is added to the job queuing section, saved in the COSMOtherm input file and run. Calculation steps are repeated for every component of interest. When the calculations are finished, results window appears with the results tabulated $pvap$ vs. $T$ with Wagner equation calculations in the last column of the results table.

### 5.1.2. Activity Coefficient Calculation

The activity coefficients of different compounds in the selected solvent or solvent mixture can be calculated in the activity coefficient panel of COSMOtherm. For the calculation of the activity coefficient at infinite dilution, the mole fraction of the compound of interest has to be set to zero in the composition of the solution. It is also possible to calculate the activity coefficients at a given finite concentration [27].

For the activity coefficient calculations in this work the compounds of interest (1-butanol, acetone, ethanol, water) are selected from the DB of TZVPD-FINE, SVP and DMOL3 QC levels. "Activity coefficient" is selected in properties panel and the temperature and composition are set in the input preparation panel. The calculation job is repeated for each compound choosing water as a solvent. For the activity coefficient calculations at infinite dilution the mole fraction of the compound is set to zero, while the mole fraction of water is set to 1.0 in the composition of the solution. The selection is transferred to the job queuing section by the "add button" and run.

### 5.1.3. Phase Equilibrium Calculations

COSMOtherm allows for the computation of phase diagrams (VLE and LLE) of binary, ternary or multinary mixtures. In COSMOtherm, these options are accessible from the vapor-liquid and liquid-liquid buttons in the property selection. It is possible to calculate phase diagrams at fixed pressure (isobaric) or at fixed temperature (isothermal). The pressure or temperature has to be given in the input. COSMOtherm automatically computes a list of concentrations covering the whole range of mole fractions of the binary, ternary or multinary mixture, calculating the excess properties $H^E$ and $G^E$, the chemical potentials $\mu_i + RTln(x_i)$, the activity coefficient $\gamma_i$,

the total vapor pressure of the system $p^{(tot)}$ and the concentrations of the compounds in the gas phase $y_i$ at each point as well as other useful information like azeotropic points for a given temperature. The binary and ternary options allow for the automatic computation of phase diagrams of two- and three-component mixtures, respectively. Phase diagrams of higher dimensionality can be computed with the multinary phase diagram option. If one of the binary, ternary, or multinary options is applied, no mole ($x = \{\}$), or mass ($c = \{\}$) fraction input is required. Instead, the program automatically computes a list of concentrations covering the whole range of possible mole fractions of the binary or ternary mixture. [27].

The concentrations of the VLE default grid are defined in mole fractions, which are unevenly spaced: the concentration steps in the grid are becoming smaller if a compound approaches infinite dilution. Thus being uneven the default VLE grid tries to cover the phase space of the computed properties as comprehensive and as effective as possible. When the “search LLE point” suboption is used, the default values are modified automatically according to any miscibility gap that has been detected.

Fig. 5-2 shows the definition window of COSMOtherm for the equilibrium calculations, where the system and its composition can be defined, temperature or pressure can be set and suboptions “search LLE point” and “compute renormalized LLE” can be used as well as the number of points to be calculated in i.e. mole fraction can be selected.

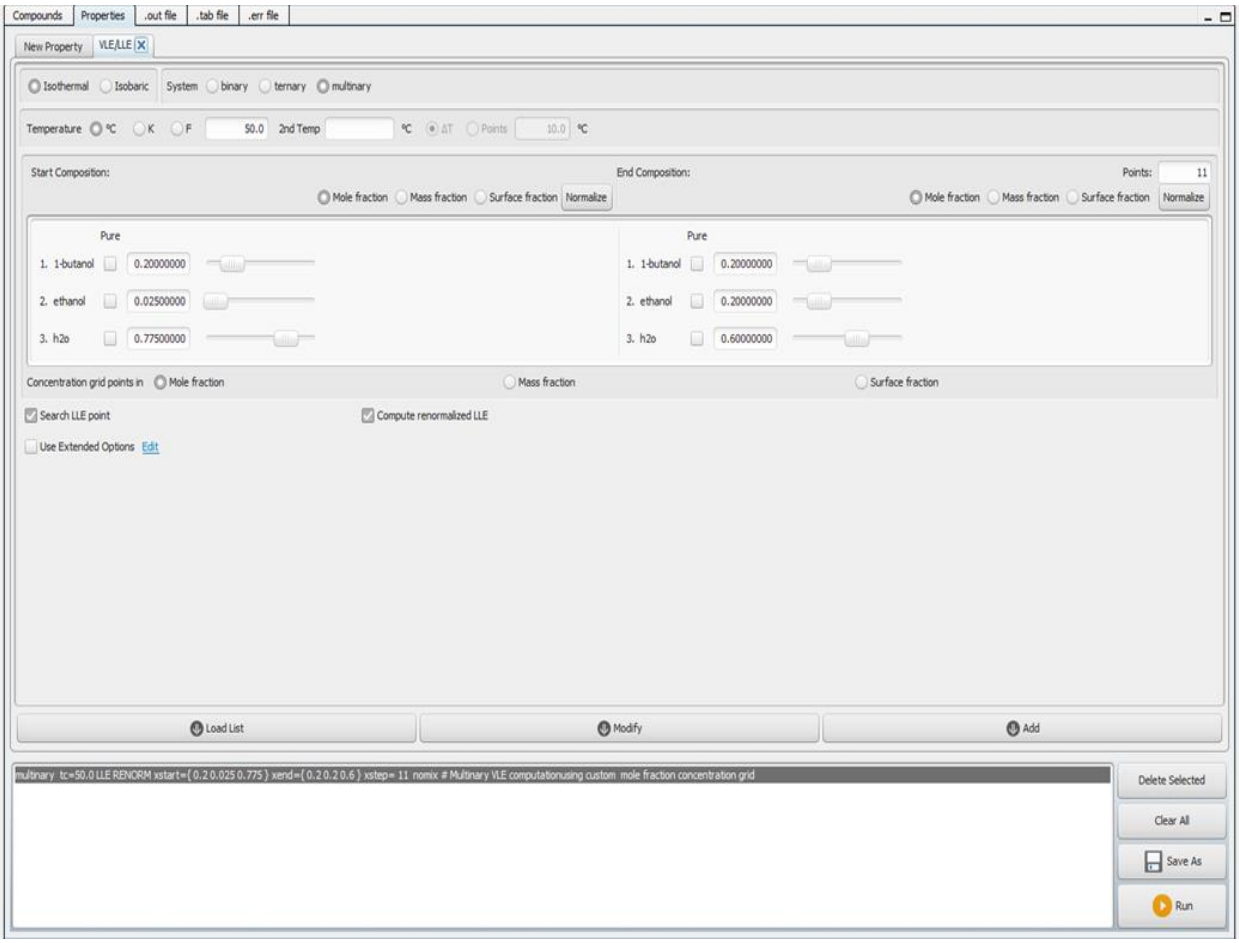


**Fig. 5-2. COSMOtherm properties area for defining phase equilibrium calculations**

**VLE Calculations of Binary Mixture 1-Butanol-Water:**

For binary phase diagram calculations, options for automatic post-processing are provided, such as fitting of the computed activity coefficients to activity coefficient models or azeotrope detection [27].

VLE calculations of binary system “1-butanol-water” in this work are done with three of the COSMOtherm QC levels TZVPD-FINE, SVP and DMOL3. After selecting components from one of these QC levels the vapor-liquid option in properties tab is selected and set to isobaric conditions defining required pressures for the calculations. Calculations are done with and without using “search LLE point” suboption. The jobs are added to the job queuing section for each QC level, pressure and run.

**LLE Calculations of Binary, Ternary and Multinary Mixtures:**

COSMOtherm offers the possibility to detect miscibility gaps for binary, ternary, and multinary mixtures, i.e. points of liquid-liquid equilibrium phase separation by activating ‘search LLE’ option. If this command is given in the same line as the binary, ternary, or multinary command, COSMOtherm will search the computed mixtures for possible points of separation and if found, writes them to the COSMOtherm output and table file. In case of a binary mixture, the binodal LLE point and the spinodal LLE point, that distinguishes the unstable region of the liquid mixture from the metastable region, will be printed in the table file. In ternary and multinary mixtures it is necessary to define a starting composition and end composition. The number of points to be calculated can also be specified. A given number of points along a straight line between these compositions is then used as starting point for the tie point search. If the composition is not inside the miscibility gap, no points will be found. Optionally, COSMOtherm can do a renormalization of LLE points accounting for thermodynamic fluctuations in the liquid mixture, if the “compute renormalized LLE” checkbox is checked [27].

For the LLE calculations of binary systems, TZVPD-FINE QC level is used. 1-Butanol and water are selected from this QC level and the calculation is specified choosing liquid-liquid in phase diagrams column. The temperatures are set and search LLE option is selected. The selection is transferred to the job queuing section by “add button” and run. Calculation is repeated also with compute renormalized LLE option.

LLE calculations of ternary and multinary systems are also done with TZVPD-FINE QC level with compounds of interest (1-butanol, acetone, ethanol, water) defining the mixture phase by entering start and end compositions for each compound in the mixture. Temperatures are defined at isothermal conditions. “Search LLE point” suboption is selected. Calculations are done with and without “compute renormalized LLE” suboption at different temperatures.

Fig. 5-3 shows results window of COSMOtherm with a ternary diagram for a liquid-liquid equilibrium calculation. A smaller ternary diagram is added to underline the binodal LLE curve/equilibrium line and indicate the line between start and end mixture composition. In COSMOtherm results window calculated points can be seen easily.

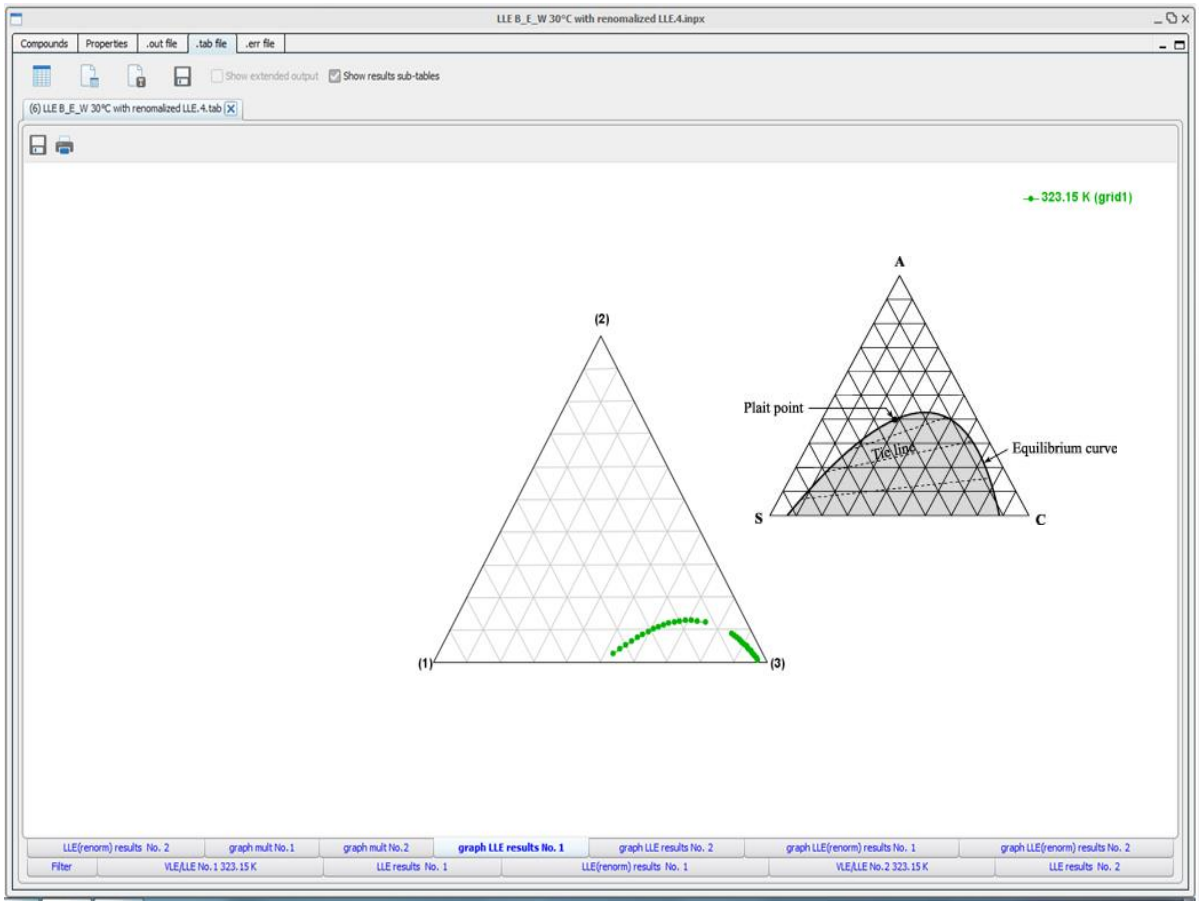


**Fig. 5-3. COSMOtherm ternary diagram in a result table for liquid-liquid equilibrium calculation**

## 5.2. Aspen Plus Calculations

Aspen Plus is a simulation software package, where Aspen is short for Advanced System for Process Engineering. Aspen Plus allows predicting the behavior of a process using basic engineering relationships such as mass and energy balances, phase and chemical equilibrium, and reaction kinetics. Aspen Plus uses mathematical models to predict the performance of the process. Given reliable themodynamic data, realistic operating conditions, and the rigorous Aspen Plus equipment models, actual plant behavior can be simulated. Aspen Plus helps design better plants and increases profitability in existing plants [32, 33].

Within Aspen Plus specifications such as flowsheet configuration, operating conditions, feed compositions can be changed interactively to run new cases and analyse alternatives [32]. In Aspen Plus, the calculation methods for thermodynamic properties are defined via what is called a “Property Method”. A property method is a collection of methods to calculate several thermodynamic (fugacity, enthalpy, entropy, Gibbs free energy, and volume) and transport (viscosity, thermal conductivity, diffusion coefficient, and surface tension) properties. In addition, Aspen Plus provides a large database of interaction parameters that are used with thermodynamic models and mixing rules to estimate mixture properties. Aspen Plus properties in this work are calculated based on defined models, however Aspen Plus can estimate missing properties by different type of calculations. A screenshot with methods and databases in properties area of Aspen Plus can be found in Appendix (fig. 8-16).

In this work Aspen Plus calculations were also made via flowsheet calculation in “Simulation” area of Aspen Plus with sensitivity analysis, defining streams and cases (values for varied variable) and other parameters such as temperature as it can be seen in Appendix (fig. 8-17, fig. 8-21).

In Aspen Plus, there are several activity coefficient models. Among the most commonly used is NRTL, which can be applied to polar mixtures. Other models include: Wilson, van Laar, UNIFAC, UNIQUAC, Flory Huggins, Electrolyte NRTL, and Scatchard Hildebrand models. In these models, the activity coefficient approach is used to calculate the liquid properties, while the vapor phase properties are assumed to behave ideal or calculated using an equation of state model (EoS) [34].

The Aspen Plus version 8.8 is used to calculate vapor pressures, activity coefficients and phase equilibriums (VLE, LLE) of ABE fermentation solvents in this work.

**Selecting and Estimating Parameters:**

In some cases, Aspen Plus might have the necessary model or interaction parameters, but the predictions do not compare well with the experimental data. In such cases parameters can be [34]:

- entered manually, if the parameters are known from other sources (literature, etc.),
- data regression of the experimental data can be used and let Aspen Plus obtain or modify the parameters of interest,
- or determined based on the structure and some physical known properties.

Databanks such as NRTL-1 VLE-IG, NRTL-1 User [35], UNIQUAC VLE-IG and UNIQUAC LLE Aspen are used from the parameters area of the simulation in this work. NRTL-1 User option includes interaction parameters regressed from a multitude of experimental data to enable the calculation of the VLLE of system 1-butanol/water over a wider range of temperature than boiling conditions at ambient pressure [35].

Interaction parameters are selected from the database in global panel (NRTL-1 User, NRTL-1 VLE-IG, UNIQUAC LLE Aspen and UNIQUAC VLE-IG). NRTL-1 User option is used only for 1-butanol calculations, since the interaction parameters from this option is available only for this component.

Fig. 5-4 shows options for databases of interaction parameters, some of which are used in this work.

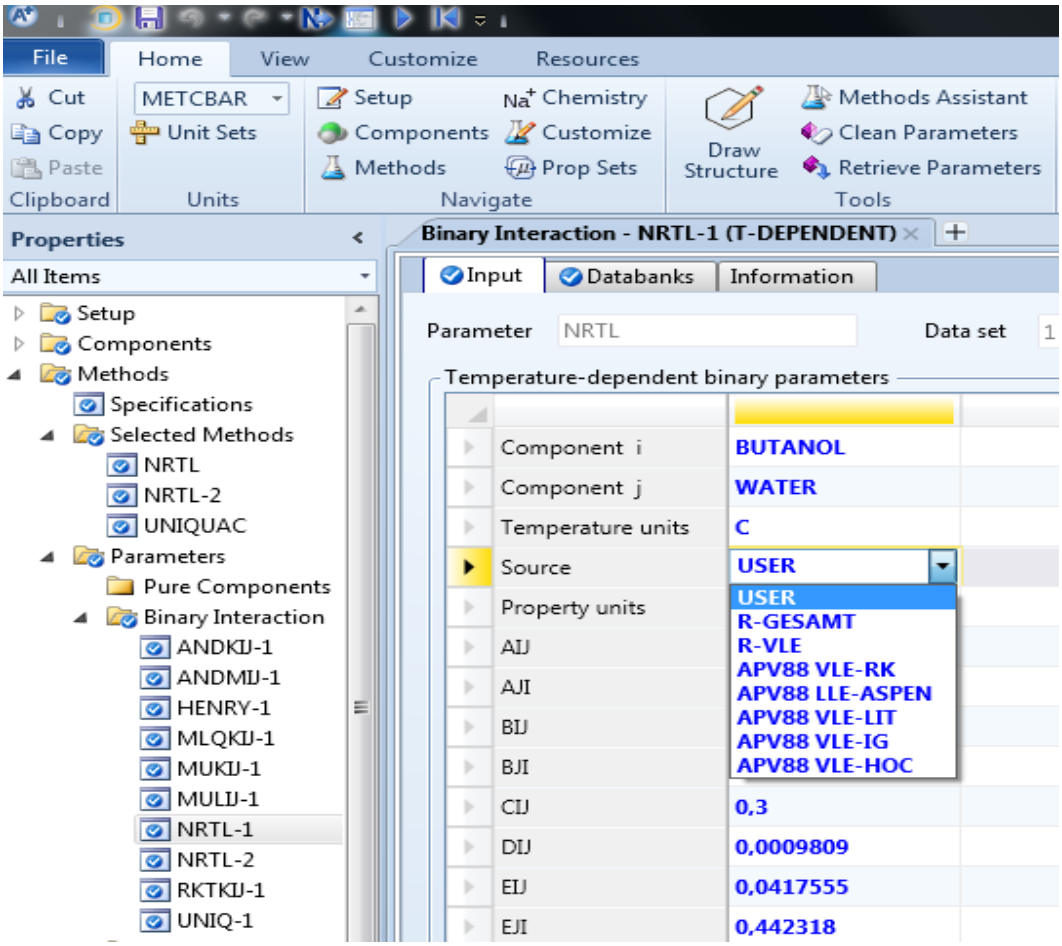


**Fig. 5-4. Aspen Plus Database**

In general, the databanks are selected in the properties area of Aspen Plus for every calculation in this work. After selecting databanks, required components are selected. Vapor pressure, activity coefficient and binary system phase equilibrium calculations are carried out directly in the properties area of Aspen Plus while more complicated calculations such as ternary and quaternary system phase equilibrium calculations need to be performed in the flowsheet area of Aspen Plus. Simulation steps of the calculations in this work are described below, some of the related screenshots from these calculations can be found in appendix.

### 5.2.1. Vapor Pressure Calculation

The pure component vapor pressures of 1-butanol, acetone, ethanol and water are calculated in properties area of Aspen Plus.

The components are selected in properties area. By default, Aspen Plus uses the Antoine equation (eq. 3.13) for the vapor pressure calculations. From the analysis area selecting “pure” gives the input section for the required calculation. In the Input section selecting “PL” and defining parameters such as temperature range (e.g. 0-200°C), number of points (51), pressure and phase (liquid) vapor pressures can be calculated. After defining these parameters, simulation is run and repeated for each component. Results are saved from the results summary panel.

## 5.2.2. Activity Coefficient Calculation

Aspen Plus activity coefficients at infinite dilutions are calculated in the properties area, “mixture” panel, using the gamma option after selecting components 1-butanol, acetone, ethanol, water. From the input section the component mass fraction is set to 0 in water to calculate activity coefficient at infinite dilutions, temperature (e.g. 0-220°C) and pressure (10 bar) are set according to available literature data, setting pressure to 10 bar has ensured defining liquid phase over the whole temperature range. The activity coefficient approach is used to calculate the liquid properties, while the vapor phase properties are calculated using an equation of state. The calculation is run and repeated for each component. Results are saved from “results summary” panel.

Fig. 5-5 shows activity coefficient calculation via mixture panel in properties area of Aspen Plus.

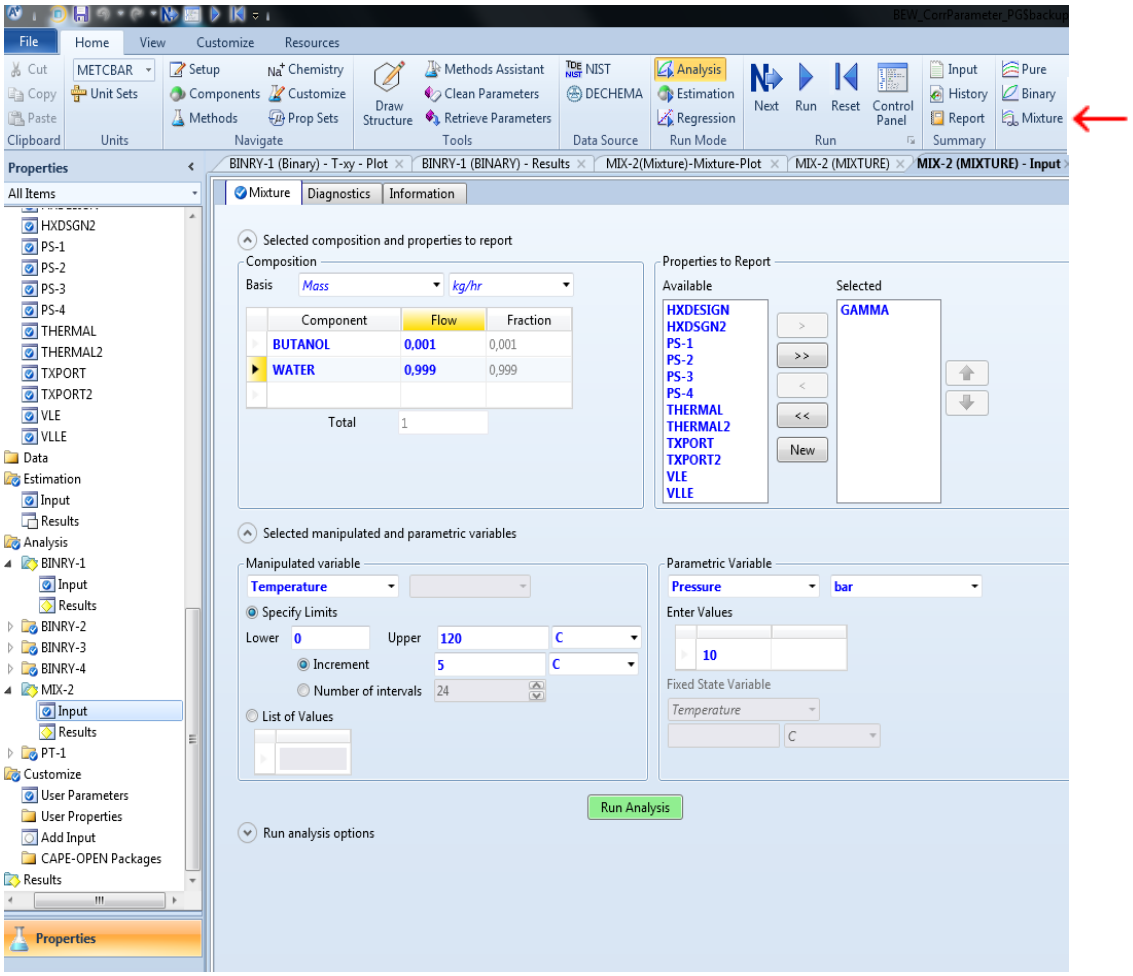


**Fig. 5-5. Activity coefficient calculation input section**

## 5.2.3. Phase Equilibrium Calculation

Phase equilibria (VLE, LLE) of binary system “1-butanol-water” are calculated in properties area of Aspen Plus. Components (1-butanol and water) are selected. In properties area “binary” can be selected from analysis section. In binary analysis section components (1-

butanol, water), composition basis (mole fraction), required phases (vapor-liquid or liquid-liquid), property method (e.g. NRTL), number of points, and pressure can be defined and calculations can be run. In this work calculations are repeated selecting databanks NRTL-1 User, NRTL-1 LLE Aspen, UNIQUAC LLE Aspen and setting the pressures to 1013.25, 1980 and 4920 mbar. Results are saved from the results summary panel.

Fig. 5-6 shows the input section of binary system calculation in properties area of Aspen Plus.

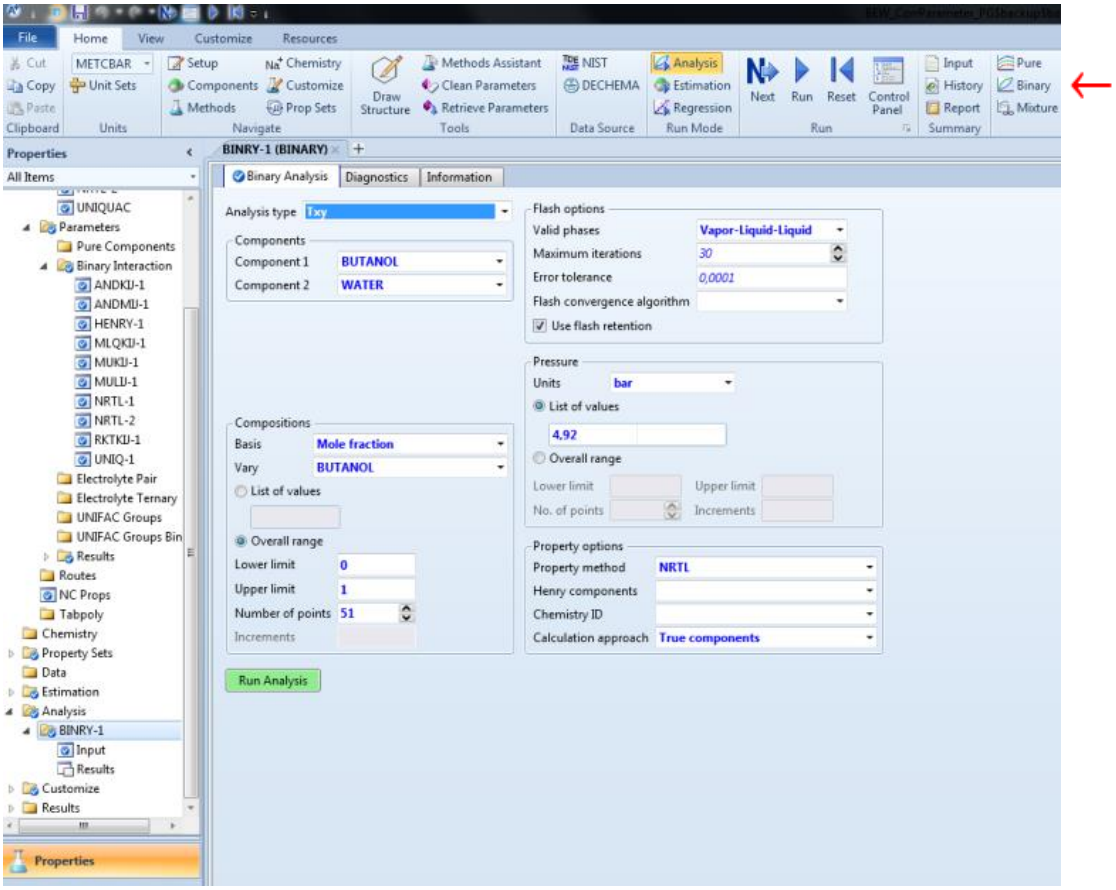


**Fig. 5-6. Binary systems calculation in properties area of Aspen Plus**

LLE calculations for ternary systems “1-butanol-acetone-water”, “1-butanol-ethanol-water” and quaternary system “1-butanol-acetone-ethanol-water” are calculated via sensitivity analysis from the simulation area of Aspen Plus since the mixture composition for ternary system calculations can’t be set in the properties area and the calculations made in properties area were not satisfactory. Quaternary system calculation via properties area was also not possible. Therefore, multinary system calculations were carried out in the flowsheet area of Aspen Plus with sensitivity analysis.

Aspen Plus model library contains flash and decanter blocks that solve appropriate material, energy balance, and equilibrium equations in the main flowsheet section under the separators tab. Flash3 block is designed to produce one vapor phase and two liquid phases in equilibrium for suitability specified process conditions. Flash3 block is also capable of solving liquid-liquid equilibrium problem under conditions where no vapor is produced. Decanter block is designed to produce two liquid phases in equilibrium in the absence of a vapor phase.

First, the model is designed for the separation process in the main flowsheet section of Aspen Plus using a decanter, a flash and a duplicate to compare the results of the two blocks. Feed

and streams are defined as in fig. 5-7. Parameters are specified in the sensitivity analysis section to define composition and temperature area of interest to be compared with literature. Required components (1-butanol, acetone, ethanol, water) are tabulated. In Input-options section, ‘reinitialize all blocks’ and ‘do not execute base case’ commands are selected and calculations are run. Results are saved from the summary panel if no error has occurred in control panel. Results of the flash3 and decanter calculations did not show any considerable amount of difference.

Fig. 5-7 shows the process model in the main flowsheet area of Aspen Plus. Feed is connected to decanter and flash through a duplicate. Liquid phases are defined as LIQ1FLSH and LIQ2FLSH for flash3 block and LIQ1DEC, LIQ2DEC for decanter block.

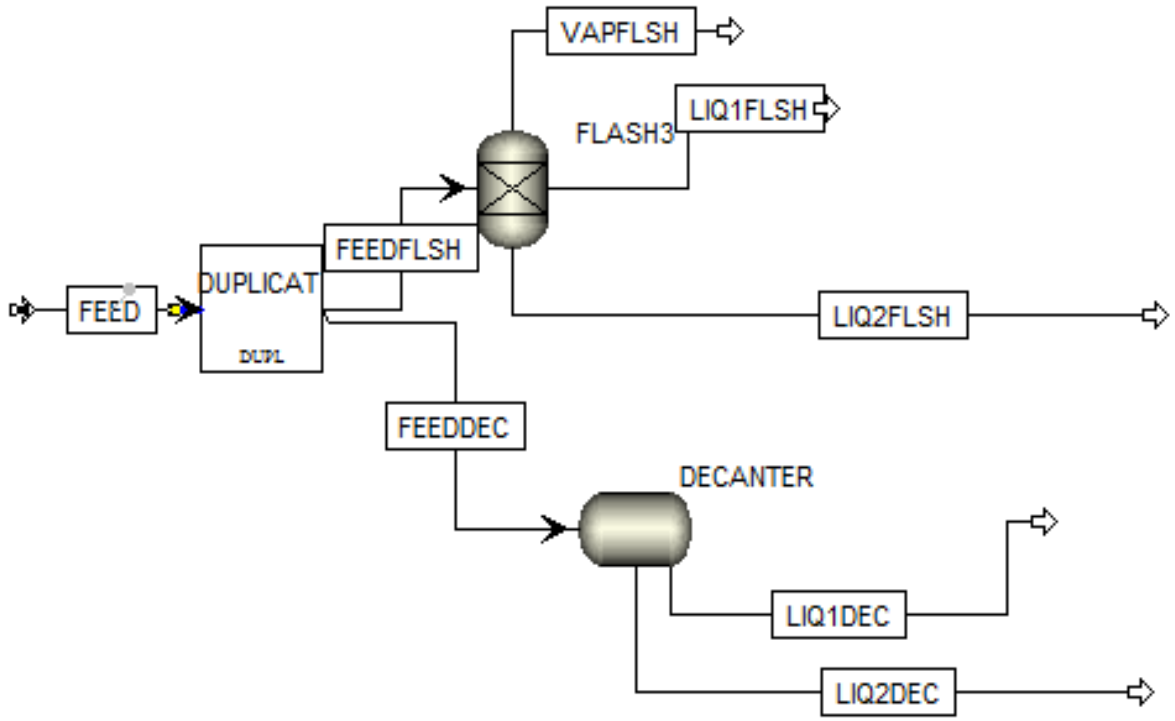


**Fig. 5-7. Main flowsheet in the simulation area of Aspen Plus**

## 5.3. Calculation Summary

The calculation options and parameters (temperature, pressure) used in calculations with COSMOtherm and Aspen Plus are summarized in tables (5.1- 5.7). The calculation parameters are based on the available literature data and the results of these calculations are presented in the results part of this thesis. Since some additional calculations are done to test the suboptions of the simulations and compare the results at different temperatures, results of these additional calculations will be presented in appendix due to results not being in accordance with the literature data or lack of literature data for comparison.

| Component | Temperature range of literature data [°C] | COSMOtherm Options | Aspen Plus Options |
|---|---|---|---|
| 1-Butanol | 20-220 | TZVD-FINE, Wagner | UNIQUAC LLE Aspen |
| Acetone | -40-200 | TZVD-FINE, Wagner | UNIQUAC LLE Aspen |
| Ethanol | 0-120 | TZVD-FINE, Wagner | UNIQUAC LLE Aspen |
| Water | 0-200 | TZVD-FINE, Wagner | UNIQUAC LLE Aspen |

**Table 5-1. Vapor pressures of pure components "1-butanol, acetone, ethanol, water" with COSMOtherm and Aspen Plus**

| Component | Temperature range of literature data [°C] | COSMOtherm Options | Aspen Plus Options |
|---|---|---|---|
| 1-Butanol/Water | 0-120 | TZVD-FINE, DMOL3, SVP | NRTL-1 User, NRTL-1 VLE-IG, UNIQUAC LLE Aspen |
| Acetone/Water | 0-100 | TZVD-FINE, DMOL3, SVP | NRTL-1 VLE IG, UNIQUAC VLE-IG |
| Ethanol/Water | 0-110 | TZVD-FINE, DMOL3, SVP | NRTL-1 VLE IG, UNIQUAC VLE-IG |

**Table 5-2. Activity coefficients of "1-butanol, acetone, ethanol, water" at infinite dilutions with COSMOtherm and Aspen Plus**

| Pressure of literature data [mbar] | COSMOtherm Options | Aspen Plus Options |
|---|---|---|
| 913 | TZVPD-FINE, DMOL3, SVP (with search LLE and without search LLE) | |
| 933 | TZVPD-FINE, DMOL3, SVP (with search LLE and without search LLE) | |
| 1013.25 | TZVPD-FINE, DMOL3, SVP (with search LLE and without search LLE) | NRTL-1 User, NRTL-1 LLE Aspen, UNIQUAC LLE Aspen |
| 1980 | TZVPD-FINE, DMOL3, SVP (with search LLE and without search LLE) | NRTL-1 User |
| 4920 | TZVPD-FINE, DMOL3, SVP (with search LLE and without search LLE) | NRTL-1 User |

**Table 5-3. Vapor Liquid Equilibrium of binary system "1-butanol-water" with COSMOtherm and Aspen Plus**

| Temperature range of literature data [°C] | COSMOtherm Options and Temperature Range | Aspen Plus Options and Temperatur Range |
|---|---|---|
| 0-120 | TZVPD-FINE (with and without compute renormalized LLE), 5-170°C | NRTL-1 User, NRTL-1 LLE Aspen, UNIQUAC LLE Aspen, 5-170°C |

**Table 5-4. Liquid-liquid equilibrium of binary system "1-butanol-water" with COSMOtherm and Aspen Plus**

| Temperatures of literature data [°C] | COSMOtherm Options and Temperature | Aspen Plus Options and Temperature |
|---|---|---|
| 20, 30, 40 | TZVPD-FINE (without compute renormalized LLE) at 25, 30, 35, 40, 50, 70°C, TZVPD-FINE (with compute renormalized LLE) at 30, 40, 50, 70°C | UNIQUAC LLE Aspen, NRTL-1 User, NRTL-1 LLE Aspen at 30, 50, 70°C |

**Table 5-5. Liquid-liquid equilibrium of ternary system "1-butanol-acetone-water" with COSMOtherm and Aspen Plus**

| Temperatures of literature data [°C] | COSMOtherm Options and Temperature | Aspen Plus Options and Temperature |
|---|---|---|
| 25 | TZVPD-FINE (without compute renormalized LLE) at 25, 30, 40, 50, 70°C, TZVPD-FINE (with compute renormalized LLE) at 30, 50, 70°C | UNIQUAC LLE Aspen, NRTL-1 User, NRTL-1 LLE Aspen at 30, 50, 70°C |

**Table 5-6. Liquid-liquid equilibrium of ternary system "1-butanol-ethanol-water" with COSMOtherm and Aspen Plus**

| Temperature of literature data [°C] | COSMOtherm Options | Aspen Plus Options and Temperature |
|---|---|---|
| 25 | TZVPD-FINE (without compute renormalized LLE) at 25, 30, 40, 50, 70°C, TZVPD-FINE (with compute renormalized LLE) at 30, 50, 70°C | UNIQUAC LLE Aspen, NRTL-1 User at 30°C |

**Table 5-7. Liquid-liquid equilibrium of quaternary system "1-butanol-acetone-ethanol-water" with COSMOtherm and Aspen Plus**

# 6. Results

Vapor pressures, activity coefficients and phase equilibria of binary, ternary and quaternary systems of the ABE fermentation products (acetone, 1-butanol, ethanol, water) are calculated by using COSMOtherm and Aspen Plus, according to the procedures explained in chapter 5. Results are displayed in diagrams in comparison with literature data from different sources.

## 6.1. Vapor Pressures

Vapor pressures of pure components are calculated with both simulations COSMOtherm and Aspen Plus according to the procedures described in chapters 5.1.1 and 5.2.1. COSMOtherm calculates vapor pressures ab initio based on QM TZVPD-FINE level as well as with Wagner coefficients from its database. Calculation in Aspen Plus are based on the correlation of Antoine.

Diagram fig. 6-1 shows the vapor pressure of pure component 1-butanol. Calculations are done for a temperature range of 20-220°C. The logarithmic values of the vapor pressures presented show an increase as the temperature increases, and COSMOtherm and Aspen Plus-Antoine options are in good accord with literature data.

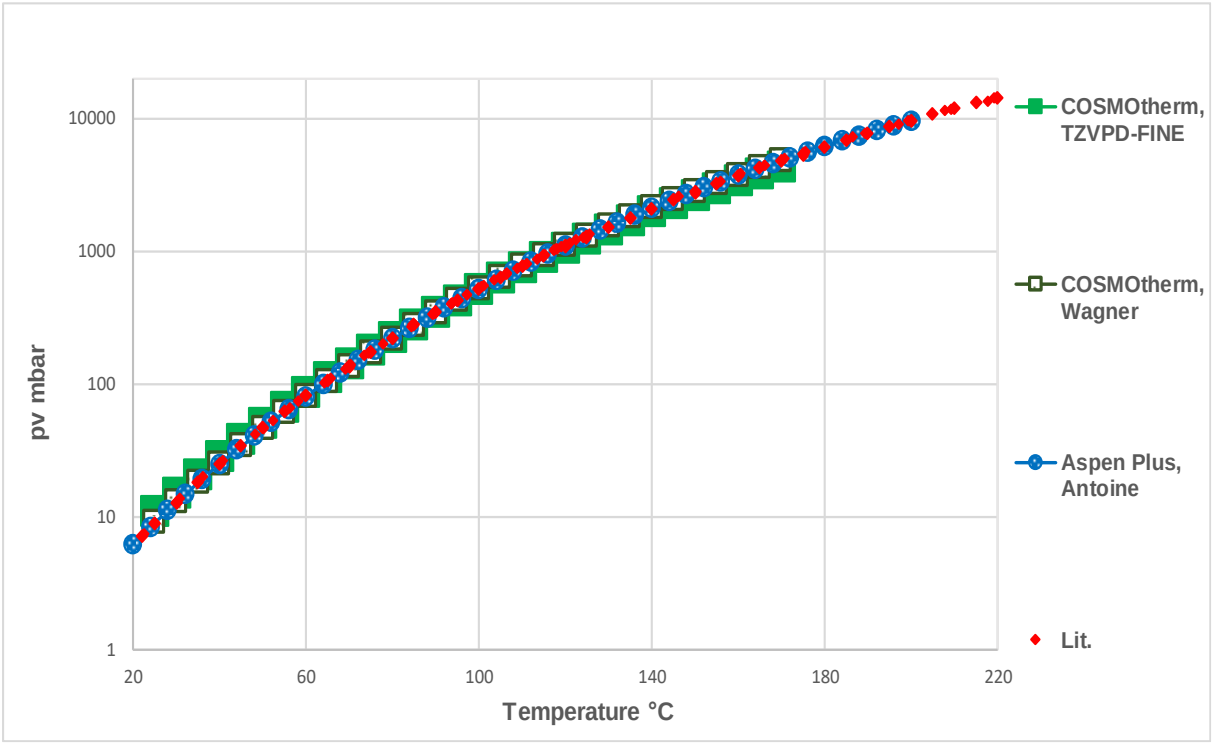


**Fig. 6-1. Vapor pressure of 1-butanol with COSMOtherm-TZVPD-FINE, Wagner, Aspen Plus-Antoine options and literature data [36-39]**

Diagram fig. 6-2 shows the vapor pressure of pure component acetone with COSMOtherm, Aspen Plus calculations and the literature data. Calculations are done at the temperature range of 0-200°C. In this diagram COSMOtherm-Wagner option and Aspen Plus-Antoine options are fitting literature data very well, but COSMOtherm-TZVPD-FINE option shows poor results with rather a lower vapor pressure line. COSMOtherm is a predictive method calculating vapor

pressures based on its quantum chemical calculations, while Aspen Plus calculations use empirical parameters like Antoine constants from its database for the vapor pressure calculations. Aspen Plus-Antoine option and COSMOtherm-Wagner option calculations are based on agreed parameters and therefore in good accordance with literature data.

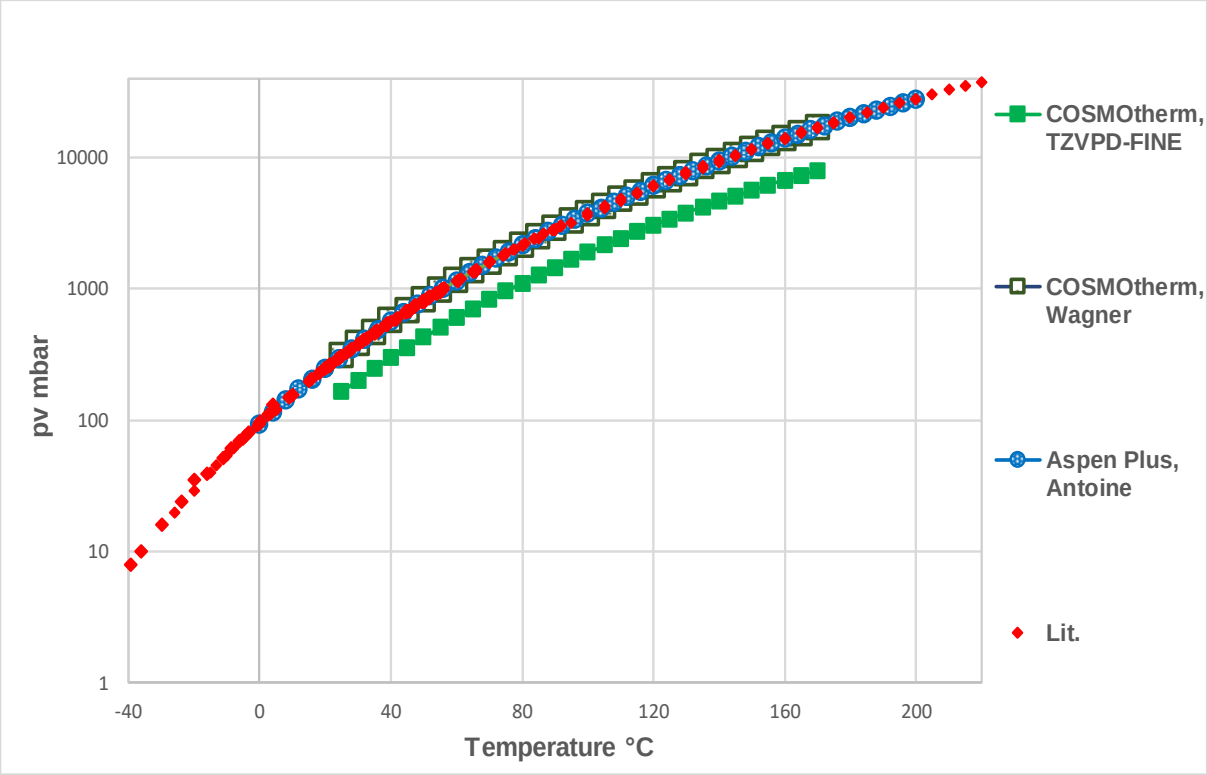


**Fig. 6-2. Vapor pressure of acetone with COSMOtherm-TZVPD-FINE, COSMO-Wagner, Aspen Plus-Antoine and literature data [37-41], [44]**

Diagram, fig. 6-3, shows the vapor pressure calculations of pure component ethanol with COSMOtherm and Aspen Plus compared with literature data at 0-120°C. COSMOtherm-Wagner and Aspen Plus-Antoine options fit literature data very well, while COSMOtherm-TZVPD-FINE option shows slightly lower vapor pressure values, which gets more remarkable at higher temperatures. From fig. 6-3, it can be concluded that it is important to choose the Wagner option for pvap calculation, if the VLE calculations of a mixture including acetone with COSMOtherm is required. Wagner coefficients are available in COSMOtherm and resulting in high accuracy, hence higher accuracy in subsequent VLE calculations can be achieved with this option.

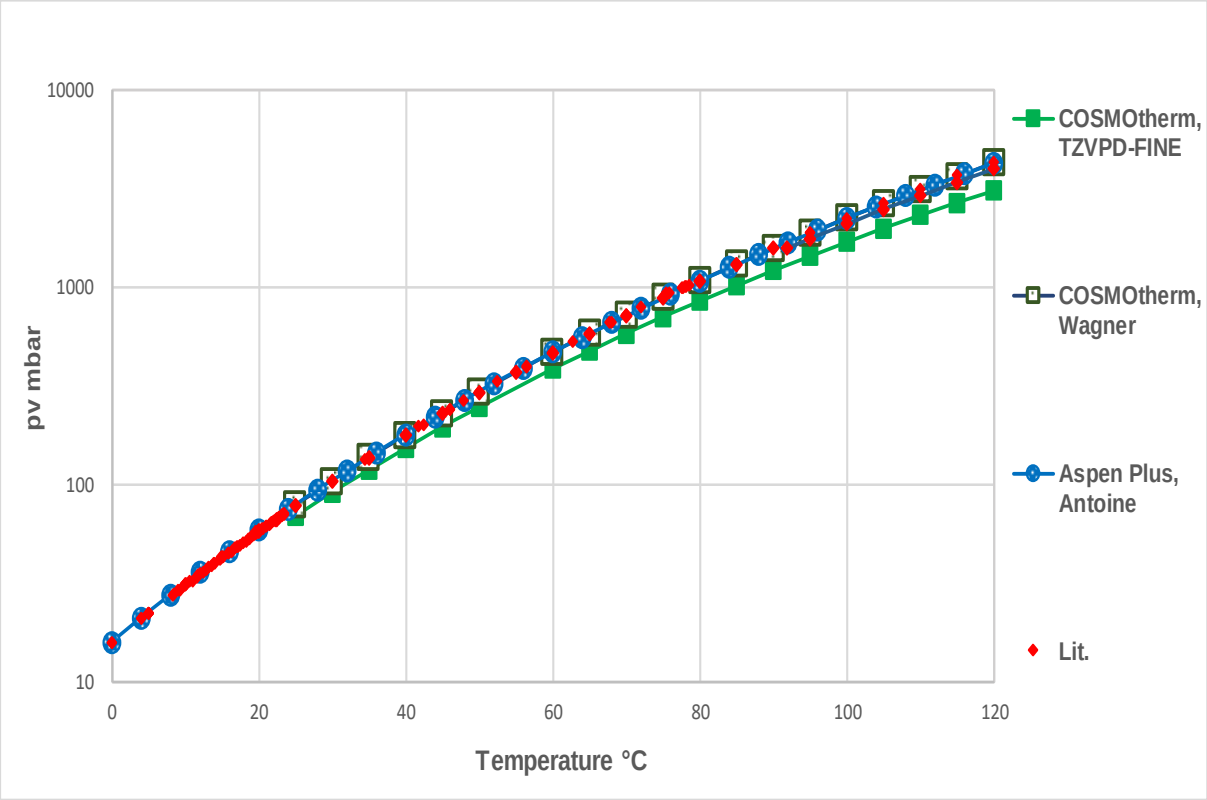


**Fig. 6-3. Vapor pressure of ethanol with COSMOtherm-TZVPD-FINE, COSMO-Wagner, Aspen Plus-Antoine and literature data [37-39], [42]**

Diagram, fig. 6-4**,** shows the vapor pressure of pure component water with COSMOtherm-TZVPD-FINE, Wagner options, Aspen Plus-Antoine option and literature data. Temperature range for these calculations is 0-200°C. COSMOtherm-TZVPD-FINE option shows here the lowest vapor pressure line at temperatures between 20 – 170°C and have no common value with COSMOtherm-Wagner calculation and Aspen Plus options or literature data (lit.1, lit.2). The parameters for the vapor pressure calculations of literature data (lit.1, lit.2) show a clear difference, resulting in two different lines with no connecting values. Lit.1 consists of different literature data, which are in accord with each other. Some of these are calculated with Antoine constants from sources such as NIST Chemistry Webbook, Dortmund Data Bank and other web sources given in references [37, 38, 43, 44] and some of them are experimentally measured values from Hartwick et al. [41]. Lit.2 is calculated with Antoine constants given in an online source [45]. While COSMOtherm-Wagner and Aspen Plus-UNIQUAC LLE Aspen options are in good accordance with lit.1, lit.2 is between COSMOtherm-TZVPD-FINE, and other two options, showing lower literature data line, without having any connection point with any other option.

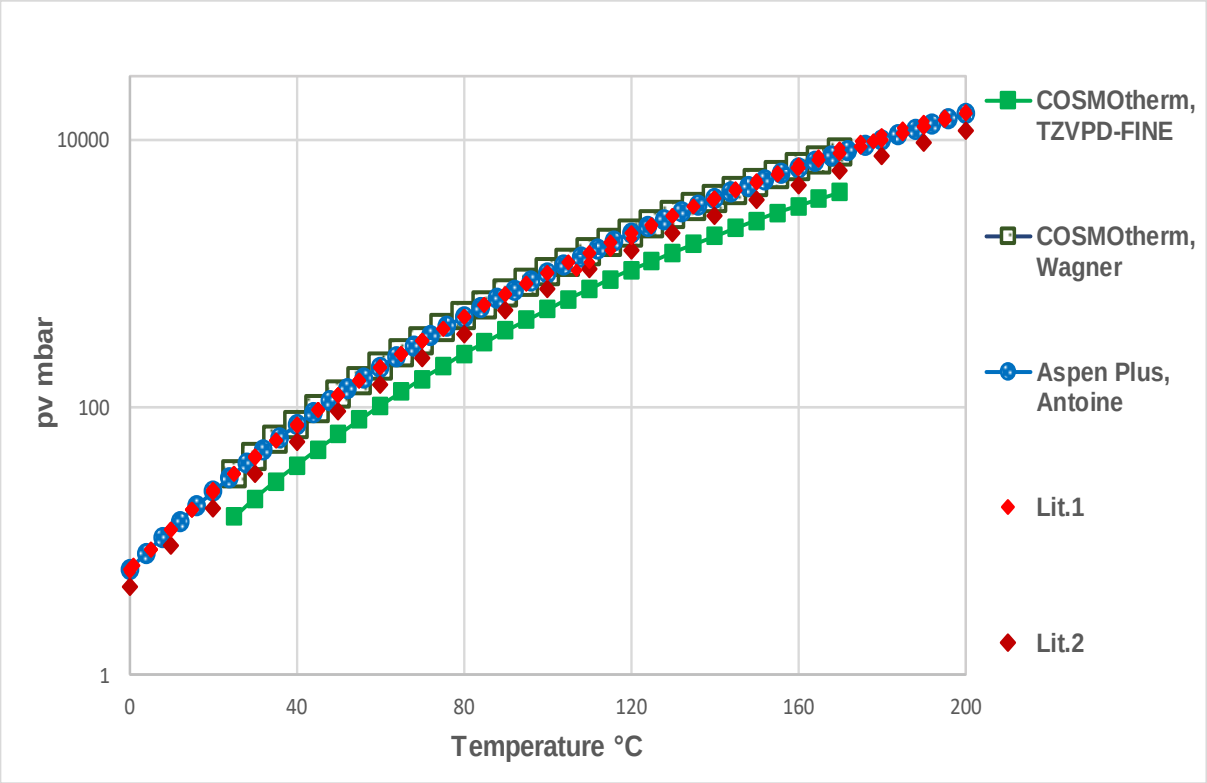


**Fig. 6-4. Vapor pressure of water with COSMOtherm-TZVPD-FINE, COSMO-Wagner, Aspen Plus-Antoine, literature data [37-38], [41], [43-45]**

## 6.2. Activity Coefficients

Activity coefficient calculations are of importance for the calculations of phase equilibria. Activity coefficients at infinite dilution in water, $\gamma^{\infty}$, of the components 1-butanol, acetone, ethanol are calculated by COSMOtherm and Aspen Plus and compared with the literature data according to the simulation steps explained in chapters 5.1.2 and 5.2.2.

For the activity coefficient calculations at infinite dilution with COSMOtherm-TZVPD-FINE, DMOL3 and SVP QC levels are used. Aspen Plus calculations for the activity coefficients at infinite dilution are calculated with the following options: NRTL-1 User, NRTL-1 VLE-IG, UNIQUAC LLE Aspen, UNIQUAC VLE-IG. Literature data are taken from different sources and compared with both simulation results.

Diagram, fig. 6-5**,** shows activity coefficient of 1-butanol at infinite dilution, $\gamma^{\infty}$, with COSMOtherm-TZVPD-FINE, DMOL3, SVP levels and literature data. Different behavior of activity coefficient over temperature is obtained for used COSMOtherm levels. The three COSMOtherm levels TZVPD-FINE, DMOL3, SVP give different values from each other but a similar curve form to the literature data. SVP has the highest activity coefficient values among other levels. TZVPD-FINE level activity coefficient line seems to be the closest to the literature data showing slightly lower values than literature data, while the activity coefficient values at 0°C for both literature data and TZVPD-FINE level are around 30. Both curves are at their highest point at around 60°C with the activity coefficient values ranging from 50-70. As the temperature further increases, activity coefficient values decrease for both TZVPD-FINE level and literature data to 40-50 at 120°C.

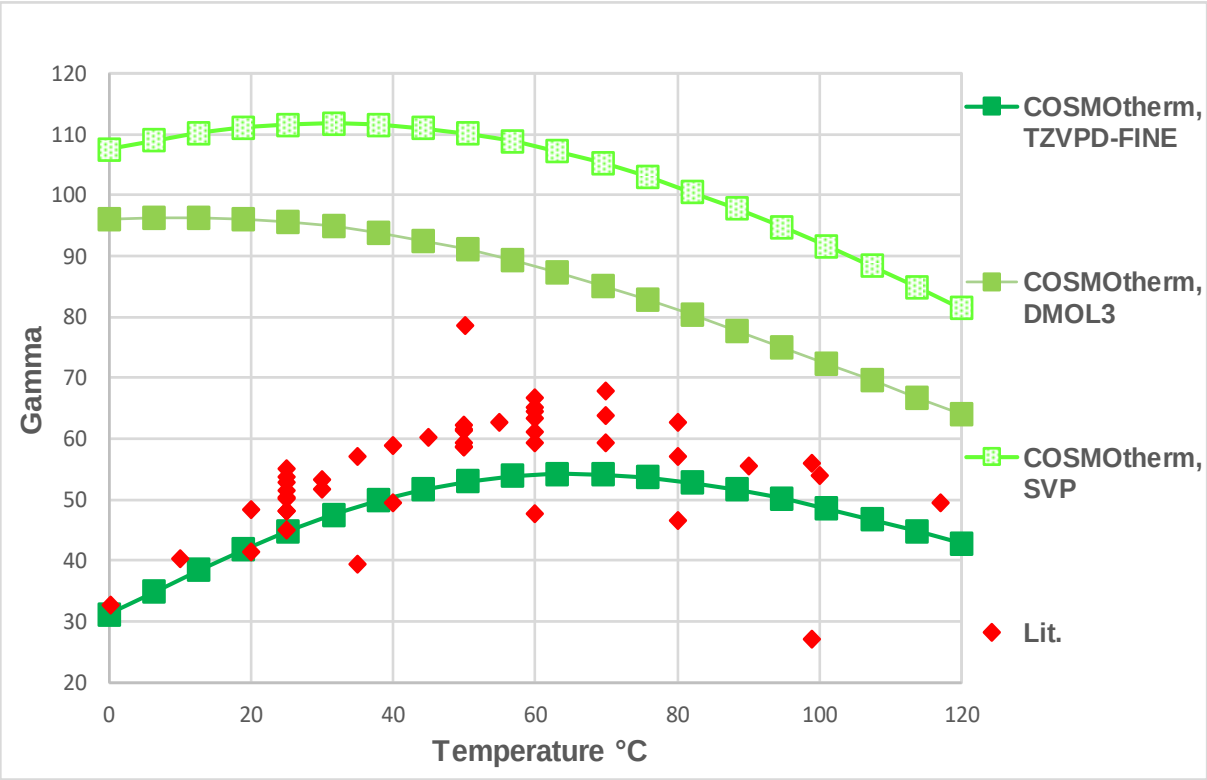


**Fig. 6-5. $\gamma^{\infty}$-1-Butanol with COSMOtherm-TZVPD-FINE, DMOL3, SVP and literature data [46]**

The calculations with three different QC levels of COSMOtherm have served to find the best QC level to calculate the activity coefficient of the required compound. As these calculations are repeated for the components acetone and ethanol the results showed that TZVPD-FINE level is the best option for 1-butanol and ethanol, and SVP level is the best option for acetone. In diagrams, fig. 6-6, fig. 6-7 and fig. 6-8, the best fitting COSMOtherm option with Aspen Plus options will be shown for acetone and ethanol. Diagrams for activity coefficients obtained for all COSMOtherm QC levels for components aqueous systems of ethanol and acetone can be found in the appendix (fig. 8.1, fig. 8-2).

Diagram, fig. 6-6, shows the activity coefficient of 1-butanol values at infinite dilution, $\gamma^{\infty}$, calculated with Aspen Plus, NRTL-1 User [35], NRTL-1 VLE-IG, UNIQUAC LLE Aspen options, COSMOtherm, TZVPD-FINE level and literature data. Literature data comes from Dechema Chemistry Data Series [46]. The values of literature data are inconsistent and showing deviations, but are indicating the behavior of infinite activity coefficient of 1-butanol with temperature. Aspen Plus calculation results are different from each other depending on the model and databank used. NRTL-1 User [35] option was adapted to fit activity coefficients and shows the best fitting results to the literature data. This option was regressed to improve calculation results compared to literature data and used only for 1-butanol calculations since the parameters are not available for other compounds. UNIQUAC LLE Aspen and COSMOtherm-TZVPD-FINE options are in literature data range. COSMOtherm data show lowest activity coefficients of all calculated options and thus strongest deviation from literature data at lower temperature. At higher temperature COSMOtherm data fit literature data better than Aspen Plus calculations based on UNIQUAC LLE Aspen option. However, COSMOtherm results never reached accuracy of Aspen Plus calculations with based on NRTL-1 User interaction parameters.

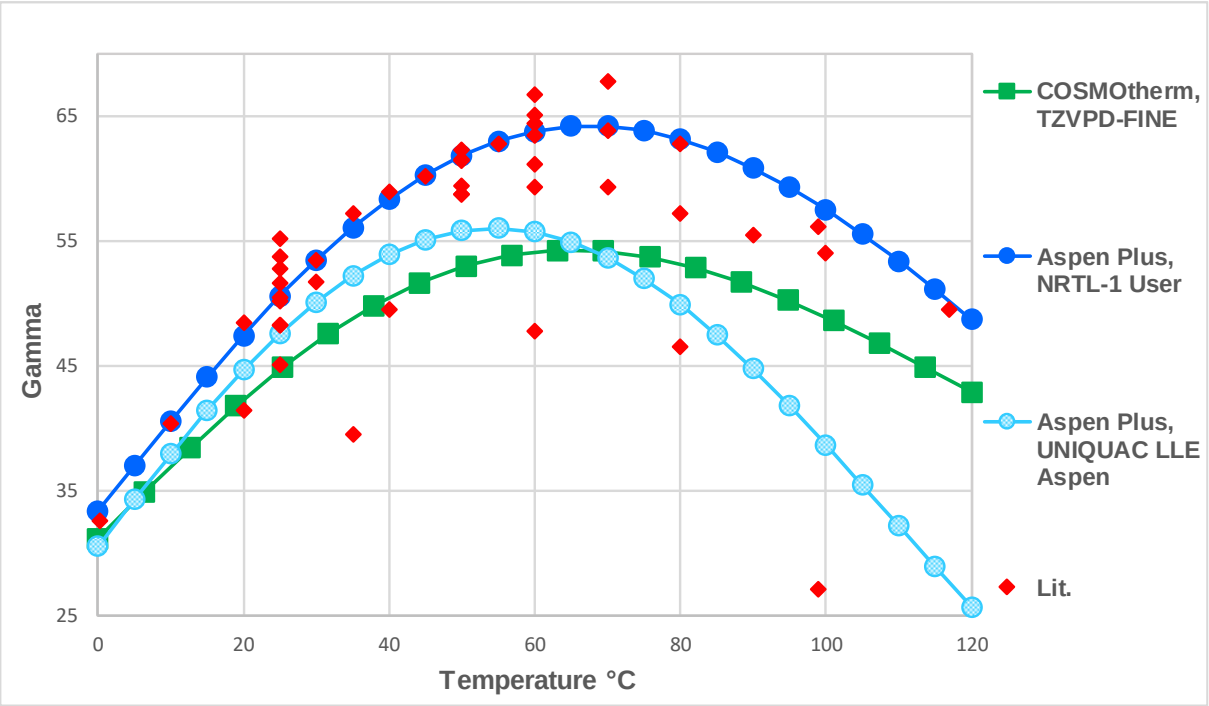


**Fig. 6-6. $\gamma^{\infty}$- 1-Butanol with COSMOtherm-TZVPD-FINE, Aspen Plus-NRTL-1 User [35], NRTL-1 VLE-IG, UNIQUAC LLE Aspen and literature data [46]**

Activity coefficient at infinite dilution of acetone with Aspen Plus-NRTL-1 VLE IG, UNIQUAC VLE-IG options, COSMOtherm-TZVPD-FINE level and literature data is displayed in fig. 6-7. Literature data for the activity coefficient of acetone at infinite dilutions is coming from an article [41] and Dechema Chemistry Data Series [47]. Calculations with COSMOtherm and Aspen Plus are based on the temperature range of the available literature data. Literature data in fig.6-7 is mostly up to 60°C which is a little bit higher than the boiling point temperature of acetone 56.05°C (at 1 atm), with some deviations. Until temperatures of around 60°C, calculations show deviations from literature data but both Aspen Plus-NRTL-1 VLE-IG, UNIQUAC VLE-IG options and COSMOtherm-SVP level are in good accord with literature data. For temperatures higher than 60°C COSMOtherm levels both show an increase of activity coefficients while Aspen Plus options show a decrease. Since at higher temperatures than 60°C literature data is most likely not available, it is hard to tell the form of the literature data line and compare with the calculated values.

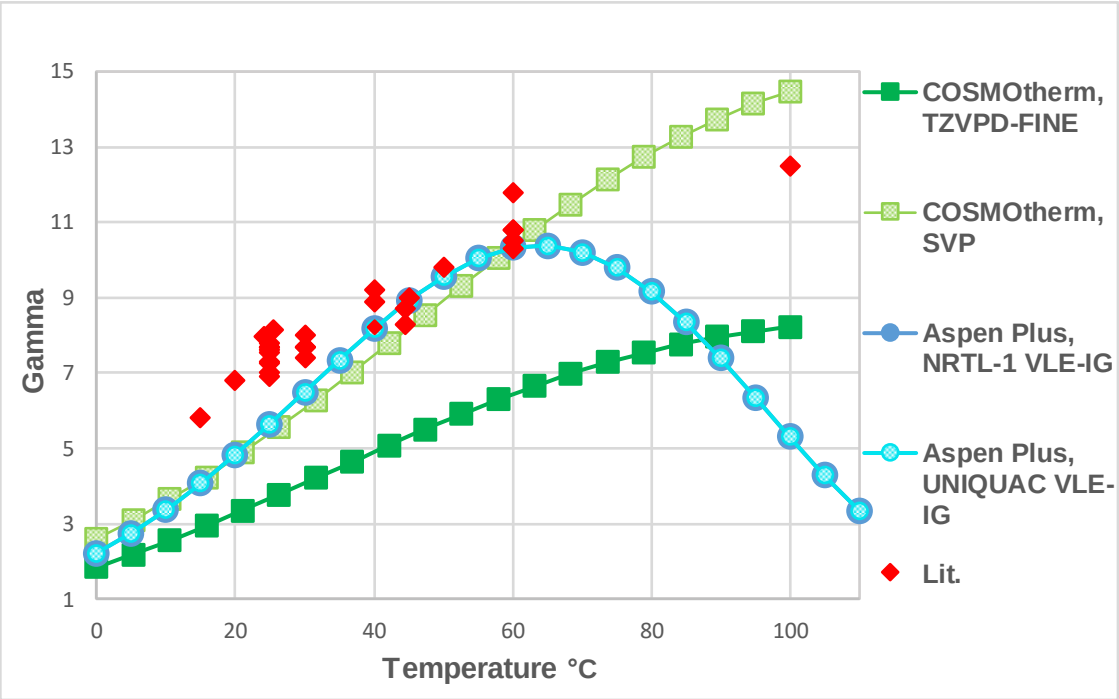


**Fig. 6-7. $\gamma^{\infty}$- Acetone with COSMOtherm-TZVPD-FINE, SVP, Aspen Plus-NRTL-1 VLE-IG, UNIQUAC VLE-IG and literature data [41], [47]**

Calculations with COSMOtherm-TZVPD-FINE level and Aspen Plus-NRTL-1 VLE-IG, and UNIQUAC VLE-IG options for the activity coefficient of ethanol at infinite dilution are displayed with literature data in fig. 6-8. Literature data in this diagram is taken from Dechema Chemistry Data Series [48], showing strongly inconsistent values and deviations. There are many literature data values at temperatures 25°C and 40°C, showing that these temperatures are more favored for the experimental measurements. The calculations for activity coefficient calculations of ethanol with Aspen Plus are carried out with different options than other compounds because of the availability of parameters in Aspen Plus database. In fig. 6-8, Aspen Plus calculations based on UNIQUAC and NRTL-1 seem to better follow literature data over the temperature range. COSMOtherm results show a stronger dependence on temperature, but seem to fit literature data at higher temperature better than Aspen Plus calculations.

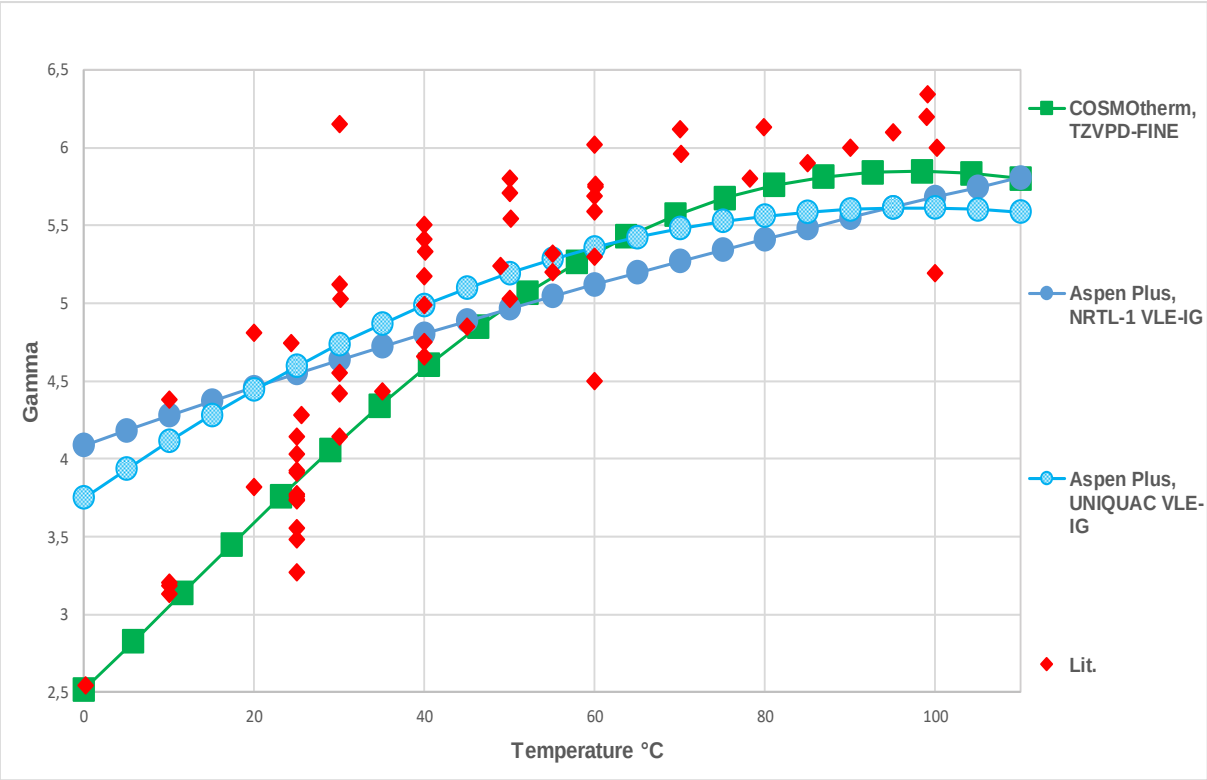


**Fig. 6-8. $\gamma^{\infty}$- Ethanol COSMOtherm-TZVPD-FINE, Aspen Plus-NRTL-1 VLE-IG, UNIQUAC VLE-IG and literature data [48]**

## 6.3. Vapor-Liquid Equilibrium of Binary System „1-Butanol-Water“

In this part the behavior of vapor-liquid equilibrium (VLE) of binary system “1-butanol-water” is investigated to find by calculations the temperatures, pressures, and compositions of phases in equilibrium. Phase equilibrium calculations of the binary system VLE, “1-butanol-water” are carried out by COSMOtherm and Aspen Plus simulations, according to the procedures explained in chapters 5.1.3 and 5.2.3. The simulation results are compared with the literature data at different temperature and pressure settings. The calculations with COSMOtherm are done with and without using “search LLE” suboption. Since “search LLE” option gave better results for the calculations, calculations of COSMOtherm with this option will be presented in this chapter. Calculations without using “search LLE” suboption can be found in Appendix (fig. 8-3, fig. 8-4).

### 6.3.1. Vapor-Liquid Equilibrium of Binary System „1-Butanol-Water“ with COSMOtherm

Fig. 6-9 shows the vapor-liquid equilibrium of binary system “1-butanol-water” with COSMOtherm levels, TZVPD-FINE, DMOL3, SVP and literature data at 1013.25 mbar, for evaluating the accuracy and suitability of COSMOtherm QC levels. The results displayed in fig. 6-9 are calculated with search LLE suboption. Literature data for VLE of binary system “1-butanol-water” is taken from Dechema Chemistry Data Series [49] and Koichi et al. [50].

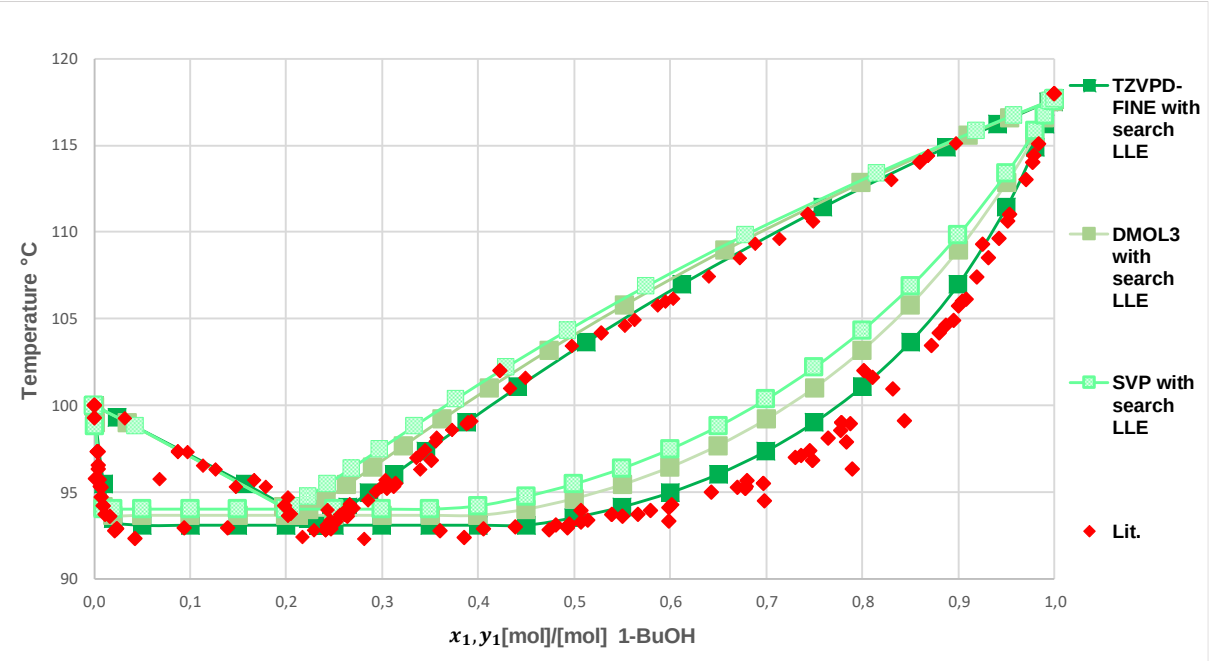


**Fig. 6-9. Temperature [°C] vs. mole fraction, $x_1$, $y_1$ [-] diagram for VLE of binary system, "1-butanol-water" with COSMOtherm-TZVPD-FINE, DMOL3, SVP with search LLE option and literature data at 1013.25 mbar [49-50]**

Literature data in fig. 6-9 shows dew point curve and bubble point curve with rather small deviations. The azeotropic point mole fraction is around 0.24 for 1-butanol at around 93°C Calculations in COSMOtherm levels show the same form as the literature data dew point and bubble point curves with an azeotropic point but slightly different results between each other and the literature data. TZVPD-FINE level calculations give the best results among the three QC levels of COSMOtherm, bubble point curve showing deviations from the literature data with slightly higher temperatures. When three of the QC levels of COSMOtherm are compared, DMOL3 level is the second best option for this calculation and SVP level comes as a third option giving the highest deviations from literature data especially for the bubble point curve and azeotropic point at a slightly higher temperature and a lower 1-butanol mole fraction.

### 6.3.2. Vapor-Liquid Equilibrium of Binary System „1-Butanol-Water" with Aspen Plus

Fig. 6-10 shows the vapor-liquid equilibrium of binary system "1-butanol-water" with Aspen Plus, NRTL-1 User [35], NRTL-1 LLE Aspen, UNIQUAC LLE Aspen options, and literature data at 1013.25 mbar, to investigate the best Aspen plus option. Calculations are carried out according to the procedure explained more detailed in chapter 5.2.3. Literature data for the VLE of binary system "1-butanol-water" is taken from Dechema Chemistry Data Series and Koichi et al. [49-50].

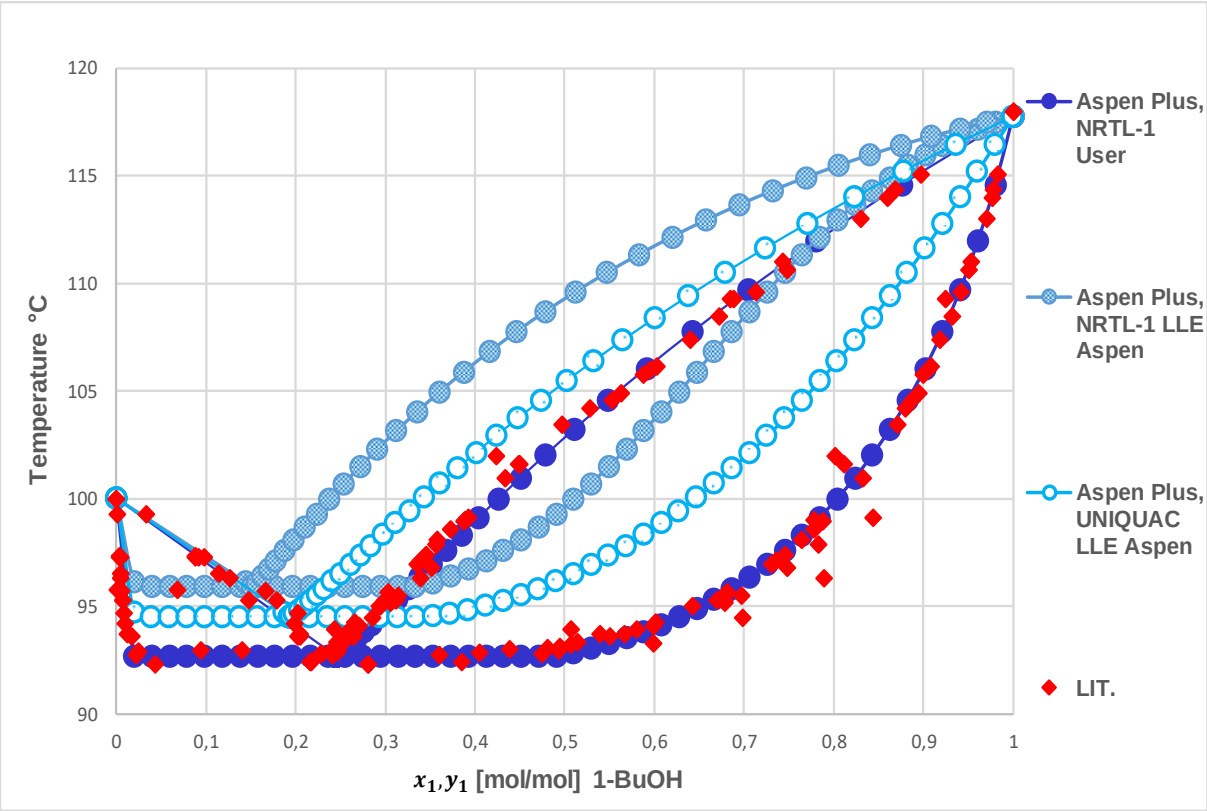


**Fig. 6-10. Temperature [°C] vs. mole fraction, $x_1$, $y_1$ [-] diagram for VLE of binary system, "1-butanol-water", with Aspen Plus-NRTL-1 User [35], NRTL-1 LLE Aspen, UNIQUAC LLE Aspen options and literature data at 1013.25 mbar [49-50]**

In fig. 6-10, Aspen Plus-NRTL-1 User option [35] is showing good accordance with literature data taken from different sources fitting dew point, bubble point curves and azeotropic point very well. The other Aspen Plus options UNIQUAC LLE Aspen and NRTL-1 LLE Aspen have azeotropic points considerably shifted to higher temperatures and lower mole fractions of 1-butanol.

### 6.3.3. Vapor-Liquid Equilibrium of Binary System „1-Butanol-Water" with COSMOtherm and Aspen Plus

The previous diagrams, fig. 6-9 and fig. 6-10, showed the the vapor–liquid equilibrium calculations of binary system "1-butanol-water" with COSMOtherm and Aspen Plus calculations separately. In fig. 6-11, Aspen Plus-NRTL-1 User option [35], COSMOtherm-TZVPD-FINE level with search LLE option and the literature data [49-50] at 1013.25 mbar are displayed. COSMOtherm-TZVPD-FINE level and Aspen Plus-NRTL-1 User option are in good accordance with the literature data at 1013.25 mbar. Aspen Plus-NRTL-1 User option calculations based on empirical parameters gives only slightly better results than the predictive calculations of COSMOtherm-TZVPD-FINE level.

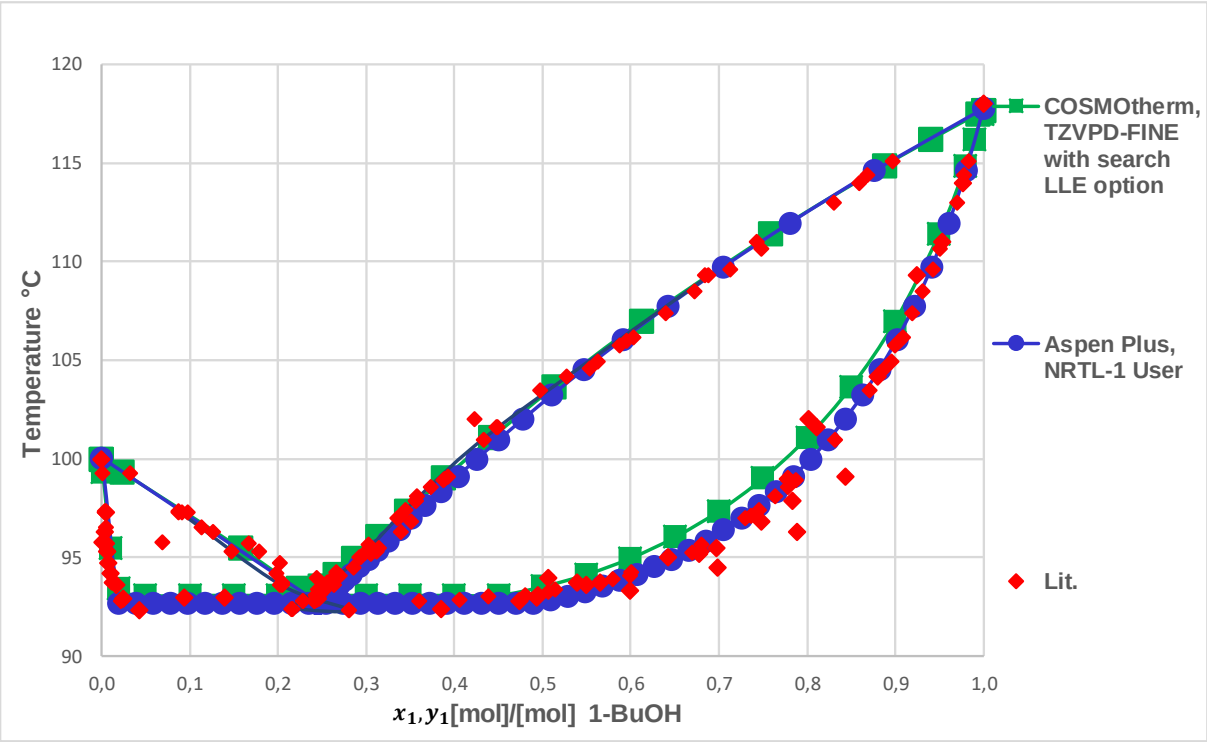


**Fig. 6-11. Temperature [°C] vs. mole fraction, $x_1$, $y_1$ [-] diagram for VLE of binary system, "1-butanol-water", with COSMOtherm-TZVPD-FINE with search LLE option, Aspen Plus-NRTL-1 User option [35] and literature data at 1013.25 mbar [49-50]**

### 6.3.4. Vapor-Liquid Equilibrium of Binary System „1-Butanol-Water" with COSMOtherm and Aspen Plus at 1013.25, 1980 and 4920 mbar

In fig. 6-12, vapor-liquid equilibrium of binary system "1-butanol-water" calculated with Aspen Plus-NRTL-1 User option [35] and COSMOtherm-TZVPD-FINE level with search LLE option, are displayed at three different pressures, 1013.25, 1980 and 4920 mbar together with literature data [49-50]. Less data points are available for higher pressures in literature but the dew point and bubble point curves have a clear form. Aspen Plus and COSMOtherm calculations fit literature data very good as explained in chapter 6.3.3 more detailed. When the calculated values at higher pressures, 1980 and 4920 mbar are compared with the literature data at these pressures the same behavior as the calculations at 1013.25 mbar regardless the pressures. For the calculations at higher pressures TZVPD-FINE level is still the best QC level as it can be seen in Appendix (fig. 8-4).

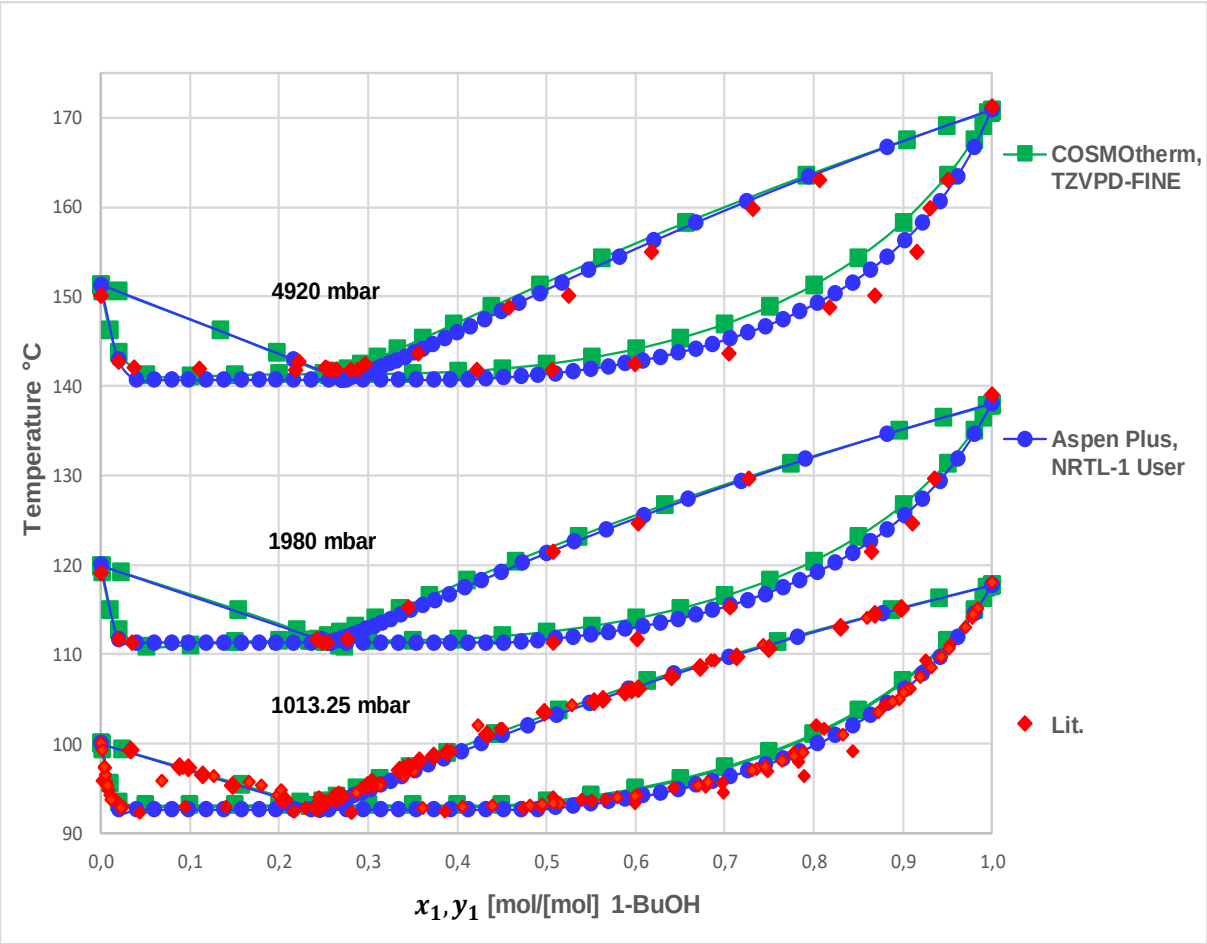


**Fig. 6-12. Temperature [°C] vs. mole fraction, $x_1$, $y_1$ [-] diagram for VLE of binary system, "1-butanol-water" with COSMOtherm-TZVPD-FINE with search LLE option, Aspen Plus-NRTL-1 User option [35], and literature data at 1013.25, 1980 and 4920 mbar [49-50]**

## 6.4. Liquid-Liquid Equilibrium of Binary System "1-Butanol-Water"

Liquid-liquid equilibrium of binary system "1-butanol-water" is calculated to understand multinary systems (ternary and quaternary systems) including "1-butanol-water". COSMOtherm and Aspen Plus calculations for liquid-liquid-equilibrium of binary system "1-butanol-water" are carried out according to the procedure explained in chapters 5.1.3 and 5.2.3.

COSMOtherm-TZVPD-FINE level with and without "compute renormalized LLE" options and Aspen Plus-NRTL-1 User [35], NRTL-1 LLE Aspen, UNIQUAC LLE Aspen options are used for the liquid-liquid equilibrium calculation of the binary system "1-butanol-water" at constant temperatures varying the temperatures for each calculation from 5 to 170°C. The following fig. 6-13 shows the temperature [°C] vs. mole fraction, $x_1$ (mole fraction of water) and $x_2$ (mole fraction of 1-butanol) [-] diagram of the liquid-liquid equilibrium of binary system "1-butanol-water" with COSMOtherm and Aspen Plus options in comparison with literature data from Dechema Data Bank [51].

In fig. 6-13, literature data shows a miscibility gap between temperatures of 0°C and about 125 °C and 1-butanol mole fraction of around 0.01 to 0.51 with small deviations at higher 1-butanol mole fractions. The miscibility gap diminishes with temperature increase. Aspen Plus options

NRTL-1 LLE Aspen and UNIQUAC LLE Aspen have similar form with literature data liquid-liquid phase equilibrium line except the curving of the equilibrium lines with the calculated values at higher 1-butanol concentrations, yet UNIQUAC LLE Aspen option gives slightly better results when compared to the literature data. NRTL-1 User option [35] does not have the same form as the other Aspen Plus options and the values show a remarkable difference when compared to these two options. Although NRTL-1 User option showed good accordance with the literature data for the activity coefficients and vapour-liquid equilibrium calculations, it shows less compatible results for the liquid-liquid equilibrium calculations of "1-butanol-water" with mole fraction of 1-butanol, $x_1$, reaching around 0.64 at 0°C for the liquid-liquid equilibrium line. Both COSMOtherm options show a similar form to the literature data but they also show a curving at higher 1-butanol mole fractions like the two Aspen Plus options, NRTL-1 LLE Aspen and UNIQUAC LLE Aspen. COSMOtherm-TZVPD-FINE level with renormalization of LLE points accounting for thermodynamic fluctuations in the liquid mixture gives more realistic results. The miscibility gap with renormalized LLE reaches temperatures of around 135°C, while the calculations without this option reaches relatively higher temperatures of 170°C. Thus TZVPD-FINE level with "compute renormalized LLE" option is more compatible than the calculations without "compute renormalized LLE" option for the LLE calculations with COSMOtherm.

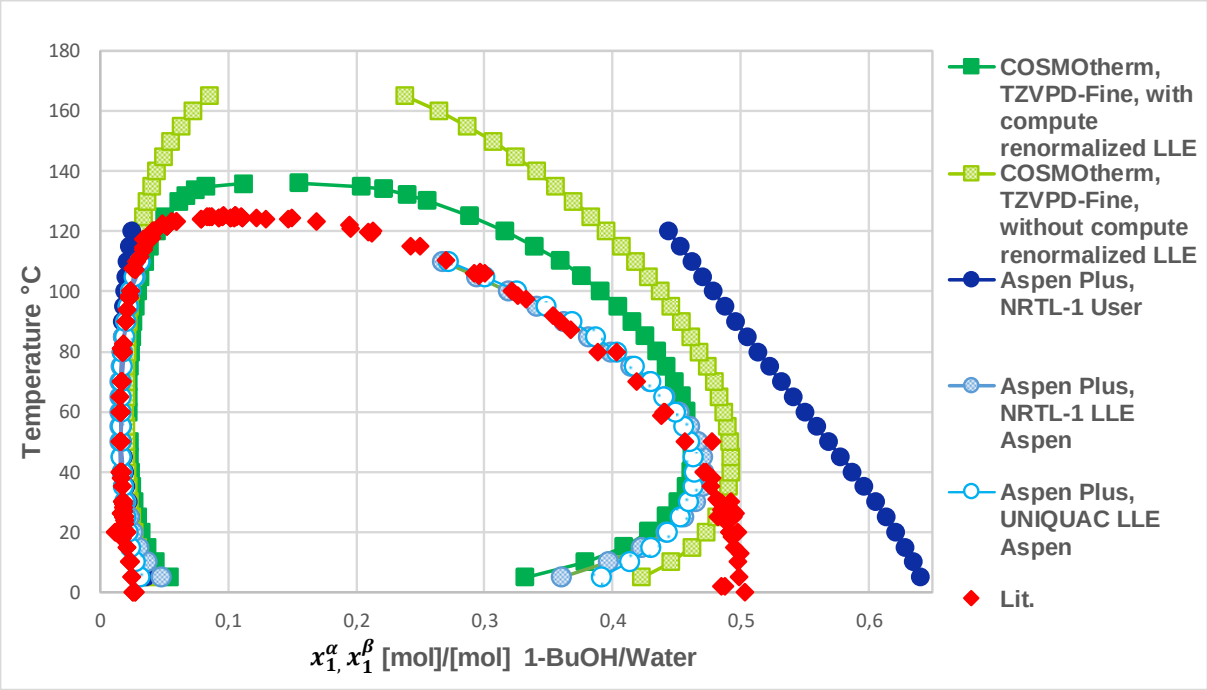


**Fig. 6-13. Temperature [°C] vs. mole fraction, $x_1$, $x_2$[-] diagram for LLE of binary system, "1-butanol-water" with COSMOtherm-TZVPD-FINE with and without renormalized LLE options, Aspen Plus-NRTL-1 User [35], NRTL-1 LLE Aspen, UNIQUAC LLE Aspen options and literature data [51]**

## 6.5. Liquid-Liquid Equilibrium of Ternary Systems

The presence of a third liquid component can sometimes be very useful in changing the mutual solubility of two other components. Besides temperature, an auxiliary component can be exploited to drive the separation of butanol from water. This third chemical species may lead

to additional phase equilibria. Also, systems that contain more than three chemical species can be created. The miscibility gap of the system is important for the separation, as 1-butanol rich phase is easier to separate than 1-butanol poor phase which can be influenced by the third chemical species. The effect of the third chemical species is to be investigated and discussed in this part with calculations of liquid-liquid equilibriums (LLE) of ternary systems “1-butanol-acetone-water” and “1-butanol-ethanol-water” carried out by COSMOtherm and Aspen Plus simulations. The procedures of the simulations are explained in chapters 5.1.3 and 5.2.3. Calculations are done with COSMOtherm, TZVPD-FINE level with compute renormalized LLE option and Aspen Plus-NRTL-1 User [35] and UNIQUAC LLE Aspen options as these options are used for the previous LLE calculations. Calculation parameters (temperatures) are chosen based on the available literature data.

### 6.5.1. Liquid-Liquid Equilibrium of Ternary System “1-Butanol-Acetone-Water”

#### 6.5.1.1. Liquid-Liquid Equilibrium of Ternary System “1-Butanol-Acetone-Water” with COSMOtherm

Fig. 6-14 shows calculations of LLE “1-butanol-acetone-water” with COSMOtherm-TZVPD-FINE level with “compute renormalized LLE” option in comparison with literature data from Dechema Chemistry Data Series, Spottke et al. and Fania et al. [52-54]. Literature data is available for three different temperatures showing the same equilibrium line with small deviations at higher 1-butanol concentrations. Literature data and COSMOtherm liquid-liquid equilibrium lines have the same form and very close values to each other even though the calculations have been done for three different temperatures. COSMOtherm calculations with the three different temperatures show the same form and similar values when they are compared to each other. It could be expected that the higher temperatures have positive effects on the miscibility and therefore as a result smaller miscibility gaps than the calculations at lower temperatures but in this case the calculations with COSMOtherm at 30°C show slightly lower equilibrium line than the calculations at 40°C and 50°C. Some additional calculations at different temperatures with and without “compute renormalized LLE” option can be found in Appendix (fig. 8-5, fig. 8-6, fig. 8-7, fig. 8-8).

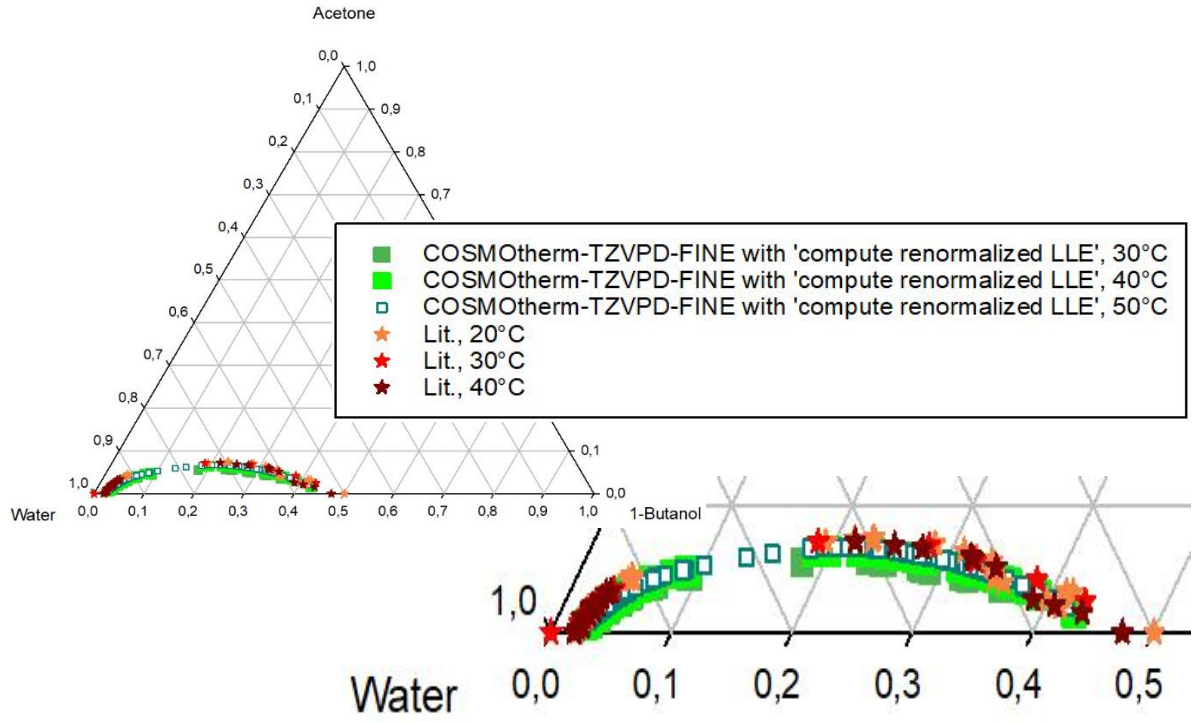


**Fig. 6-14. LLE diagram of "1-butanol-acetone-water" with COSMOtherm, TZVPD-FINE level with 'compute renormalized LLE' option and literature data [52-54], (mole fractions)**

### 6.5.1.2. Liquid-Liquid Equilibrium of Ternary System "1-Butanol-Acetone-Water" with Aspen Plus

In fig. 6-15**,** Aspen Plus calculations with NRTL-1 User [35], UNIQUAC LLE Aspen options and literature data [52-54] from same sources as explained in chapter 6.5.1.1 are displayed. UNIQUAC LLE option shows good accordance with literature data unlike NRTL-1 User option as this option gave similar results for the binary system calculations showing a relatively higher miscibility gap than literature data, even though the plait point reaches a higher acetone mole fraction than literature data. 1-Butanol mole fractions for the temperatures 30°C and 50°C are lower than literature data 1-butanol mole fractions as well. NRTL-1 User option shows a miscibility gap with higher acetone mole fraction for calculations at 30°C than for calculations at 50°C and 1-butanol mole fraction at 30°C higher than at 50°C, having a smaller miscibility gap at higher temperatures. Thus UNIQUAC LLE Aspen option has the closest results to literature data showing deviations only for intermediate 1-butanol mole fractions and the temperature difference for the given temperatures do not seem to make a considerable effect on this option.

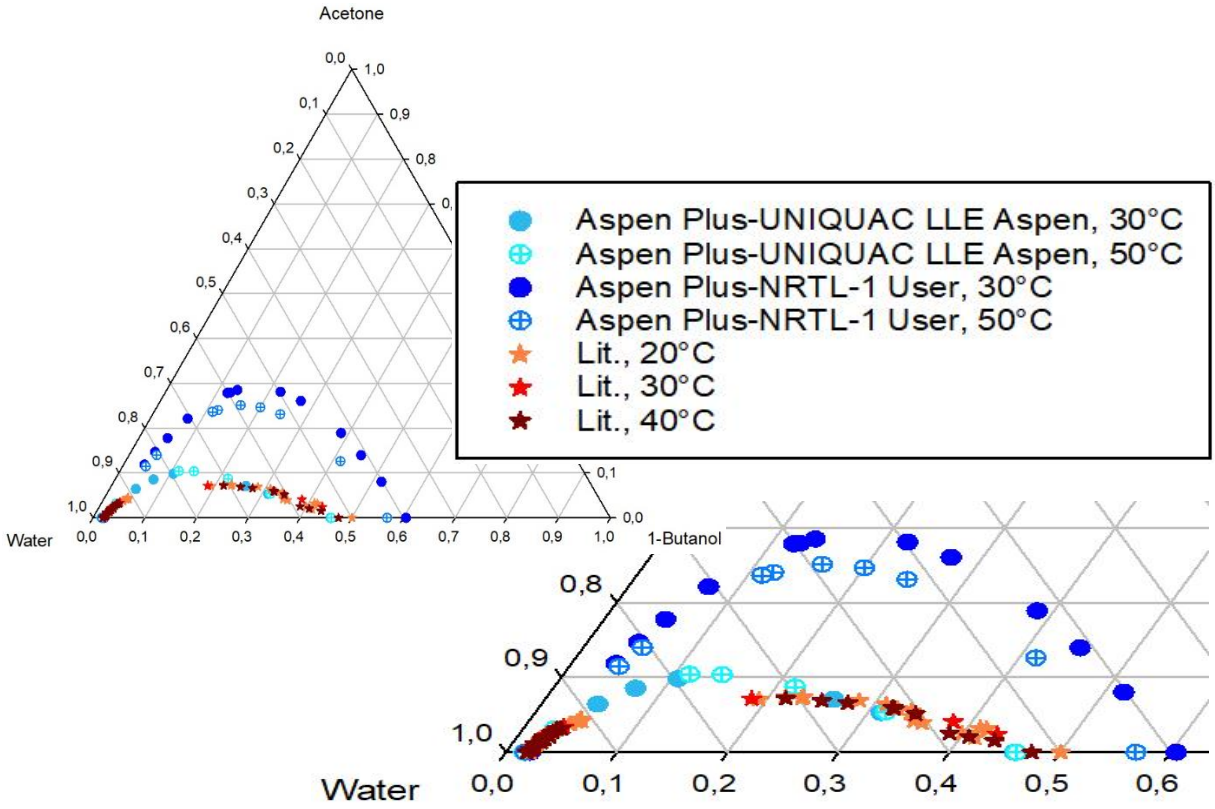


**Fig. 6-15. LLE diagram of "1-butanol-acetone-water" with Aspen Plus-UNIQUAC LLE Aspen, NRTL-1 User [35] options, and literature data [52-54], (mole fractions)**

### 6.5.1.3. Liquid-Liquid Equilibrium of Ternary System "1-Butanol-Acetone-Water" with Aspen Plus and COSMOtherm

Fig. 6-16, shows COSMOtherm-TZVPD-FINE level with "compute renormalized LLE" option, Aspen Plus-UNIQUAC LLE Aspen option and literature data from different sources [52-54]. COSMOtherm and Aspen Plus options equilibrium lines for lower and higher 1-butanol mole fractions both show good accordance to literature data. COSMOtherm results for intermediate 1-butanol mole fractions seems to fit literature data better than Aspen Plus. COSMOtherm gives a lower equilibrium line than literature data and Aspen Plus equilibrium line reaches to a higher point than literature data.

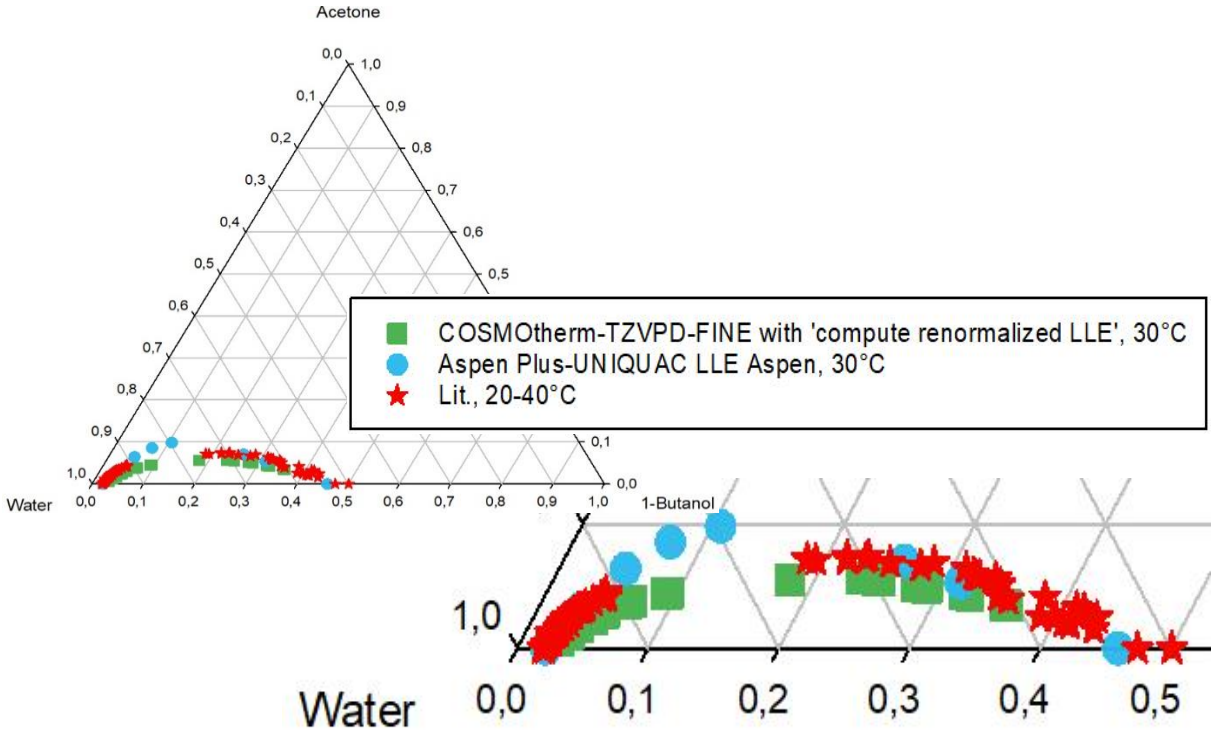


**Fig. 6-16. LLE diagram of "1-butanol-acetone-water" with COSMOtherm-TZVPD-FINE level with 'compute renormalized LLE' option, Aspen Plus-UNIQUAC LLE Aspen option and literature data [52-54], (mole fractions)**

### 6.5.2. Liquid-Liquid Equilibrium of Ternary System "1-Butanol-Ethanol-Water"

#### 6.5.2.1. Liquid-Liquid Equilibrium of Ternary System "1-Butanol-Ethanol-Water" with COSMOtherm

Fig. 6-17, shows COSMOtherm-TZVPD-FINE level with 'compute renormalized LLE' option calculated at 30°C and 50°C and literature data from Koichi et al. [50] and Dechema Chemistry Data Series [55] at 25°C. Literature data temperature shows a consistent equilibrium line with a gap and only small deviations are to be seen at higher 1-butanol mole fractions. Literature data and the calculations with COSMOtherm show an accordance in form of the equilibrium line but calculated values are lower than literature data values resulting in lower equilibrium lines. Since the calculations are done at higher temperatures than literature data temperature, a smaller miscibility gap is expected. But COSMOtherm calculations at lower temperature 30°C gives a lower equilibrium line with lower ethanol and 1-butanol fractions than the calculations at higher temperature 50°C and therefore a smaller miscibility gap. The difference between COSMOtherm and literature data equilibrium line is not significant, therefore it can be assumed that the temperature difference is negligible and the LLE lines for COSMOtherm calculations are in good accord with literature data. An additional diagram with COSMOtherm-TZVPD-FINE level calculation without "compute renormalized LLE" option at 25°C and literature data can be found in Appendix (fig. 8-9), as well as some other calculations at different temperatures with and without this option (fig. 8-10, fig. 8-11, fig. 8-12, fig. 8-13).

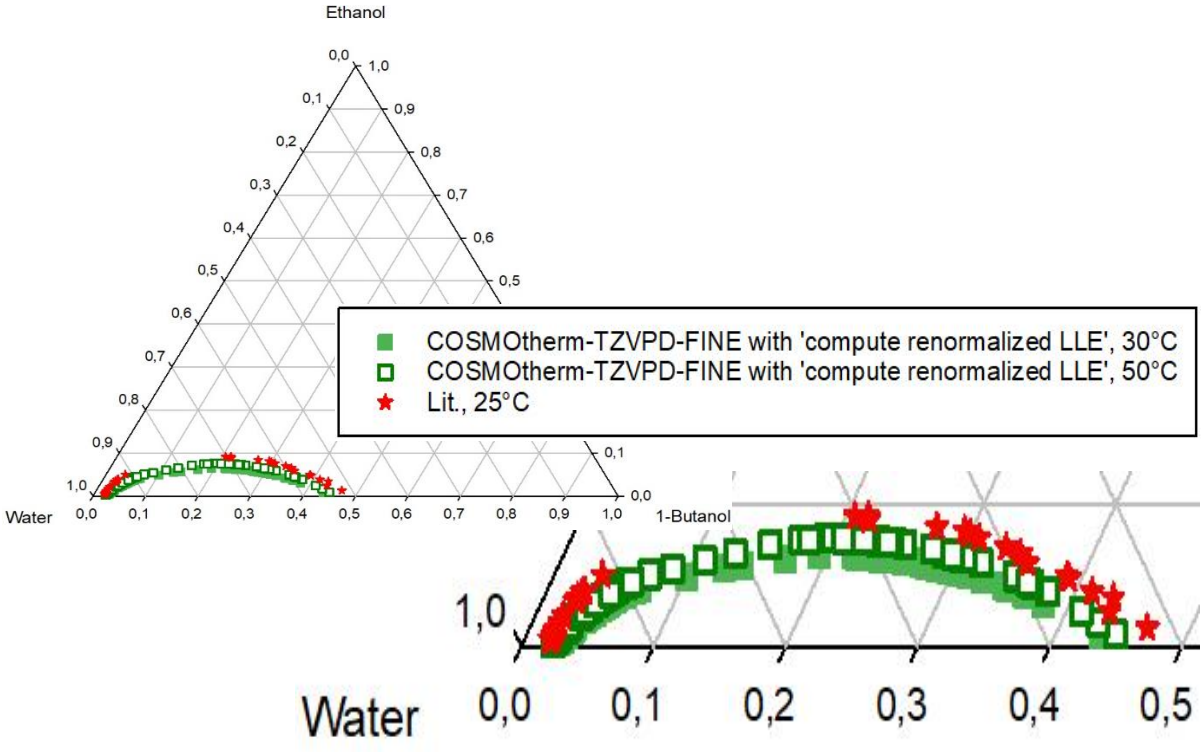


**Fig. 6-17. LLE diagram of "1-butanol-ethanol-water" with COSMOtherm-TZVPD-FINE level with 'compute renormalized LLE' option and literature data [50], [55], (mole fractions)**

### 6.5.2.2. Liquid-Liquid Equilibrium of Ternary System "1-Butanol-Ethanol-Water" with Aspen Plus

Diagram, fig. 6-18, shows the Aspen Plus calculations of LLE "1-butanol-ethanol-water" with NRTL-1 User and UNIQUAC LLE Aspen options with the literature data [50], [55]. Aspen Plus calculation with UNIQUAC LLE Aspen option has closer values to literature data than NRTL-1 User option as for the previous binary and ternary system phase equilibrium calculations. Ethanol mole fraction for calculated values are higher than literature data miscibility gap. UNIQUAC LLE Aspen option at 30 and 50°C show similar values for LLE lines with each other. Equilibrium line at 50°C is slightly lower than at 30°C. Both LLE lines with this option and literature data are in good accordance for low and high butanol mole fractions but results do not match well for intermediate mole fractions (0.1 to 0.3) resulting in a larger miscibility gap. NRTL-1 User option equilibrium line values show a decrease as the calculation temperature increases. From these values, it can be assumed that the temperature effect is considerably small and this option is not in good accord with literature data.

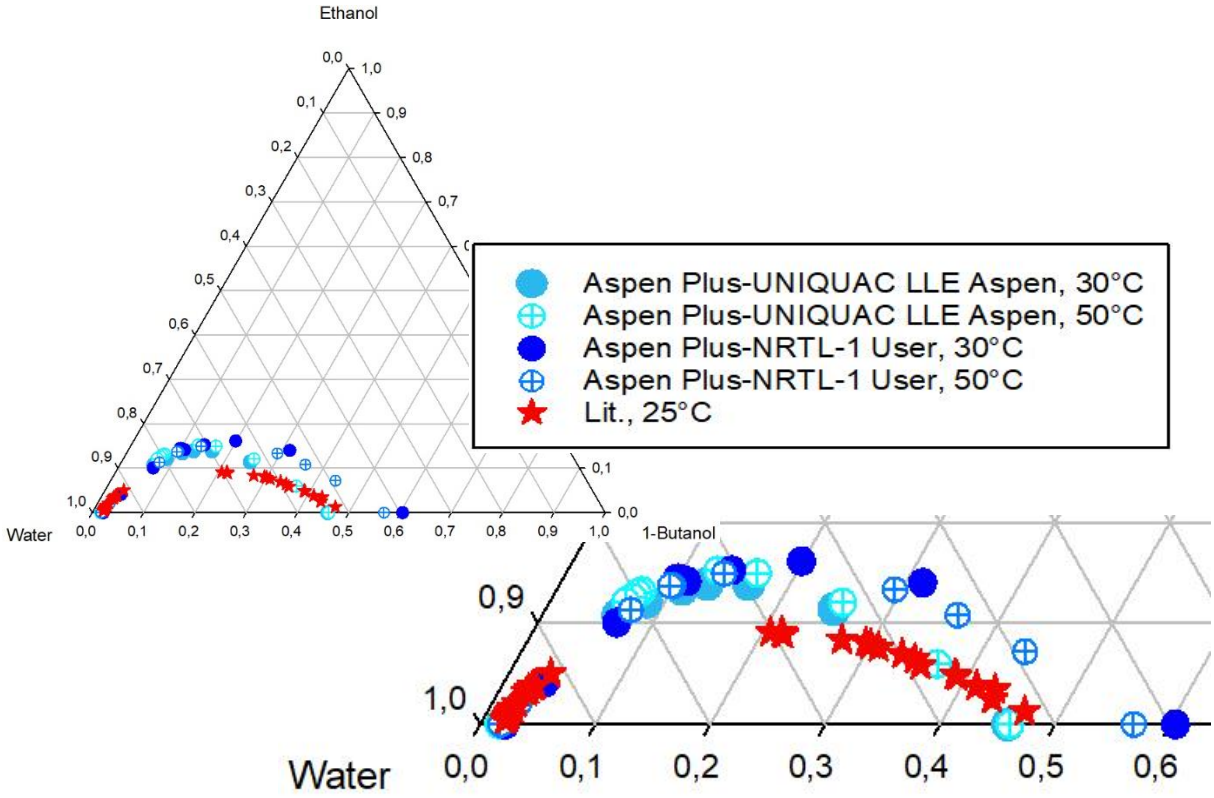


**Fig. 6-18. LLE diagram of "1-butanol-ethanol-water" with Aspen Plus, UNIQUAC LLE Aspen, NRTL-1 User [35] options and literature data [50], [55], (mole fractions)**

### 6.5.2.3. Liquid-Liquid Equilibrium of Ternary System "1-Butanol-Ethanol-Water" with Aspen Plus and COSMOtherm

Diagram, fig. 6-19**,** displays COSMOtherm-TZVPD-FINE level with "compute renormalized LLE" option, Aspen Plus-UNIQUAC LLE Aspen option and literature data [50], [55]. Literature data LLE line is between the LLE of these options, TZVPD-FINE level showing lower values than literature data and UNIQUAC LLE Aspen showing higher values than literature data resulting in lower equilibrium line with TZVPD-FINE level and higher equilibrium line with UNIQUAC LLE Aspen option than literature data. Although UNIQUAC LLE Aspen option shows good accordance to literature data at low and high mole fractions it has a higher miscibility gap than literature data. TZVPD-FINE level calculations seem more in accordance with literature data than calculations with UNIQUAC LLE Aspen option.

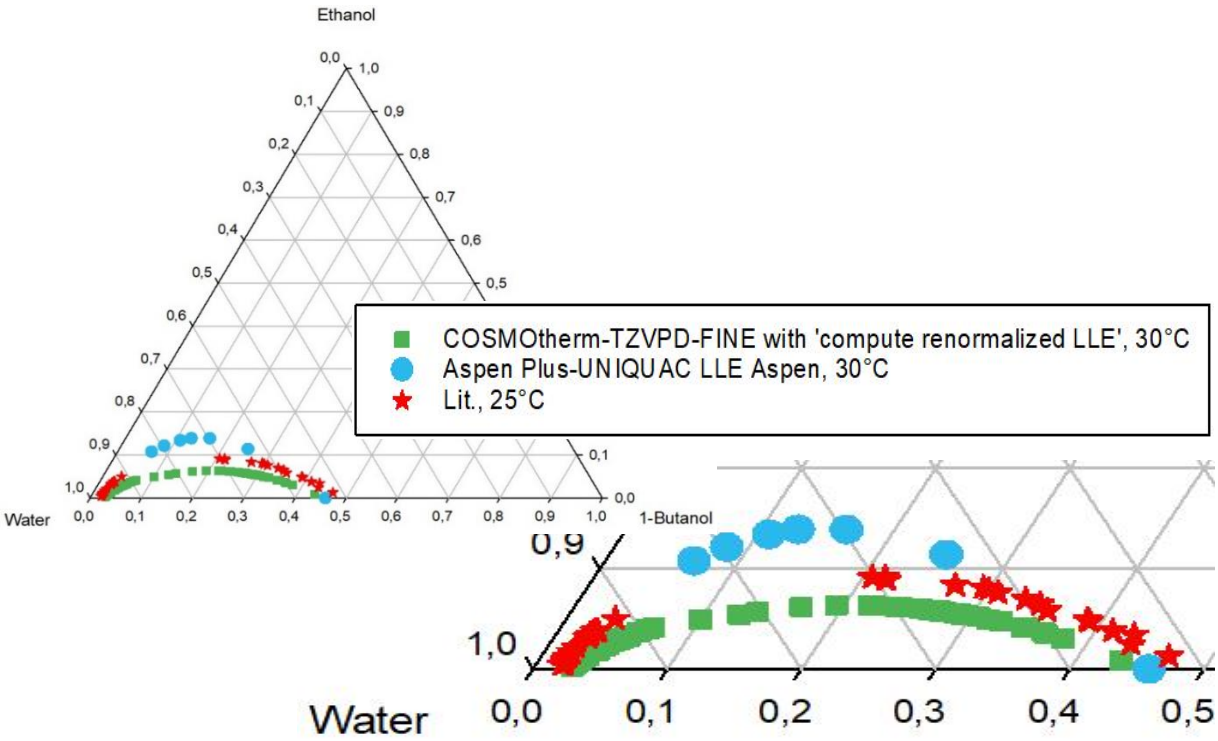


**Fig. 6-19. LLE diagram of "1-butanol-ethanol-water" with COSMOtherm-TZVPD-FINE level with 'compute renormalized LLE' option, Aspen Plus-UNIQUAC LLE Aspen option and literature data [50], [55], (mole fractions)**

### 6.5.2.4. Liquid-Liquid Equilibrium of Ternary System "1-Butanol-Ethanol-Water" with COSMOtherm and Aspen Plus

Diagram, fig. 6-20, displays calculations at 1013.25 mbar with COSMOtherm-TZVPD-FINE level with renormalized LLE option and Aspen Plus-NRTL-1 User option and literature data taken from Koichi et al. [50]. Literature data is available only at low and high 1-butanol mole fractions therefore it does not show a clear form for the miscibility gap. TZVPD-FINE level and UNIQUAC LLE Aspen option show a good accordance with literature data at low 1-butanol mole fractions, at higher 1-butanol mole fractions Aspen Plus calculations show deviations whereas COSMOtherm results fit literature data much better although its miscibility gap seems wider. NRTL-1 User option seems to fit literature data at lower 1-butanol mole fractions as well but at higher 1-butanol mole fractions shows a significant difference to literature data 1-butanol mole fraction.

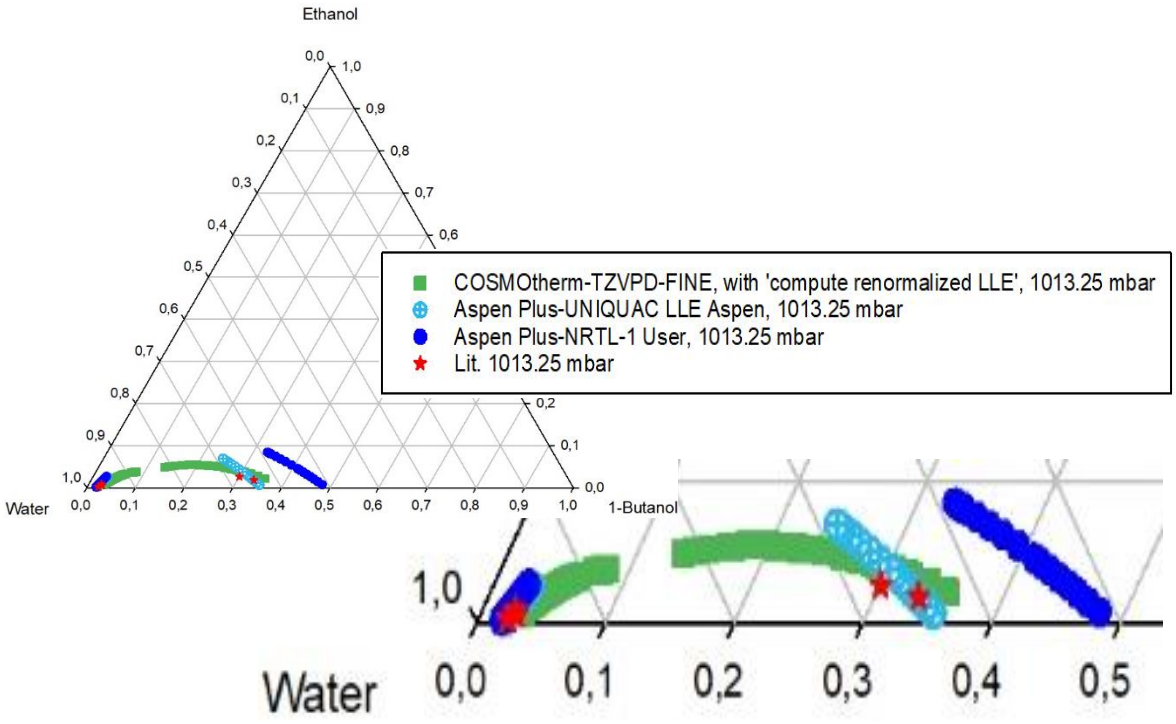


**Fig. 6-20. LLE of "1-butanol-ethanol-water" at 1013.25 mbar with COSMOtherm-TZVPD-FINE with 'renormalized LLE', Aspen Plus-UNIQUAC LLE Aspen, NRTL-1 User [35] options, literature data [50], (mole fractions)**

## 6.6. Liquid-Liquid Equilibrium of Quaternary System "1-Butanol-Acetone-Ethanol-Water"

Quaternary systems are four-component systems, which contain 1-butanol, acetone, ethanol and water in this work. Quaternary systems require a multi dimensional display (a tetrahedral diagram) for a complete representing. To avoid multi-dimensional diagrams that cannot be read with a high degree of accuracy, only two-dimensional ternary diagrams are displayed for quaternary systems here.

Acetone and ethanol affect the phase separation because of their miscibility with butanol and water. However, degree of their effects can vary because they have different physicochemical properties. The previous calculations of ternary systems showed that acetone and ethanol have similar effects on the system "1-butanol-water" and displaying the quaternary system of 1-butanol, acetone, ethanol and water with a ternary diagram therefore is possible, showing different concentrations of acetone and ethanol at a fixed butanol concentration. The composition diagram for "1-butanol-water" systems under isothermal conditions are calculated by COSMOtherm and Aspen Plus simulations according to the procedure in chapters 5.1.3 and 5.2.3.

In fig. 6-21 the two ternary systems, "1-butanol-acetone-water" and "1-butanol-ethanol-water" calculated by COSMOtherm-TZVPD-FINE level with "compute renormalized LLE" option, Aspen Plus-UNIQUAC LLE Aspen option and literature data [50], [52-55] are displayed to compare the effects of acetone and ethanol on "1-butanol-water" system. Literature data equilibrium lines for mole fractions of ethanol and acetone show similar values with a lower

equilibrium line for acetone. COSMOtherm results for both equilibrium lines with ethanol and acetone are very close to each other but mole fraction of acetone is slightly lower than ethanol mole fraction. The two systems are in good accord with each other but they have smaller miscibility gaps than literature data. UNIQUAC LLE Aspen option for both systems show also a similar result with a smaller miscibility gap for the ternary mixture with acetone than with ethanol and both systems have with bigger miscibility gaps than literature data. The results indicate that acetone and ethanol have similar influence on the miscibility gap of ternary systems with 1-butanol and water. Therefore, it is possible to display the effect of ethanol and acetone present at the same time in a quaternary system in a ternary diagram.

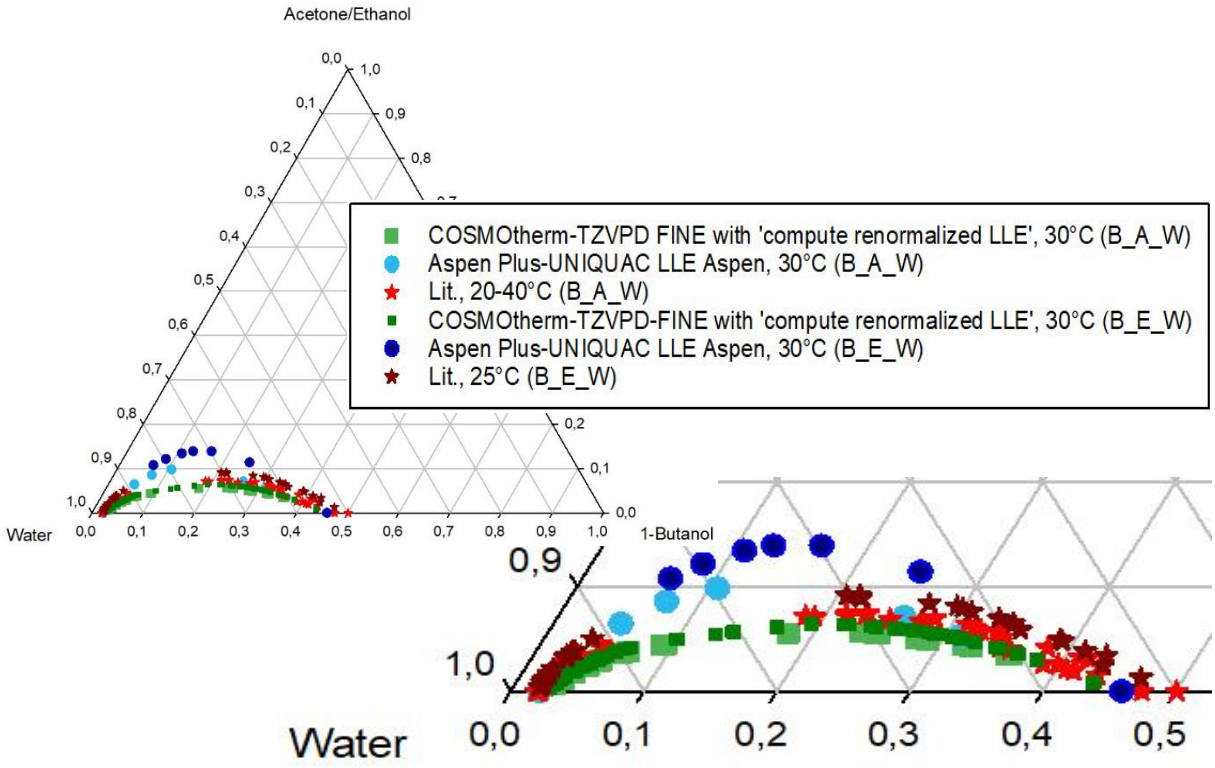


**Fig. 6-21. LLE diagram of "1-butanol-acetone-water" and "1-butanol-ethanol-water" with COSMOtherm-TZVPD-FINE level with 'compute renormalized LLE' option, Aspen Plus-UNIQUAC LLE Aspen option and literature data [50], [52-55], (mole fractions)**

Ternary diagram in fig. 6-22, shows results for liquid-liquid equilibrium of quaternary system "1-butanol-acetone-ethanol-water" calculated at 30°C by COSMOtherm-TZVPD-FINE level with 'compute renormalized LLE' option, Aspen Plus-UNIQUAC LLE Aspen option and literature data at 25°C from Dechema Chemistry Data Series [56]. In order to display the quaternary system in a ternary diagram acetone and ethanol values are summed for each calculation and literature data. Literature data shows a consistent liquid-liquid equilibrium line at lower 1-butanol mole fractions but shows inconsistent values at higher 1-butanol mole fractions. LLE lines of COSMOtherm-TZVPD-FINE level and Aspen Plus-UNIQUAC LLE Aspen option are in good accordance with literature data at lower 1-butanol mole fractions. At higher 1-butanol mole fractions, Aspen Plus and COSMOtherm seem to fit literature data range with UNIQUAC LLE Aspen option showing slightly lower equilibrium line than the equilibrium line calculated with COSMOtherm. Since literature data at this part of the equilibrium is not forming a clear line it is hard to tell which equilibrium line is a better fit to literature data. From the diagram, fig. 6-22, the differences for both COSMOtherm and Aspen Plus options are

insignificant and both simulations are in good accordance with literature data. Thus, these simulations give reliable results for the liquid-liquid equilibrium calculations of quaternary system “1-butanol-acetone-ethanol-water”.

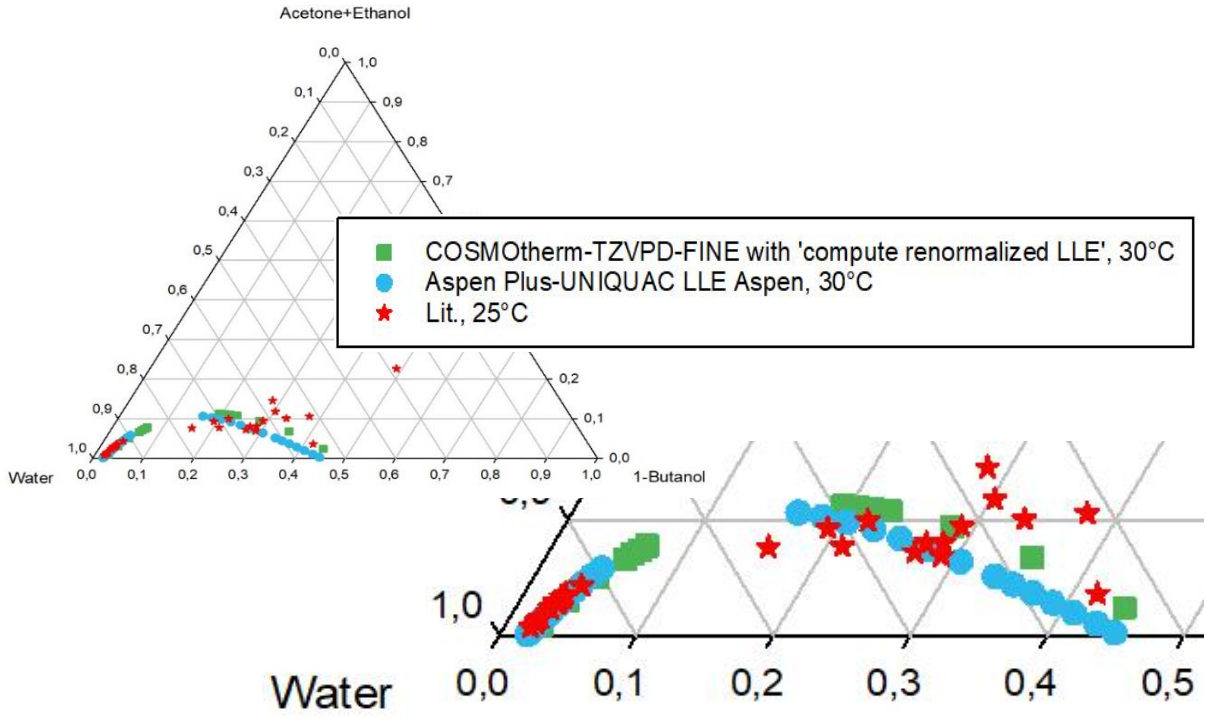


**Fig.6- 22. LLE diagram of “1-butanol-acetone-ethanol-water”, COSMOtherm-TZVPD-FINE with ‘compute renormalized LLE’, Aspen Plus-UNIQUAC LLE Aspen and literature data [56], (mole fractions)**

# 7. Summary, Conclusion and Outlook

Renewable 1-butanol is produced from the fermentation of carbohydrates in a process called ABE fermentation, after its major chemical products: acetone, butanol and ethanol. The production of acetone, butanol and ethanol (ABE) mixtures using the anaerobic bacterium Clostridium acetobutylicum has potential commercial significance. However, a barrier for the commercial development of the fermentation process is the fact that it suffers severely from product inhibition caused principally by butanol. One way to overcome this would be to couple the fermentation process to a continuous product removal technique, so that inhibitory product concentrations are never reached [4]. The classical distillation process for the removal of butanol is far too energy demanding, an economical biofuel/biobutanol production requires further investigation in separation processes [5].

The design and optimization of the biofuel purification requires a model that can describe the phase equilibria of water-alcohol systems. The capacity to describe the water solubility in biofuels is important to insure the fuel quality during production, since water affects biofuel calorific value, shelf life and composition and can cause engine problems [7]. The accurate knowledge of the most important property data, vapor pressure, activity coefficient, liquid-liquid-equilibrium (LLE) and vapor-liquid-equilibrium (VLE) is thus essential for the design of the separation and purification processes. The thermodynamic properties of binary, ternary and quaternary mixtures including “butanol-water” lead to a wide range of options available for the recovery of butanol from aqueous solution, by varying temperature, pressure or composition. These data are documented to some extent in literature but often not in sufficient amount or only at questionable consistence available. This information can be reached via experimental methods or process simulations.

A very promising and efficient method in this context is COSMO-RS, which was investigated in this work. The main advantage of COSMO-RS is that it uses quantum chemically generated charge density surfaces to describe each molecule and its interactions with other molecules. It is therefore universally applicable without using group parameters or any system-specific adjustments. Additionally, activity coefficient models like NRTL and UNIQUAC, available via simulations environment of Aspen Plus, are used describe this multicomponent system for the calculations of vapor pressures, activity coefficients and phase equilibriums of binary, ternary and quaternary systems of the ABE fermentation solvents (acetone, 1-butanol, ethanol, water). Several options (databanks, QC levels) of both simulations are used for the calculations and comparison with the literature data has been performed in order to assess the prediction quality of the calculation tools under different conditions in the named multi-component system.

### Results summary:

#### Vapor pressures:

- Vapor pressure of pure component 1-butanol. COSMOtherm and Aspen Plus-Antoine options are in good accordance with literature data.
- Vapor pressure of pure component acetone, COSMOtherm-Wagner option and Aspen Plus-Antoine options are fitting literature data very well, but COSMOtherm-TZVPD-FINE option shows poor results with rather a lower vapor pressure line. Aspen Plus-Antoine option and COSMOtherm-Wagner option calculations are based on agreed parameters and therefore in good accordance with literature data.

- Vapor pressure of pure component ethanol, COSMOtherm-Wagner and Aspen Plus-Antoine options fit literature data very well, while COSMOtherm-TZVPD-FINE option shows lower vapor pressure values, which gets more remarkable at higher temperatures. it can be concluded that it is important to choose the Wagner option for pvap calculation, if the VLE calculations of a mixture including acetone with COSMOtherm is required. Wagner coefficients are available in COSMOtherm and resulting in high accuracy, hence higher accuracy in subsequent VLE calculations can be achieved with this option.
- Vapor pressure of pure component water, COSMOtherm-TZVPD-FINE option shows the lowest vapor pressure line at temperatures between 20 – 170°C and have no common value with literature data. The parameters for the vapor pressure calculations of literature data (lit.1, lit.2) show a clear difference, resulting in two different lines with no connecting values. Lit.1 consists of different literature data, which are in accord with each other. While COSMOtherm-Wagner and Aspen Plus-UNIQUAC LLE Aspen options are in good accordance with lit.1, lit.2 is between COSMOtherm-TZVPD-FINE, and other two options, showing lower literature data line, without having any connection point with any other option.

**Activity Coefficients:**

- For the activity coefficient of 1-butanol at infinite dilution, different behavior of activity coefficient over temperature is obtained for used COSMOtherm levels. The three COSMOtherm levels TZVPD-FINE, DMOL3, SVP give different values from each other but a similar curve form to literature data. SVP has the highest activity coefficient values among other levels. TZVPD-FINE level activity coefficient line seems to be the closest to literature data showing slightly lower values than literature data.
- As the calculations with three QC levels of COSMOtherm are repeated for the components acetone and ethanol the results showed that TZVPD-FINE level is the best option for 1-butanol and ethanol, and SVP level is the best option for acetone.
- Activity coefficient of 1-butanol values at infinite dilution, NRTL-1 User [35] option adapted to fit activity coefficients shows the best fitting results to literature data. UNIQUAC LLE Aspen and COSMOtherm-TZVPD-FINE options are in literature data range. COSMOtherm data show lowest activity coefficients of all calculated options and thus strongest deviation from literature data at lower temperature. At higher temperature COSMOtherm data fit literature data better than Aspen Plus calculations based on UNIQUAC LLE Aspen option. However, COSMOtherm results never reached accuracy of Aspen Plus calculations with based on NRTL-1 User interaction parameters.
- Calculations with Aspen Plus-NRTL-1 VLE-IG, UNIQUAC VLE-IG options and COSMOtherm-SVP level for the activity coefficient at infinite dilution of acetone show deviatios from literature data until temperatures of around 60°C, but they are in good accord with literature data. For temperatures higher than 60°C COSMOtherm levels both show an increase of activity coefficients while Aspen Plus options show a decrease. It is hard to compare calculated values with literature data at higher temperatures than 60°C, since at higher temperatures literature data is not available in sufficient amount.
- Literature data values for activity coefficient of ethanol at infinite dilution are strongly inconsistent values showing deviations. Aspen Plus calculations based on UNIQUAC and NRTL-1 seem to better follow literature data over the temperature range. COSMOtherm

results show a stronger dependence on temperature, but seem to fit literature data at higher temperature better than Aspen Plus calculations.

**Vapor-liquid-equilibrium of binary system "1-butanol-water":**

- Vapor-liquid equilibrium of binary system "1-butanol-water" calculations with COSMOtherm levels at 1013.25 mbar for evaluating the accuracy and suitability of COSMOtherm QC levels with "search LLE" suboption gives TZVPD-FINE level as the best among the three QC levels of COSMOtherm, bubble point curve showing deviations from literature data with slightly higher temperatures. DMOL3 level is the second best option for this calculation and SVP level comes as a third option giving the highest deviations from literature data especially for the bubble point curve and azeotropic point at a slightly higher temperature and a lower 1-butanol mole fraction.
- Vapor-liquid equilibrium of binary system "1-butanol-water" calculations with Aspen Plus, at 1013.25 mbar give Aspen Plus-NRTL-1 User option [35] as the best fitting option, showing good accordance with literature data, fitting dew point, bubble point curves and azeotropic point very well. UNIQUAC LLE Aspen and NRTL-1 LLE Aspen have azeotropic points considerably shifted to higher temperatures and lower mole fractions of 1-butanol.
- COSMOtherm-TZVPD-FINE level and Aspen Plus-NRTL-1 User option are in good accordance with the literature data at 1013.25 mbar. Aspen Plus-NRTL-1 User option calculations based on empirical parameters gives only slightly better results than the predictive calculations of COSMOtherm-TZVPD-FINE level.
- Less data points are available for higher pressures in literature, for the vapor-liquid equilibrium of binary system "1-butanol-water" at 1013.25, 1980 and 4920 mbar, but dew point and bubble point curves have a clear form. When the calculated values of Aspen Plus-NRTL-1 and COSMOtherm-TZVPD-FINE level with search LLE option at higher pressures, 1980 and 4920 mbar are compared with literature data at these pressures the same behavior as the calculations at 1013.25 mbar regardless the pressures. For the calculations at higher pressures TZVPD-FINE level is still the best QC level.

**Liquid-liquid-equilibrium of binary system "1-butanol-water":**

- Aspen Plus options NRTL-1 LLE Aspen and UNIQUAC LLE Aspen calculations for liquid-liquid equilibrium of binary system "1-butanol-water" have similar form with literature data LLE line except the curving of the equilibrium lines with the calculated values at higher 1-butanol concentrations, yet UNIQUAC LLE Aspen option gives slightly better results when compared to literature data. NRTL-1 User option [35] does not have the same form for the equilibrium line as the other Aspen Plus options and the values show a remarkable difference to literature data. Although NRTL-1 User option showed good accordance with literature data for the activity coefficients and VLE calculations, it shows less compatible results for the LLE calculations of "1-butanol-water". Both COSMOtherm options show a similar form to literature data but they also show a curving at higher 1-butanol mole fractions like the two Aspen Plus options, NRTL-1 LLE Aspen and UNIQUAC LLE Aspen. COSMOtherm-TZVPD-FINE level with renormalization of LLE points accounting for thermodynamic fluctuations in the liquid mixture gives more realistic results. The miscibility gap without 'compute renormalized LLE' option reaches relatively higher temperatures than with this option. Thus TZVPD-FINE level with 'compute renormalized LLE' is more

compatible than the calculations without “compute renormalized LLE” option for the LLE calculations with COSMOtherm.

**Liquid-liquid-equilibrium of ternary system “1-butanol-acetone-water”:**

- LLE “1-butanol-acetone-water” literature data is available for three different temperatures showing the same equilibrium line with small deviations at higher 1-butanol concentrations. COSMOtherm LLE lines have the same form and very similar values with literature data even though the calculations have been done for three different temperatures. COSMOtherm calculations with three different temperatures show the same equilibrium line form and similar values when they are compared to each other. It could be expected that the higher temperatures have positive effects on the miscibility and as a result smaller miscibility gaps than the calculations at lower temperatures, but in this case the calculations with COSMOtherm at 30°C show lower equilibrium line than the calculations at 40°C and 50°C.
- UNIQUAC LLE Aspen option shows good accordance with literature data unlike NRTL-1 User option as this option gave similar results for the binary system “1-butanol-water”. NRTL-1 User option shows a bigger miscibility gap for calculations at 30°C than for calculations at 50°C and literature data. UNIQUAC LLE option shows closer results to literature data with 1-Butanol mole fractions lower than literature data and deviations from literature data for intermediate 1-butanol mole fractions. The temperature difference at given temperatures do not seem to make a considerable effect on the calculations with this option. Thus UNIQUAC LLE Aspen option is more reliable option for this calculation.
- COSMOtherm-TZVPD-FINE level with ‘compute renormalized LLE’ option and Aspen Plus-UNIQUAC LLE Aspen option equilibrium lines have similar 1-butanol mole fraction to literature data. Literature data equilibrium line is between COSMOtherm and Aspen Plus equilibrium lines, where COSMOtherm has a lower equilibrium line and Aspen Plus has a higher equilibrium line than literature data. Aspen Plus shows a good accordance with literature data at higher 1-butanol mole fractions.
- COSMOtherm show an accordance with literature data in form of the equilibrium line but calculated values are lower than literature data values resulting in lower equilibrium lines. Since the calculations are done at higher temperatures than literature data temperature, a smaller miscibility gap is expected. But COSMOtherm calculations at lower temperature 30°C gives a lower equilibrium line than the calculations at higher temperature 50°C and therefore a smaller miscibility gap. The difference between COSMOtherm and literature data equilibrium line is not significant, therefore it can be assumed that the temperature difference is negligible and the LLE lines for COSMOtherm calculations are in good accord with literature data.

**Liquid-liquid-equilibrium of ternary system “1-butanol-ethanol-water”:**

- Aspen Plus calculation with UNIQUAC LLE Aspen option has closer values to literature data than NRTL-1 User option as for the previous binary and ternary system phase equilibrium calculations. Calculated values have higher equilibrium line than literature data. UNIQUAC LLE Aspen option at 30 and 50°C show similar values for LLE lines to each other. Equilibrium line at 50°C is slightly lower than at 30°C. Both LLE lines with this option and literature data are in good accordance for low and high butanol mole fractions but

results do not match well for intermediate mole fractions (0.1 to 0.3) resulting in a larger miscibility gap. NRTL-1 User option equilibrium line values show a decrease as the calculation temperature increases. From these values, it can be assumed that the temperature effect is considerably small and NRTL-1 User option is not in good accord with literature data.

- Literature data LLE line is between the LLE of COSMOtherm-TZVPD-FINE level with "compute renormalized LLE" option, Aspen Plus-UNIQUAC LLE Aspen option. TZVPD-FINE level has lower equilibrium line than literature data and UNIQUAC LLE Aspen option shows good accordance to literature data at low and high 1-butanol mole fractions but it has a higher equilibrium line than literature data. TZVPD-FINE level calculations seem more in accordance with literature data than calculations with UNIQUAC LLE Aspen option.
- Literature data is available only at low and high 1-butanol mole fractions for LLE line at 1013.25 mbar. Therefore, it does not show a clear form for the miscibility gap. Calculations at 1013.25 mbar with TZVPD-FINE level and UNIQUAC LLE Aspen option show a good accordance with literature data at low 1-butanol mole fractions, at higher 1-butanol mole fractions Aspen Plus calculations show deviations whereas COSMOtherm results fit literature data much better although its miscibility gap seems wider. NRTL-1 User option seems to fit literature data at lower 1-butanol mole fractions as well but at higher 1-butanol mole fractions shows a significant difference to literature data 1-butanol mole fraction.

**Liquid-liquid-equilibrium of ternary system "1-butanol-acetone-ethanol-water":**

- Two ternary systems, "1-butanol-acetone-water" and "1-butanol-ethanol-water" equilibrium lines for mole fractions of ethanol and acetone show similar values with a lower equilibrium line for acetone. COSMOtherm results show smaller miscibility gaps than literature data for both systems. UNIQUAC LLE Aspen option for both systems show bigger miscibility gaps than literature data. The results indicate that acetone and ethanol have similar influence on the miscibility gap of ternary systems with 1-butanol and water. Therefore, it is possible to display the effect of ethanol and acetone present at the same time in a quaternary system in a ternary diagram.
- LLE of quaternary system "1-butanol-acetone-ethanol-water" calculated at 30°C by COSMOtherm-TZVPD-FINE level with 'compute renormalized LLE' option, Aspen Plus-UNIQUAC LLE Aspen option and literature data at 25°C is displayed in a ternary diagram by summing acetone and ethanol values. Literature data is consistent at lower 1-butanol mole fractions but shows inconsistent values at higher 1-butanol mole fractions. LLE lines of COSMOtherm-TZVPD-FINE level and Aspen Plus-UNIQUAC LLE Aspen option are in good accordance with literature data at lower 1-butanol mole fractions. At higher 1-butanol mole fractions, Aspen Plus and COSMOtherm seem to fit literature data range with UNIQUAC LLE Aspen option showing slightly lower equilibrium line than COSMOtherm. Since literature data at this part of the equilibrium is not forming a clear line it is hard to tell which equilibrium line is a better fit to literature data. Differences for both COSMOtherm and Aspen Plus options are insignificant and both simulations are in good accordance with literature data. Thus, these simulations give reliable results for the liquid-liquid equilibrium calculations of quaternary system "1-butanol-acetone-ethanol-water".

## Conclusion:

The results showed that quantum chemical calculations of COSMO-RS (mostly TZVPD-FINE level) and Aspen Plus (UNIQUAC LLE Aspen option for most cases and NRTL-1 User option for some cases) give closest results to literature data. COSMO-RS theory provides good predictions of chemical potentials and activity coefficients and can be extended in many other directions by the addition of small pieces of empiricism. The concept of surface polarization charge densities $\sigma$, as local polarity measures, of $\sigma$ -profiles, and of $\sigma$-potentials, provides a relatively simple and understandable pathway from the molecular details to the macroscopic thermodynamics of liquid systems. It proves to be very robust in many cases. If the suitable QC level and databank are used, both simulations COSMOtherm and Aspen Plus can provide reliable data for further research in optimizing the separation of aqueous acetone-butanol-ethanol mixtures, which results in more efficient and economical renewable liquid biofuel production.

## Outlook:

Some calculations can be repeated by varying temperatures, pessures, databanks, mixture concentrations as well as mixture combinations. Calculations can also be repeated via different simulations and experimental methods for comparison. Multinary systems can be displayed in multi-dimensional diagrams. Due to the approximations made within COSMO-RS and the limits of quantum chemistry, predictions are not perfect. The physical origins of the errors can be addressed by COSMO-RS specialists and a general improvement without special adjustments can be achieved for better results via this simulation.

# 8. Appendix

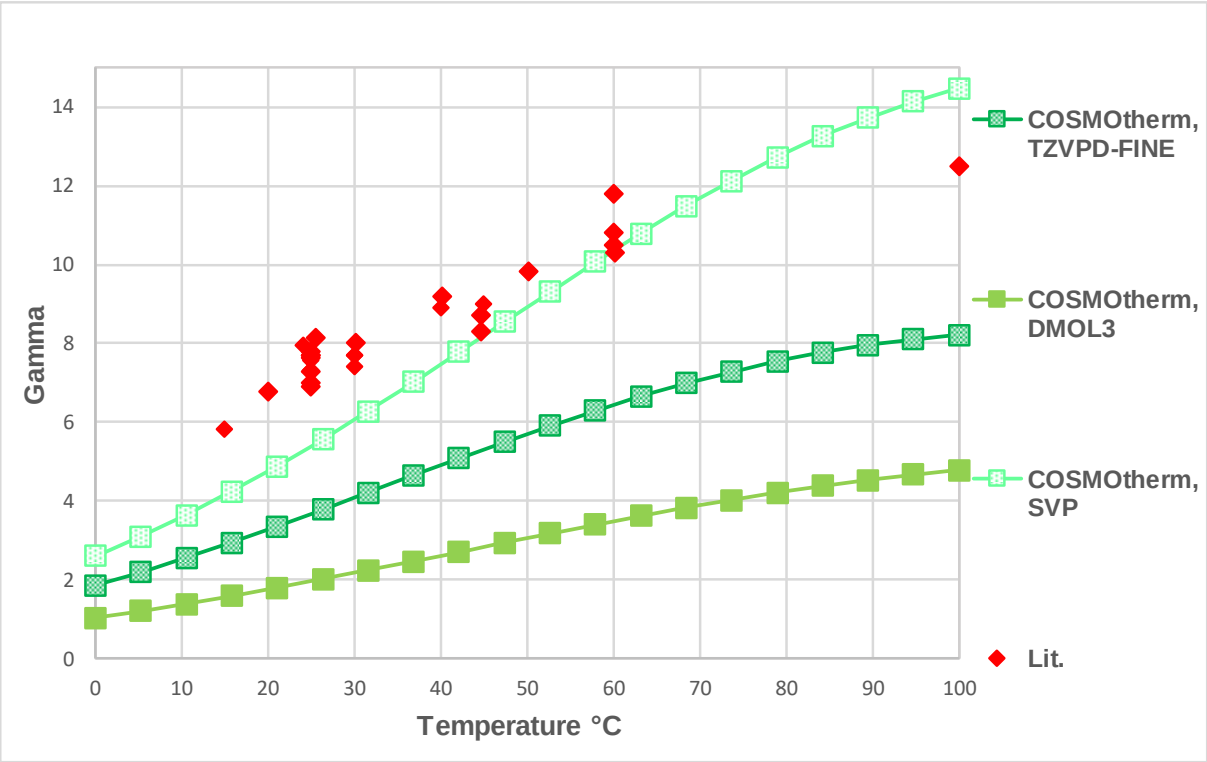


**Fig. 8-1. $\gamma^{\infty}$- Acetone at infinite dilutions with COSMOtherm-TZVPD-FINE, SVP, DMOL3 and literature data [42], [48]**

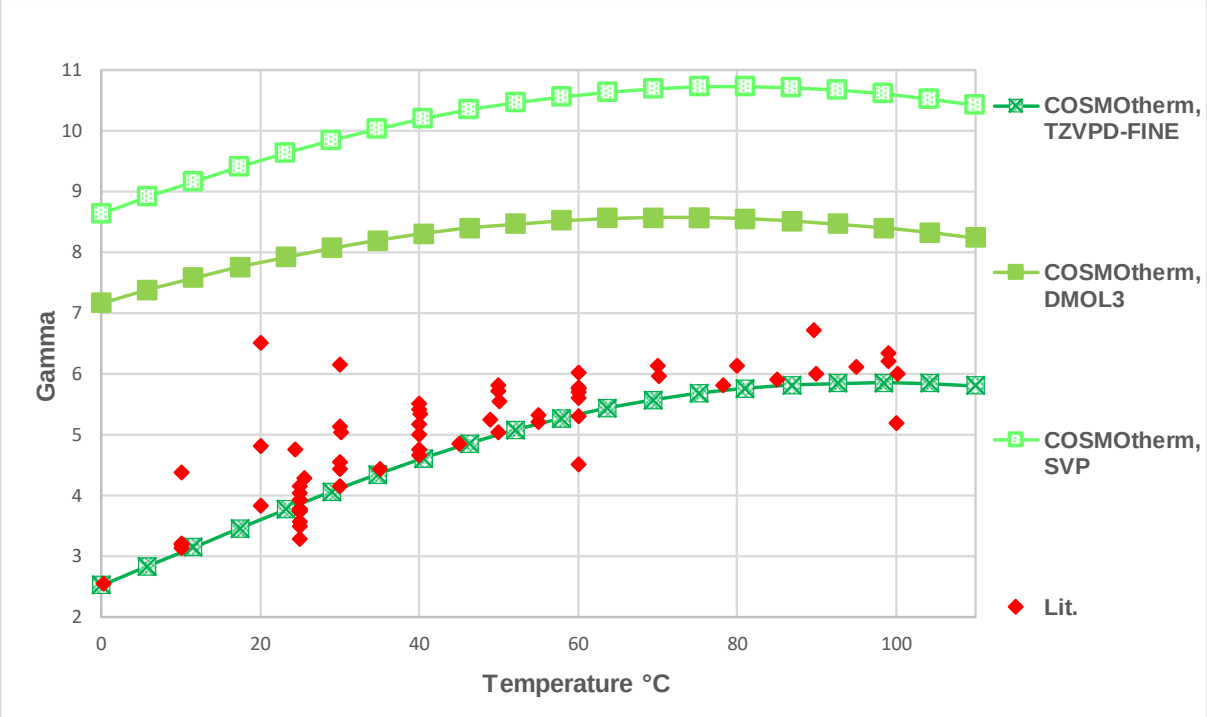


**Fig. 8-2. $\gamma^{\infty}$- Ethanol at infinite dilutions with COSMOtherm-TZVPD-FINE, DMOL3, SVP and literature data [49]**

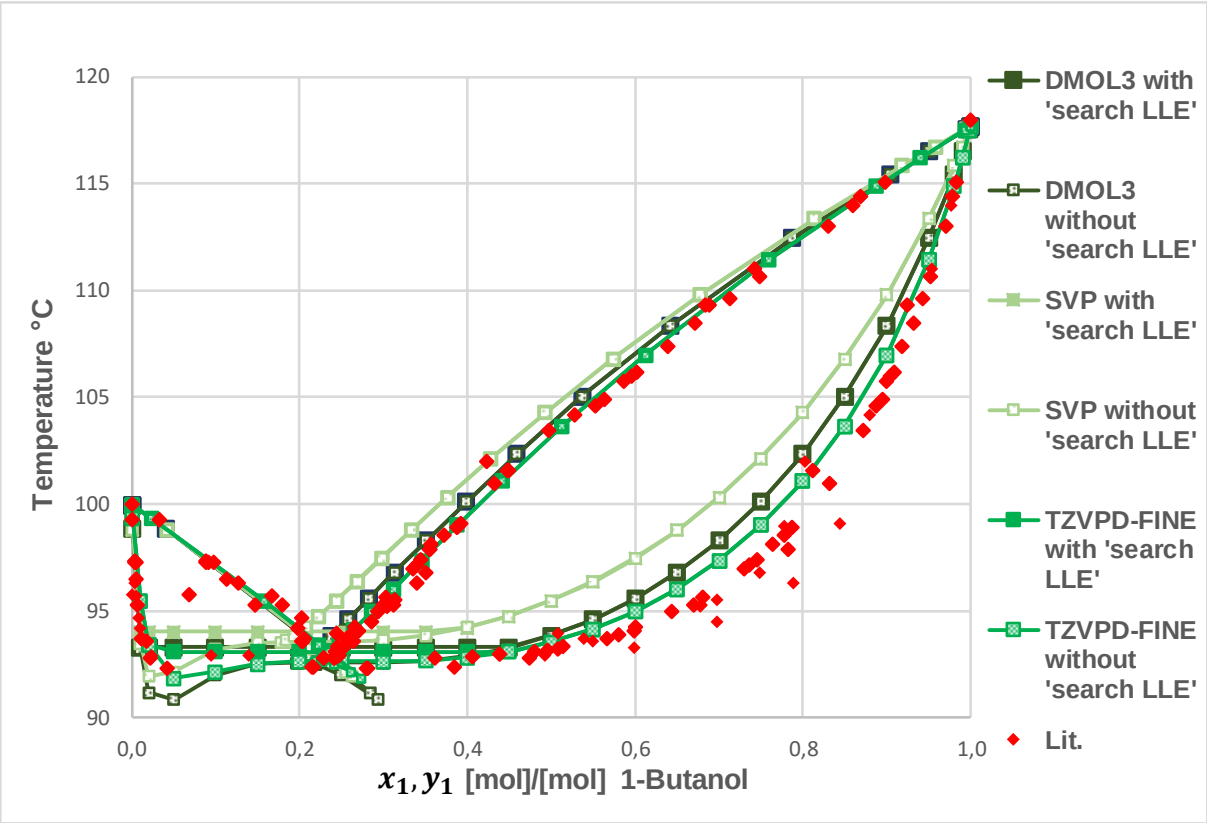


**Fig. 8-3. VLE of "1-butanol-water" at 1013.25 mbar, with COSMOtherm QC levels DMOL3, SVP, TZVPD-FINE with and without 'search LLE' option, literature data [49, 50]**

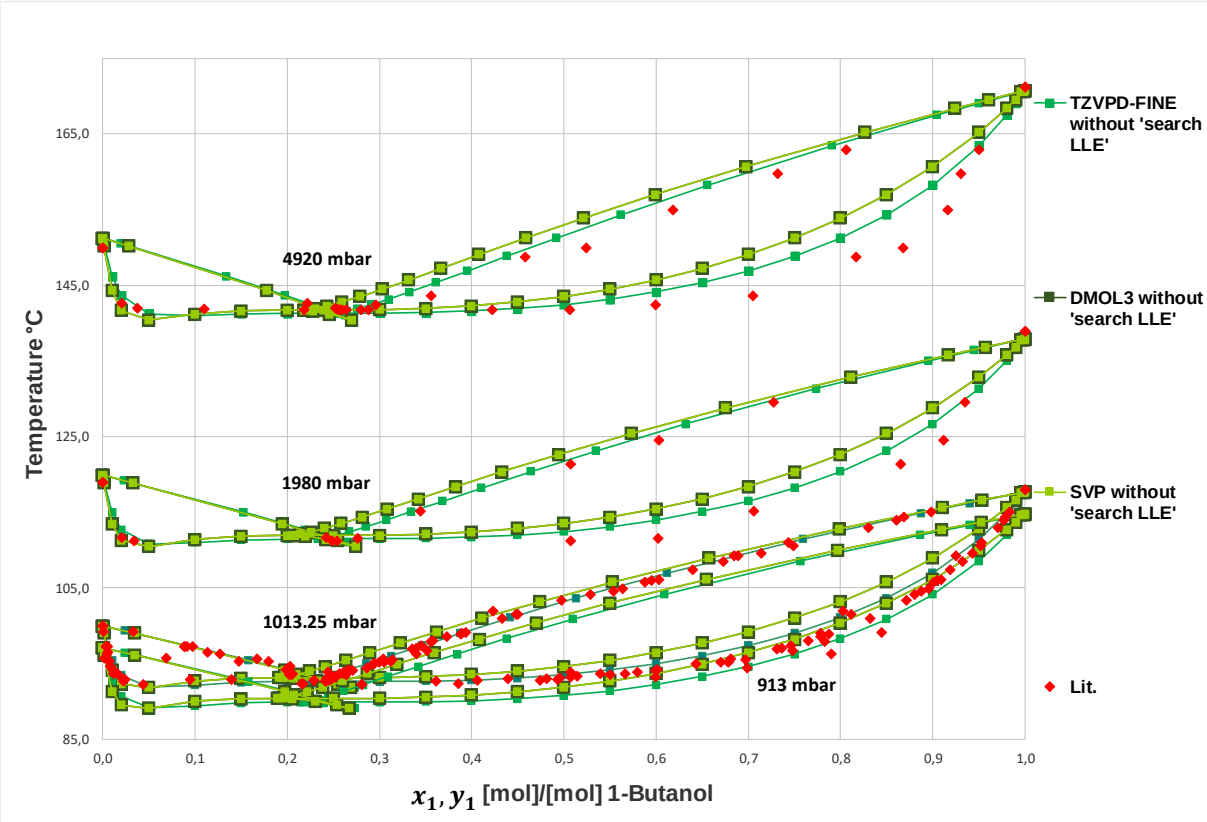


**Fig. 8-4. VLE of "1-butanol-water" at 913, 1013.25, 1980, 4920 mbar, with COSMOtherm QC levels DMOL3, SVP, TZVPD-FINE without 'search LLE' option and literature data [49, 50]**

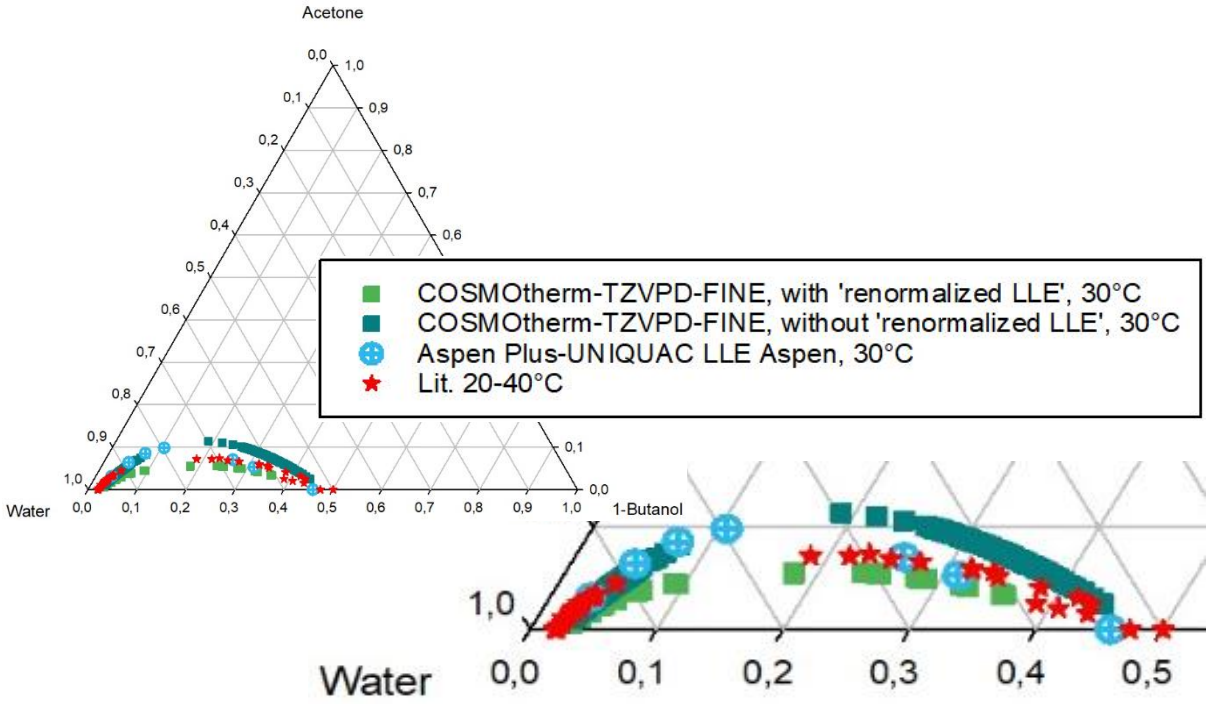


**Fig. 8-5. LLE of "1-butanol-acetone-water" at 30°C with COSMOtherm-TZVPD-FINE with and without 'renormalized LLE', Aspen Plus-UNIQUAC LLE Aspen options, literatur data [52-54], (mole fractions)**

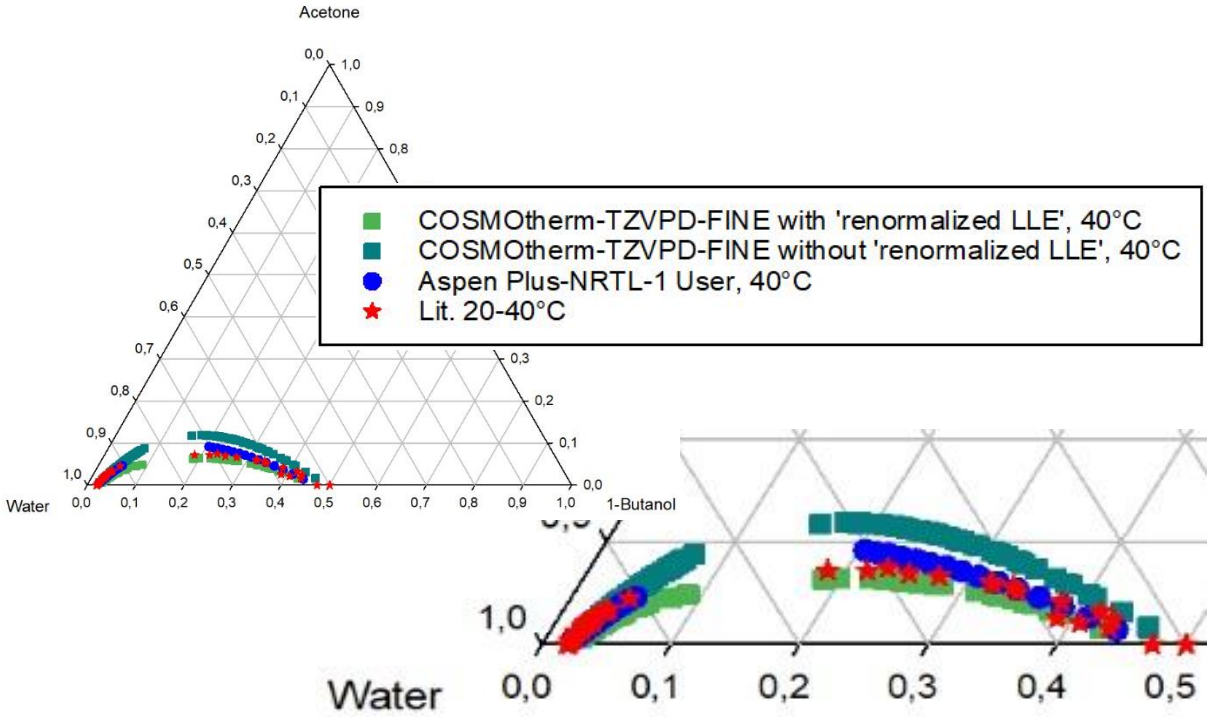


**Fig. 8-6. LLE of "1-butanol-acetone-water" at 40°C with COSMOtherm-TZVPD-FINE with and without 'renormalized LLE', Aspen Plus-NRTL-1 User [35] options, literatur data [52-54],(mole fractions)**

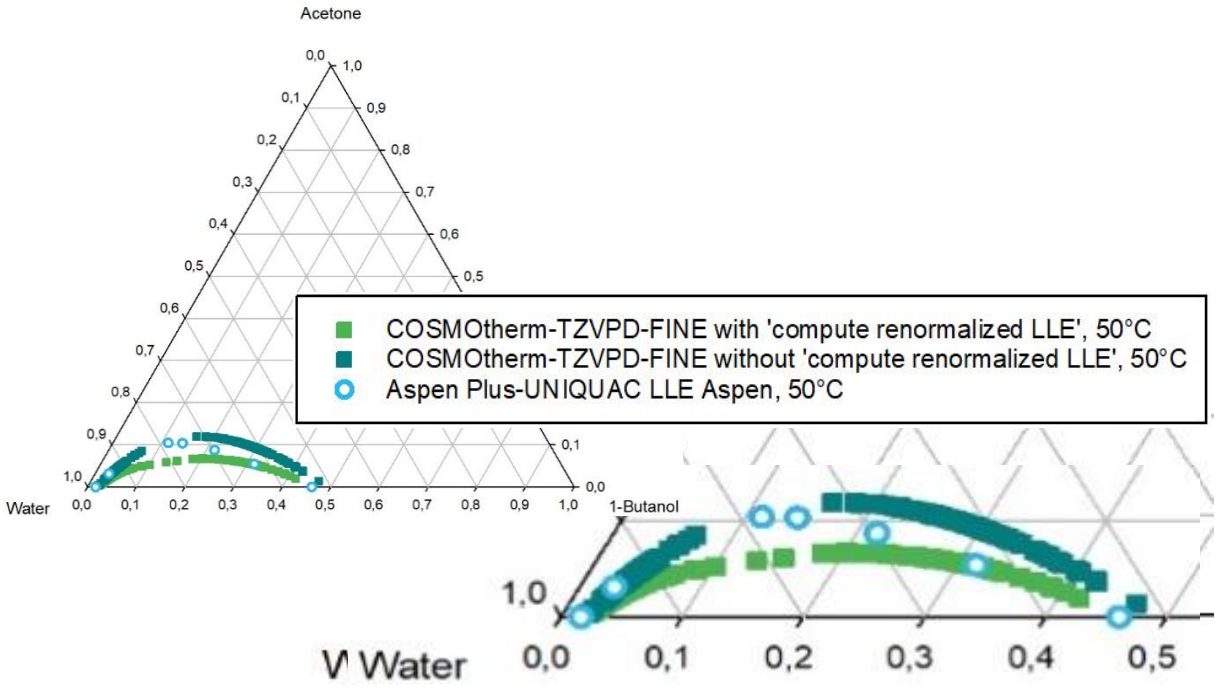


**Fig. 8-7. LLE of "1-butanol-acetone-water" at 50°C with COSMOtherm-TZVPD-FINE with and without 'renormalized LLE', Aspen Plus-UNIQUAC LLE Aspen options, (mole fractions)**

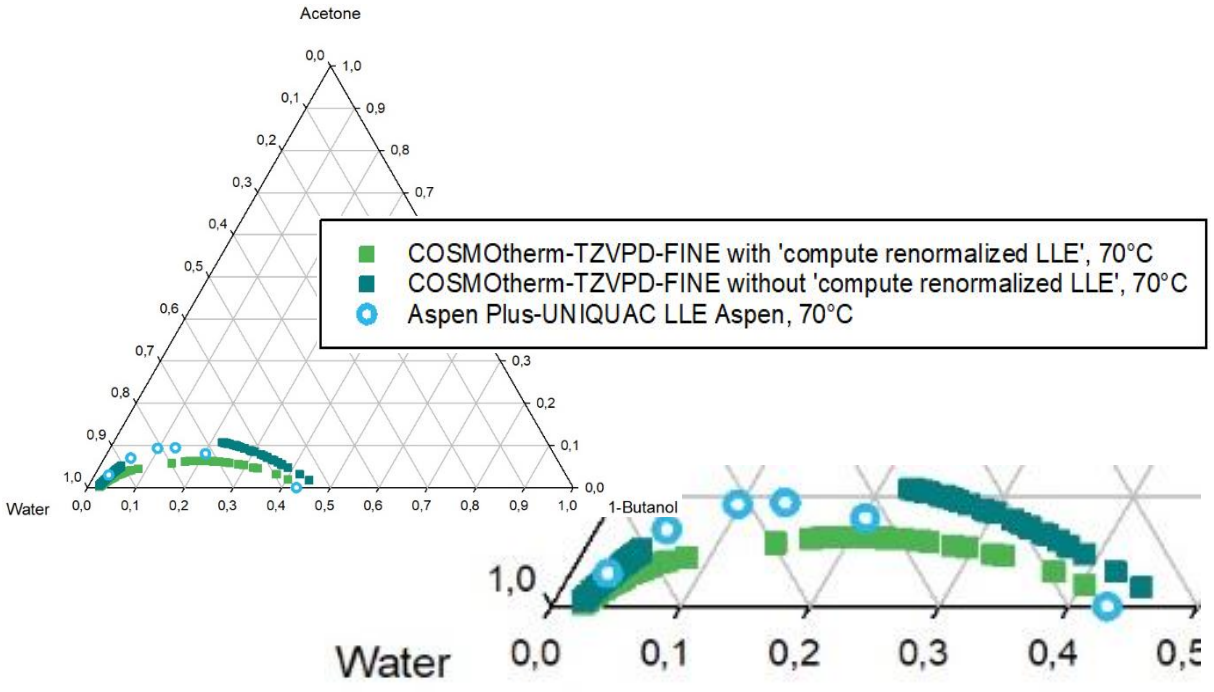


**Fig. 8-8. LLE of "1-butanol-acetone-water" at 70°C with COSMOtherm-TZVPD-FINE with and without 'renormalized LLE', Aspen Plus-UNIQUAC LLE Aspen options, (mole fractions)**

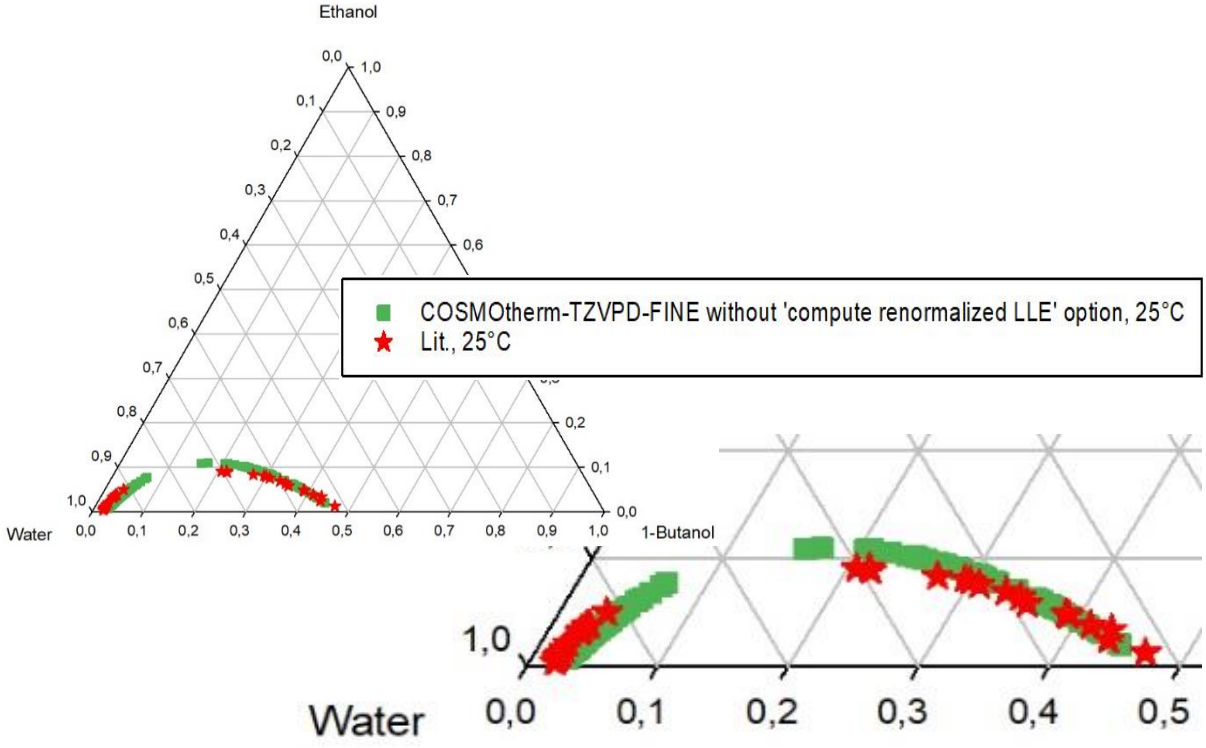


**Fig. 8-9. LLE of "1-butanol-ethanol-water" at 25°C with COSMOtherm-TZVPD-FINE without 'compute renormalized LLE' option and literature data [55], (mole fractions)**

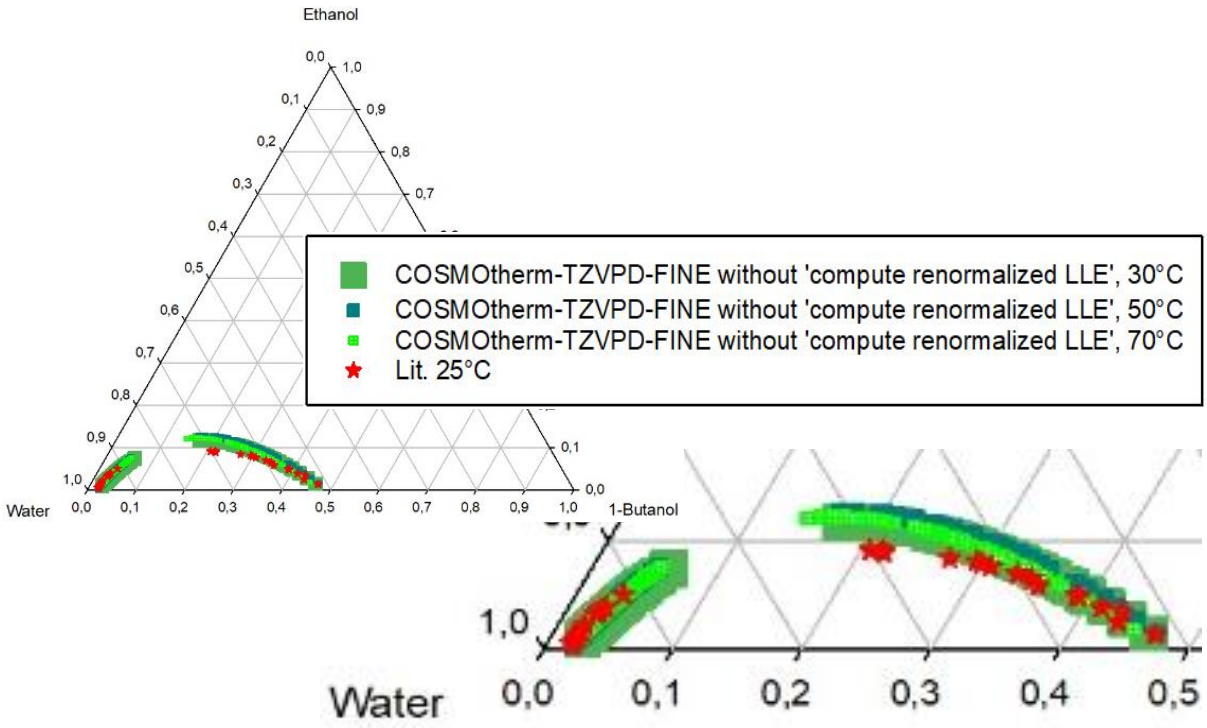


**Fig. 8-10. LLE of "1-butanol-ethanol-water" at 30, 50, 70°C with COSMOtherm-TZVPD-FINE without 'renormalized LLE' option, literature data [55], (mole fractions)**

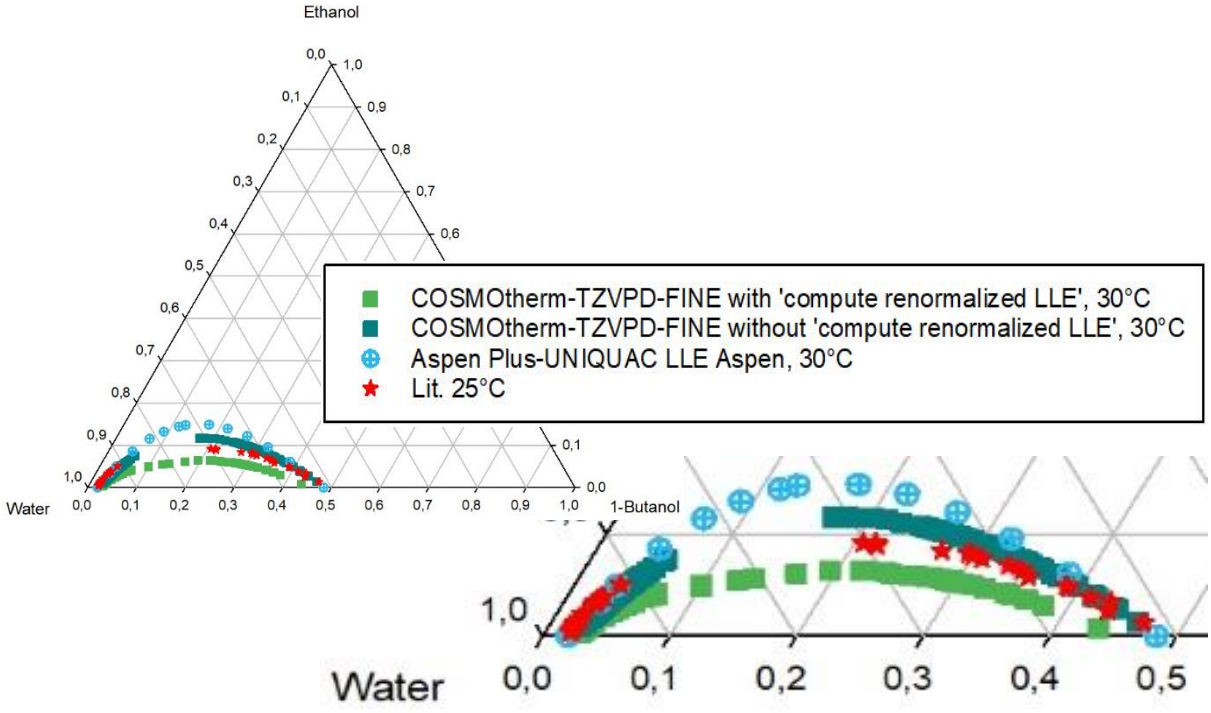


**Fig. 8-11. LLE of "1-butanol-ethanol-water" at 30°C with COSMOtherm-TZVPD-FINE with and without 'renormalized LLE', Aspen Plus-UNIQUAC LLE Aspen options, literature data [55], (mole fractions)**

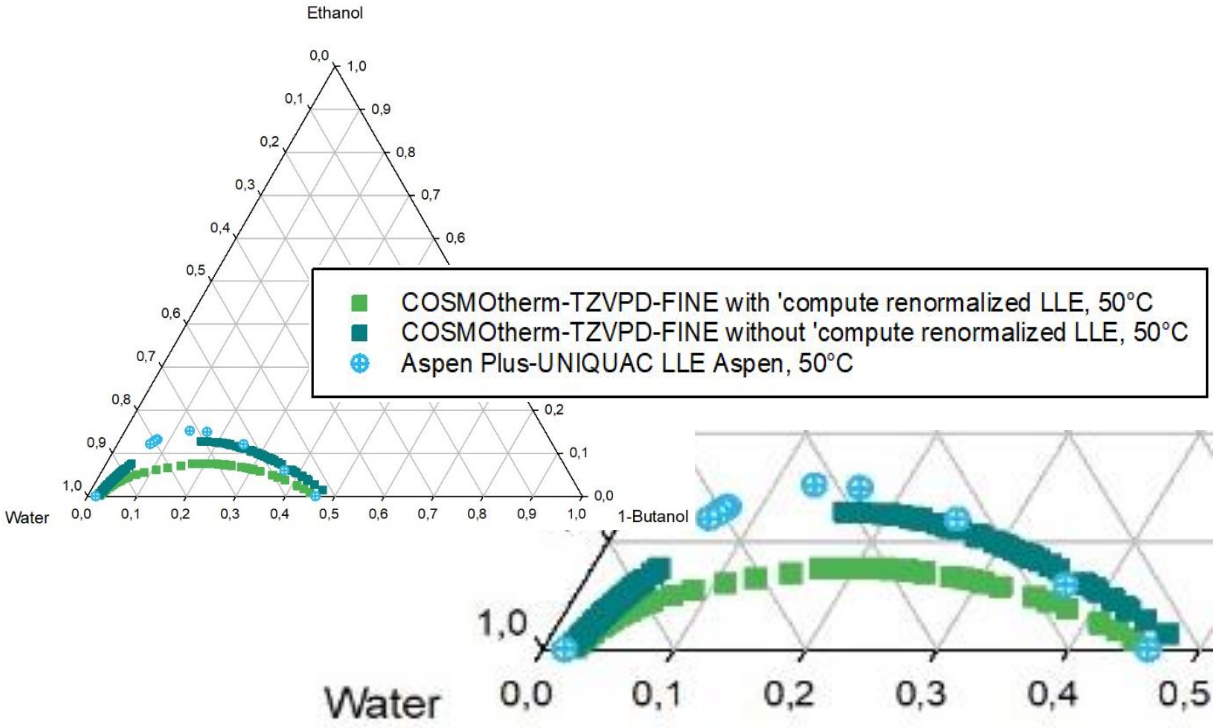


**Fig. 8-12. LLE of "1-butanol-ethanol-water" at 50°C with COSMOtherm-TZVPD-FINE with and without 'renormalized LLE', Aspen Plus-UNIQUAC LLE Aspen options, (mole fractions)**

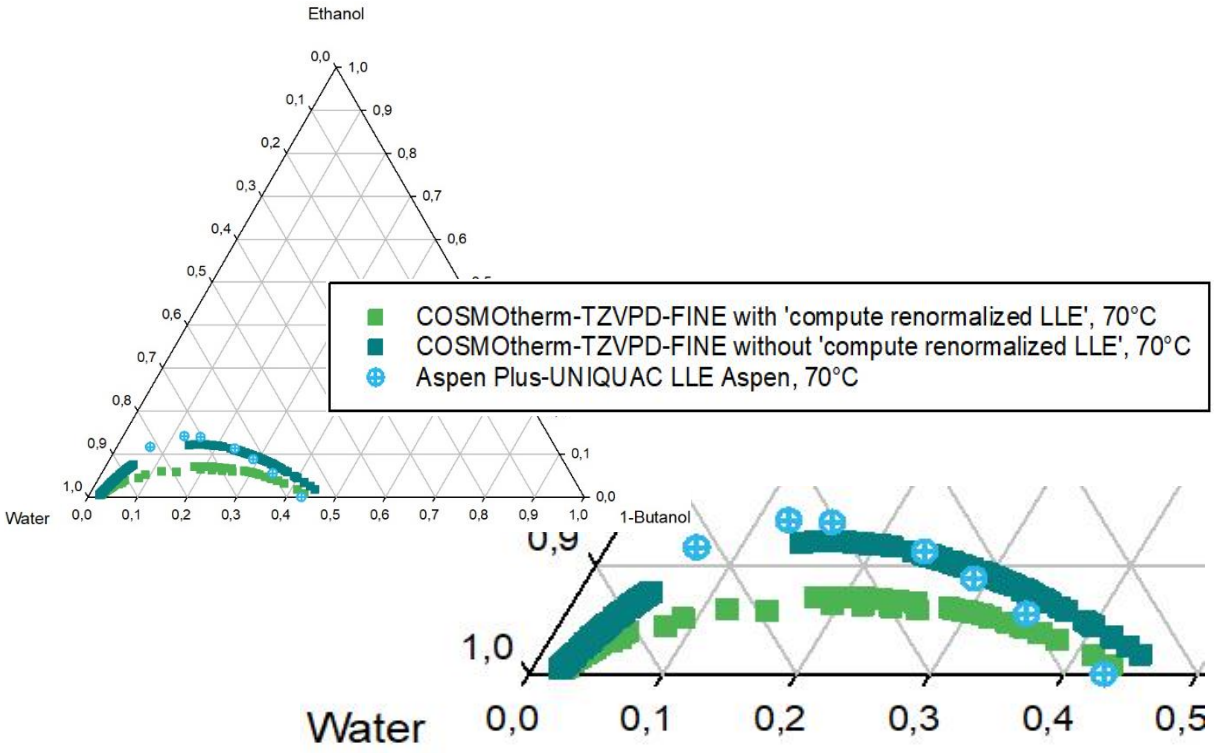


**Fig. 8-13. LLE of "1-butanol-ethanol-water" at 70°C with COSMOtherm-TZVPD-FINE with and without 'renormalized LLE', Aspen Plus-UNIQUAC LLE Aspen options, (mole fractions)**

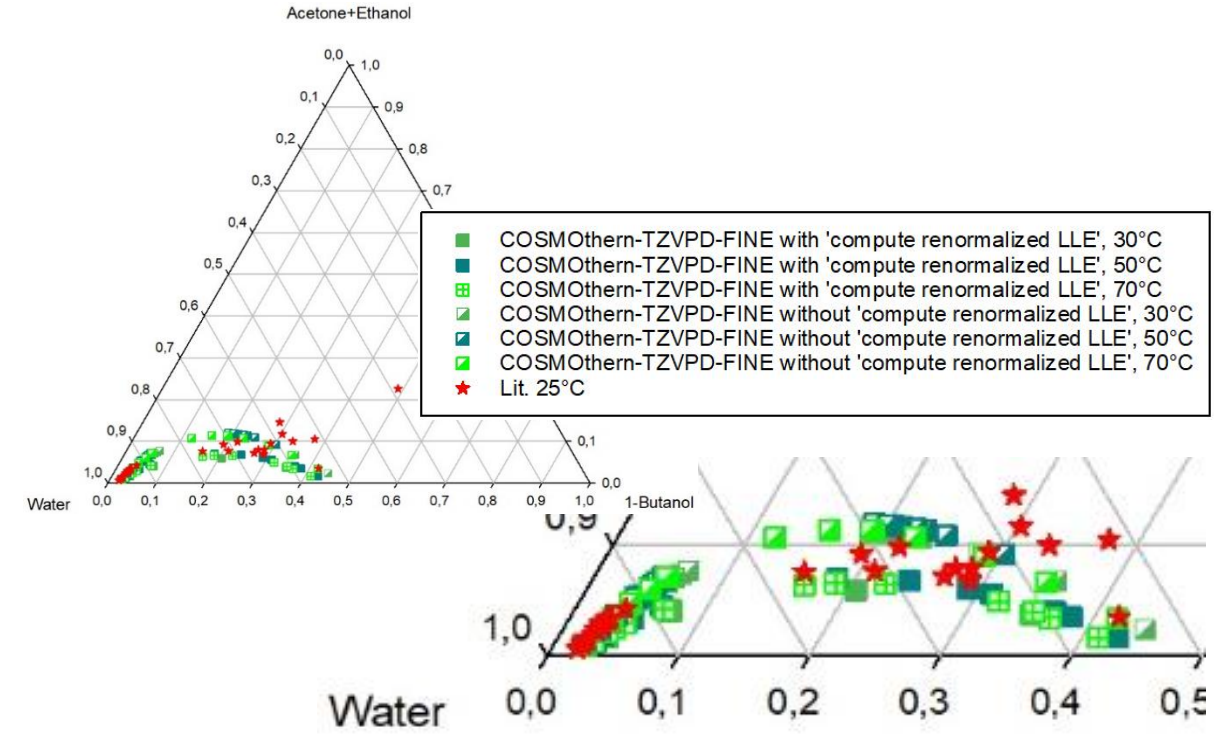


**Fig. 8-14. LLE of "1-butanol-ethanol-acetone-water" at 30, 50, 70°C mbar with COSMOtherm-TZVPD-FINE with and without 'compute renormalized LLE' options, literature data [56], (mole fractions)**

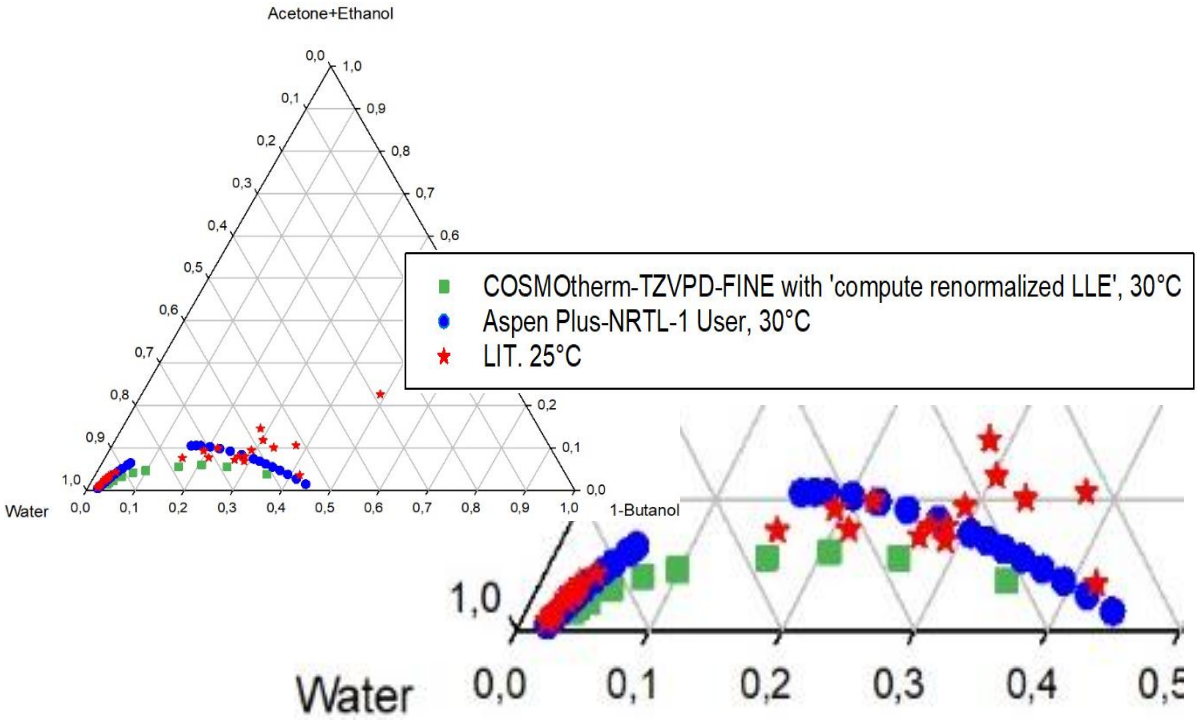


**Fig. 8-15. LLE of "1-butanol-ethanol-acetone-water" at 30°C with COSMOtherm-TZVPD-FINE with 'compute renormalized LLE', Aspen Plus-NRTL-1 User [35] options, literature data [56], (mole fractions)**

## Aspen Plus- Screen Shots:

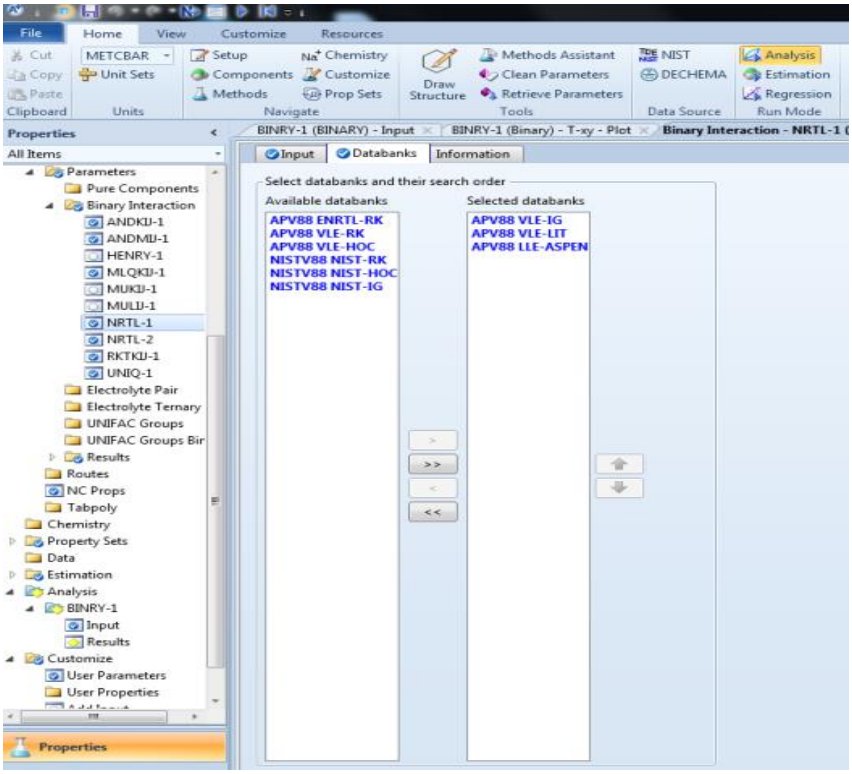


**Fig. 8-16. Methods and databases in properties area of Aspen Plus**

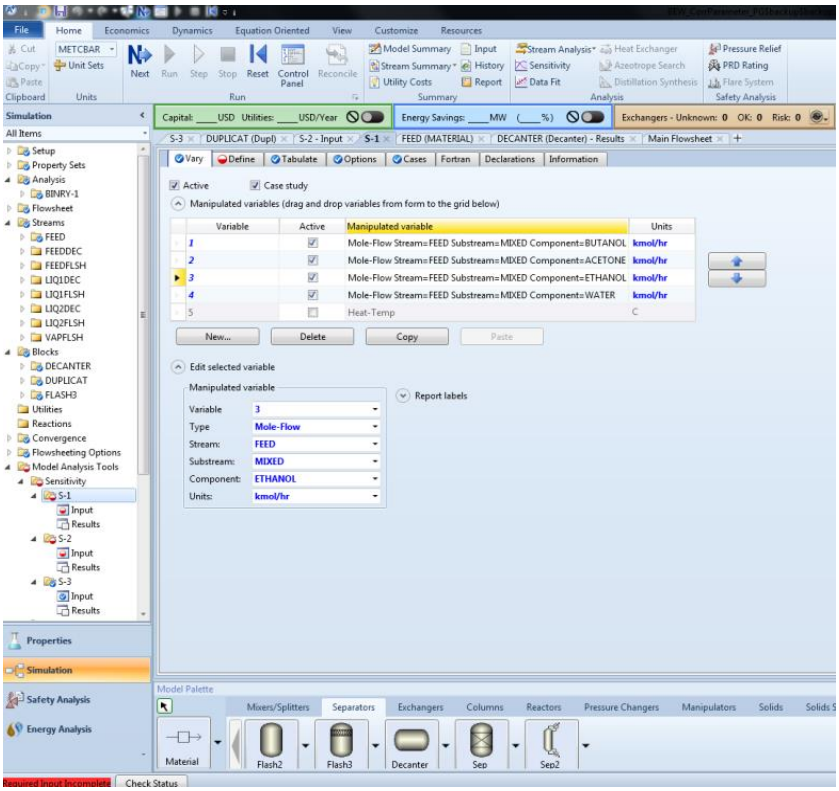


**Fig. 8-17. Flowsheet calculation in simulation area of Aspen Plus with sensitivity analysis-1 for calculations with flash (used for ternary and quaternary Systems)**

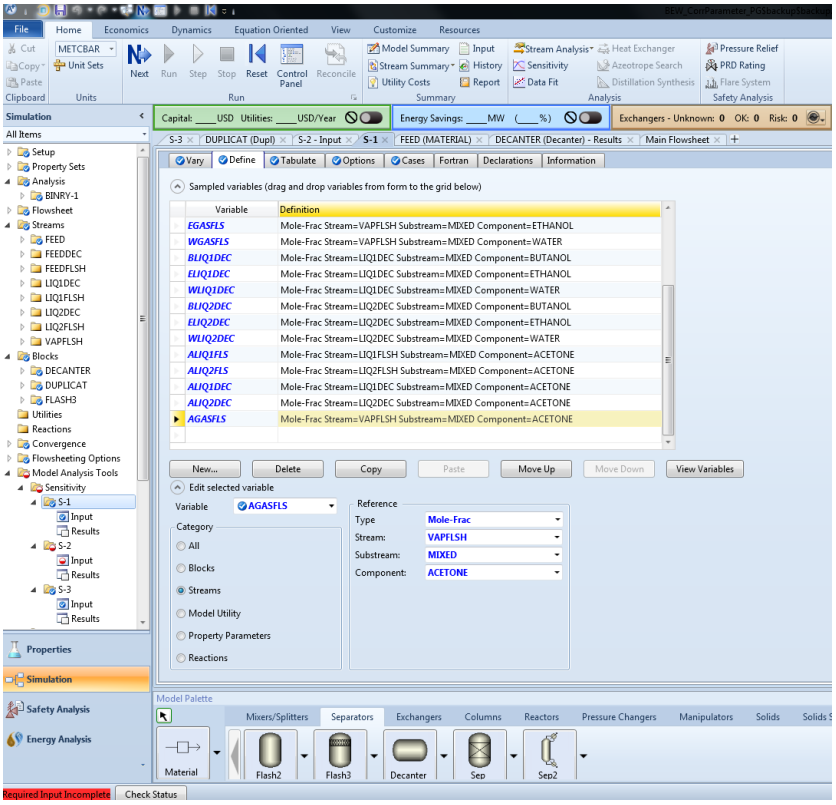


**Fig. 8-18. Defining streams in sensitivity analysis-1 (calculations with flash) for Aspen Plus flowsheet calculation**

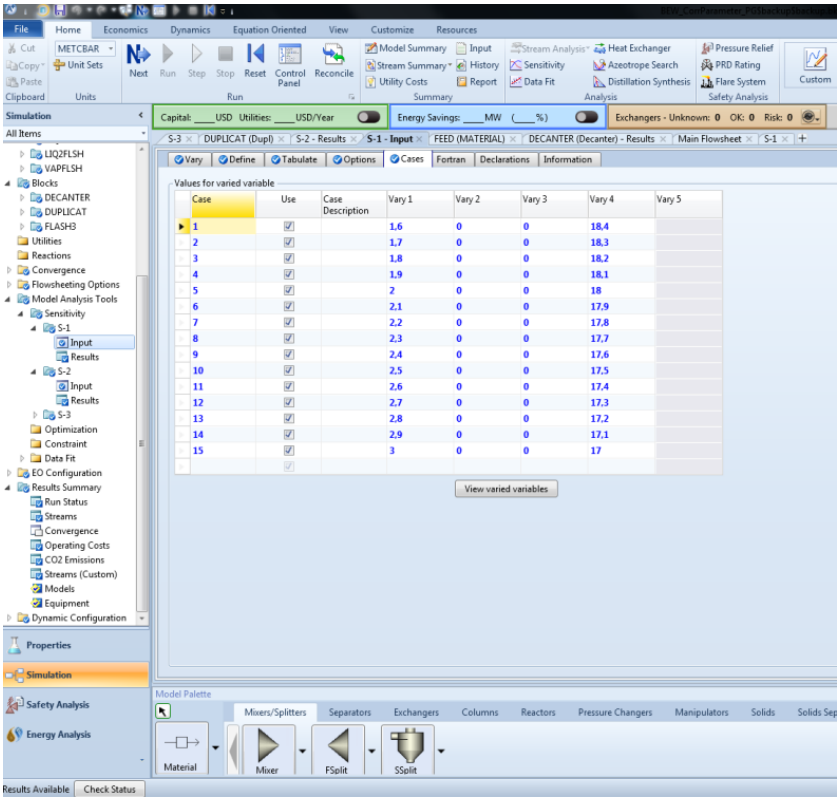


**Fig. 8-19. Case definition in senstivity analysis-1 for Aspen Plus flowsheet calculation**

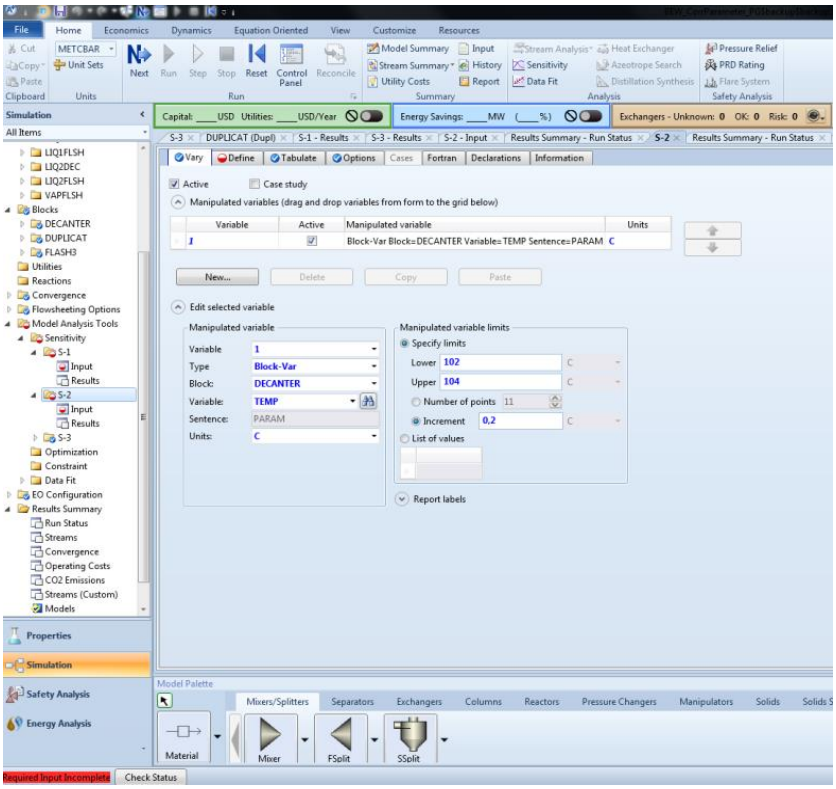

**Fig. 8-20. Defining decanter temperature in sensitivity analysis-2 for Aspen Plus flowsheet calculation**

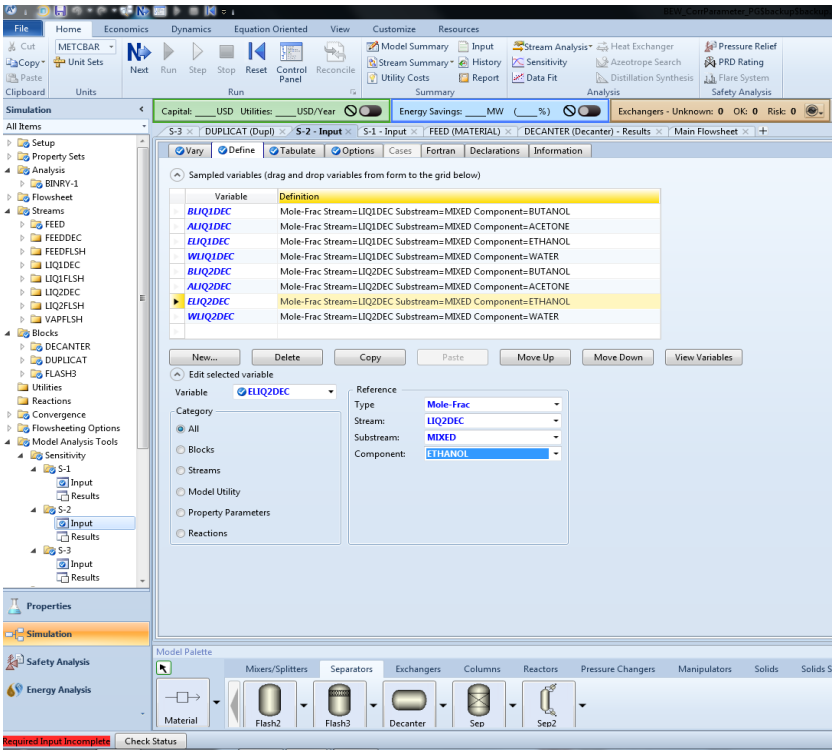

**Fig. 8-21. Defining sensitivity analysis-2 (calculations with decanter) for Aspen Plus flowsheet calculation**

# 9. References


1. Y. S., Jang, A. Malaviya, C. Cho, J. Lee, S. Y. Lee, (2012): Butanol production from renewable biomass by clostridia. *Bioresource Technology* 123, S. 653–663. DOI: 10.1016/j.biortech.2012.07.104.
2. P. Dürre (1525): Biobutanol. An attractive biofuel. *Biotechnology Journal* 2 (12), S. 1525–1534. DOI: 10.1002/biot.200700168.
3. A. Kujawska, J. Kujawski, M. Bryjak, W. Kujawski (2015): ABE fermentation products recovery methods-A review. *Renewable and Sustainable Energy Reviews* 48, S. 648–661. DOI: 10.1016/j.rser.2015.04.028.
4. I. S. Maddox, N. Qureshi, K. Roberts-Thomson (1995): Production of acetone-butanol-ethanol from concentrated substrate using clostridium acetobutylicum in an integrated fermentation-product removal process. *Process Biochemistry* 30 (3), S. 209–215. DOI: 10.1016/0032-9592(95)85001-5.
5. A. Friedl (2016): Downstream process options for the ABE fermentation. *FEMS Microbiology Letters* 363 (9), fnw073. DOI: 10.1093/femsle/fnw073.
6. W. Kaminski, E. Tomczak and A. Gorak (2011): Biobutanol-Production and Purification Methods. *Ecological Chemistry and Engineering S* (Vol. 18, No. 1).
7. M. B. Oliveira: Phase Equilibria Modeling for Biofuels Production. Online: http://path.web.ua.pt/file/Tese_MarianaBelo_ppt.pdf, 08.2018.
8. J. Jeevahan, G. Sriramanjaneyulu, R.B. Durairaj, G. Mageshwaran (2018): Experimental investigation of the suitability of 1-butanol blended with biodiesel as an alternative biofuel in diesel engines. *Biocatalysis and Agricultural Biotechnology* 15, S. 72–77. DOI: 10.1016/j.bcab.2018.05.013.
9. N. Abdehagh, F. H. Tezel, J. Thibault (2014): Separation techniques in butanol production. Challenges and developments. *Biomass and Bioenergy* 60, S. 222–246. DOI: 10.1016/j.biombioe.2013.10.003.
10. Wikipedia: n-Butanol. Online: https://en.wikipedia.org/wiki/N-Butanol, 08.2018.
11. E. M. Green, (2011): Fermentative production of butanol - the industrial perspective. *Current Opinion in Biotechnology* 22 (3), S. 337–343. DOI: 10.1016/j.copbio.2011.02.004.
12. Wikipedia: Butanol fuel. Online: https://en.wikipedia.org/wiki/Butanol_fuel, 11.2018.
13. R. West. Online: http://slideplayer.com/slide/9117480/27/images/10/abe+fermentation, 11.2018.
14. Wikipedia: Acetone-butanol-ethanol fermentation. Online: https://en.wikipedia.org/wiki/Acetone–butanol–ethanol_fermentation, 11.2018.
15. N. Qureshi, S. Hughes, I.S. Maddox and M.A. Cotta (2005): Energy-efficient recovery of butanol from model solutions and fermentation broth by adsorption. In: *Bioproc. Biosyst. Eng*. (27), S. 215–222.
16. D. Ramey (2004): Butanol. Online: http://lightparty.com/Energy/Butanol.html, 11.2018.
17. E. Larsson, M. Max-Hansen, A. Pålsson, R. Studeny (2008): A feasibility study on conversion of an ethanol plant to a butanol plant. Online: https://www.chemeng.lth.se/ket050/Finalreport2008/StatoilHydroButanol2008.pdf, 11.2018.
18. I. Tosun, (2013): The Thermodynamics of Phase and Reaction Equilibria, Netherlands: Elsevier, 1st Edition.
19. G. M. Kontogeorgis, G.K. Folas (2010). Front Matter. Thermodynamic Models for Industrial Applications, UK: John Wiley & Sons, Ltd., 1st Edition.
20. J. M. Smith, H. C. Van Ness, M. M. Abbott (2005): Introduction to Chemical Engineering Thermodynamics. USA: McGraw-Hill's chemical Enginering Series, 7th Edition.
21. A. Oudshoorn, L. A. M. van der Wielen, A. J. J. Straathof (2009): Assessment of Options for Selective 1-Butanol Recovery from Aqueous Solution. *Ind. Eng. Chem. Res., 48, 15, 7325-7336.*
22. T. Zheng (2014): Applicability of Henry's law and Raoult's law for a binary gas-liquid system. Online: https://www.researchgate.net/publication/281616958_Numerical_Analysis_of_Modeling_Concepts_for_Salt_Precipitation_and_Porosity_-_Permeability_Evolution_during_Brine_Evaporation/figures?lo=1, 11.2018.

23. Activity models. Online: http://tekim.undip.ac.id/staf/istadi/files/2013/11/AdvanceThermodynamics_Materi_6.pdf, 08.2018.

24. B. E. Poling, J.M. Prausnitz, J.P. O'Connell (2001). The Properties of Gases and Liquids, 5th edition. USA: McGraw-Hill Professional.

25. Wikipedia: Van Laar equation. Online: https://en.wikipedia.org/wiki/Van_Laar_equation, 08.2018.

26. E. Muzenda (2013): From UNIQUAC to Modified UNIFAC Dortmund: A Discussion. *3rd International Conference on Medical Sciences and Chemical Engineering (ICMSCE'2013) Dec. 25-26, Bangkok (Thailand)*, 2013.

27. COSMOlogic: COSMOthermX User Guide Version C30_1701.

28. Wikipedia: COSMO-RS. Online: https://en.wikipedia.org/wiki/COSMO-RS, 11.2018.

29. A. Klamt (2005): COSMO-RS, From Quantum Chemistry to Fluid Phase Thermodynamics and Drug Design. Neteherlands: Elsevier Science, 1st Edition.

30. F. Eckert: COSMOtherm Reference Manual, Version C3.0 Release 17.01, 1999 - 2016.

31. COSMO-RS Manual ADF Modeling Suite 2018. Online: https://www.scm.com/doc/COSMO-RS/index.html, 11.2018.

32. Aspen Plus User Guide (2000): Version 10.2. Online: https://web.ist.utl.pt/ist11038/acad/Aspen/AspUserGuide10, 11.2018

33. C. Lira: Aspen Tutorial. Online: https://www.chems.msu.edu/resources/tutorials/ASPEN, 11.2018.

34. Aspen Plus, Thermodynamic models & physical properties. Online: http://www.just.edu.jo/~yahussain/files/Thermodynamic%20Models.pdf, 08.2018.

35. A. Rom, W. Wukovits, A. Friedl (2014): "Development of a vacuum membrane distillation unit operation: From experimental data to a simulation model". *Chemical Engineering and Processing: Process Intensification*, 86 (2014) 90-95.

36. Dortmund Data Bank: Online: http://www.ddbst.com/en/EED/PCP/VAP_C39.php, 11.2018, (Vapor Pressure of 1-Butanol).

37. NIST Chemistry Webbook: Online: http://webbook.nist.gov/cgi/cbook.cgi?ID=C71363&Mask=4&Type=ANTOINE&Plot=on, 08.2018, (Vapor Pressure of 1-Butanol, Acetone, Ethanol, Water).

38. Elliot, Lira, Introductory Chemical Engineering: Online: www.personal.utulsa.edu/~geoffrey-price/.../AntoineConstants.xls, 08.2018, (Vapor Pressure of 1-Butanol, Acetone, Ethanol, Water).

39. B. E. Poling, J. M. Prausnitz, and J. P. O'Connell (2001): The Properties of Gases and Liquids, 5th ed., App. A, McGraw-Hill, New York. Online: https://de.scribd.com/doc/41541675/Antoine-Constants, 08.2018.

40. Dortmund Data Bank: Online: http://www.ddbst.com/en/EED/PCP/VAP_C4.php, 11.2018, (Vapor Pressure of Acetone).

41. R. P. Hartwick, C. S. Howat (1995): Infinite Dilution Activity Coefficients of Acetone in Water. A New Experimental Method and Verification. *Journal of Chemical and Engineering Data*, v 40, n 4, p 738-745, July 1, 1995. (Vapor Pressure of Water, Acetone) (Activity Coefficient of Acetone).

42. Dortmund Data Bank: Online: http://www.ddbst.com/en/EED/PCP/VAP_C11.php, 11.2018, (Vapor Pressure of Ethanol).

43. Dortmund Data Bank: Online: http://www.ddbst.com/en/EED/PCP/VAP_C174.php, 11.2018, (Vapor Pressure of Water).

44. D. R. Lide (2000-2001), CRC Handbook of Chemistry and Physics, USA: CRC Press, 81st Edition, (Vapor Pressure of Water).

45. Online: http://www.endmemo.com/chem/vaporpressurewater.php, 08.2018 (Vapor Pressure of Water).

46. Dechema Chemistry Data Series, Activity Coefficients at Infinite Dilution, Vol. IX, Part 4, page 1654 and Part 6, page 2589, (1-Butanol).

47. Dechema Chemistry Data Series, Activity Coefficients at Infinite Dilution, Vol. IX, Part 4, page 1651 and Part 6, page 2582, (Acetone).

48. Dechema Chemistry Data Series, Activity Coefficients at Infinite Dilution, Vol. IX, Part 4, page 1649, 1650 and Part 6, page 2579, 2580, (Ethanol).

49. Dechema Chemistry Data Series, Vol. 1, Part 1, page 331 (4.920 bar), 330 (1.980 bar), page 328 (1.013 bar), 329 (1.013 bar), 332 (1.013 bar), 334 (0.933 bar), 335 (0.913 bar), (VLE Butanol-Water).

50. K. Iwakabe, H. Kosuge (2001): Isobaric vapor–liquid–liquid equilibria with a newly developed still. *Fluid Phase Equilibria* 192 (1), S. 171–186. DOI: 10.1016/S0378-3812(01)00631-8, (VLE Butanol-Water) (LLE Butanol-Ethanol-Water).

51. Dechema Chemistry Data Series, Vol. V, Part 1, page 236, (LLE Butanol-Water).

52. Dechema Chemistry Data Series, Vol. V, Part 2, page 469, 30.0°C, (LLE Butanol-Acetone-Water).

53. L. Spottke, W. Biedermann und S. Martin (1988), Mischungsverhalten der dreistoffgemische aceton-butanol-wasser und butylacetat-butanol-wasser, (LLE Butanol-Acetone-Water).

54. S. S. Fânia, S. G. d'Ávila., M. Aznar (2001), Salt effect on liquid–liquid equilibrium of water+1-butanol+acetone system. Experimental determination and thermodynamic modeling. *Fluid Phase Equilibria* 187-188, S. 265–274. DOI: 10.1016/S0378-3812(01)00541-6, (LLE Butanol-Acetone-Water).

55. Dechema Chemistry Data Series, Vol. V, Part 2, Page 340, 25.0°C, (LLE Butanol-Ethanol-Water).

56. Dechema Chemistry Data Series, Vol. V, Part 3, Page 380, 25.0°C, (LLE Butanol-Acetone-Ethanol-Water).

57. COSMO-RS Theory. Online: www.cosmologic.de/files/downloads/theory/COSMO-RS-Theory-Basics.pdf (01.2019).

58. Energy content of fuels. Online: http://www.appropedia.org/Energy_content_of_fuels (12.2018).

# 10. Abbreviations and Symbols

## 10.1. Abbreviations

| | |
|---|---|
| 3D | Three Dimensional |
| ABE | Acetone-Butanol-Ethanol |
| AD | Anaerobic Digestion |
| AD | Anaerobic digestion |
| AM1 | A semiempirical quantum chemical method |
| ASOG | Analytical Solutions of Groups |
| BP-SVP/BP-TZVP | Becke-Perdew[1,2,3] (BP) functional for density functional theory calculations with a split valence plus polarization function (SVP) or triple valence plus polarization function (TZVP) basis set. The necessary parameterization file does always correspond to one functional and basis set. The term "BP-TZVP parameterization" is thus sometimes used and refers to the COSMOtherm parameterization not the basis set specification. |
| CAS-Number | The Chemical Abstracts Services registration number is a unique identifier for compounds. |
| CBP | Consolidated BioProcessing |
| CI | Compression-Ignition |
| COSMO | COnductor like Screening MOdel |
| COSMO-RS | COnductor like Screening MOdel for Real Solvents |
| DB | Database, usually used for the COSMOtherm compound databases |
| DFT | Density Functional Theory: A quantum chemical theory used in several software packages for molecular or lattice calculations |
| EOS | Equation of State |
| F | Feed |
| GC | Group Contribution |
| GHG | Green House Gas |
| HB | Hydrogen Bonding |
| IL | Ionic Liquids |
| LC | Local Composition |
| LCST | Lower critical solution temperature |
| LLE | Liquid-Liquid Equilibrium |
| M | Mixture |
| MSW | Municipal Solid Waste |
| MW | Molecular Weight |

| | |
|---|---|
| NRTL | Non-random-two-liquid |
| NRTL-SAC | NRTL-Segment Activity Coefficient |
| QC/QM | Quantum Chemical/Quantum Mechanical |
| QCL | Quantum Chemical Level |
| QSPR | Quantitative Structure Property Relationship, also QSAR (A = activity) |
| S | Solvent |
| SCD | Surface Charge Density |
| SLE | Solid-Liquid Equilibrium |
| SMS | Sigma Match Similarity |
| TZVP | Triple Zeta Valence Polarized set |
| UCST | Upper critical solution temperature |
| UNIFAC | UNIQUAC Functional group activity coefficient |
| UNIQUAC | Universal Quasi Chemical |
| vdW | Van der Waals |
| VLE | Vapor-Liquid Equilibrium |
| VLLE | Vapor-Liquid-Liquid Equilibrium |

## 10.2. Symbols

| | |
|---|---|
| $a_i$ | Activity of component $i$ [−] |
| $a_{12}$ | Non-randomness parameter [−] |
| $A$ | Parameter related to the intermolecular potentials of the compounds [−] |
| $A_i$ | Molecular surface area for molecule $i$ |
| $A, B, C$ | Antoine constants for a given species [−] |
| $\alpha,\ b_{12}, b_{21}$ | Parameters specific to a particular pair of species, independent of composition and $T$ [−] |
| $\alpha_{eff}$ | Effective contact area [nm$^2$] |
| $c_{hb}$ | Hydrogen bonding interaction coefficient $[kcal\ mol^{-1}\ \text{Å}^4\ e^{-2}]$ |
| $C_i$ | Concentration of species $i$ $[mol/m^3]$ |
| Γ | Cross-potential |
| $\gamma$ | Activity coefficient [−] |
| $\gamma_i$ | Activity coefficient of component $i$ [−] |
| $\gamma^{\infty}$ | Activity coefficient at infinite dilution [−] |
| $E_{int}$ | Interaction energy $[kJ/mol]$ |

| | |
|---|---|
| $E_{hb}$ | Hydrogen bonding energy $[kJ/mol]$ |
| $E_{misfit}$ | Electrostatic energy $[kJ/mol]$ |
| $E_{vdw}$ | Van der Waals Energy $[kJ/mol]$ |
| $f$ | Fugacity [bar] |
| $f_i^L$ | Pure component liquid phase fugacity $[bar]$ |
| $f_i^V$ | Pure component vapor phase fugacity $[bar]$ |
| F | Degrees of freedom of the system $[-]$ |
| $g_{ij}$ | Interaction energy parameter referring to the $i-j$ interaction $[-]$ |
| $G^E$ | Excess Gibbs free energy $[J/mol]$ |
| $G$ | Molar Gibbs energy / Free enthalpy $[J/mol]$ |
| $H$ | Molar enthalpy $[J/mol]$ |
| $H_i$ | Henry constant of $i$ $[-]$, $[mol/m^3\ Pa]$ |
| $\theta_i$ | Local surface area fraction of component $i$ $[-]$ |
| $\Lambda_{ij}$ | Wilson equation parameters equal to unity in the limiting case of an ideal solution $[-]$ |
| $\mu_i$ | Chemical potential of component $i$ $[J/mol]$ |
| $M$ | Molar mass $[kg]$ |
| $n$ | Total number of moles of the system $[mol]$ |
| $\dot{n}$ | Molar flow rate $[mol/h]$ |
| $n_i$ | Number of moles for species $i$ $[mol]$ |
| $N$ | Number of the chemical species present in the system $[-]$ |
| $\pi$ | Number of the phases $[-]$ |
| $p^i(\sigma)_)$ | Distribution function of $\sigma$-profile of component $i$ $[-]$ |
| $P_i^{sat}$ | Vapor pressure of pure species $i$ $[kPa]$ |
| $P$ | Pressure $[kPa]$, $[bar]$ |
| $\sigma$ | COSMO screening charge / polarization charge density $[e/nm^2]$ |
| $\sigma - potential$ | Chemical potential of a surface segment $[kj/nm^2]$ |
| $\sigma_{acceptor}, \sigma_{donor}$ | Polarization charges of segments located on a hydrogen bond donor/acceptor atom $[e/nm^2]$ |
| $\sigma_{hb}$ | Threshold for hydrogen bonding $[e/nm^2]$ |
| $\tau_{vdw}$ | Element specific vdW interaction parameter $[-]$ |
| $\tau$ | Reduced temperature $[K]$ |
| $\phi_i$ | Fugacity coefficient of component $i$ $[-]$ |
| $q$ | Volumetric flow rate $[m^3/s]$ |

| | |
|---|---|
| $r_i, q_i$ | Molecular volume and surface area of $i$ (Van der Waals volume and area) [Å$^3$], [Å$^2$] |
| $R_k, Q_k$ | Volume, surface area parameter of each functional group $k$ $[-]$ |
| $R$ | Ideal gas constant $[J/mol\ K]$ |
| $S$ | Molar entropy $[J/mol\ K]$ |
| $T$ | Temperature [°C], $[K]$ |
| $T_u$ | Upper consolute temperature $[K]$ |
| $T_L$ | Lower critical solution temperature $[K]$ |
| $V$ | Volume $[m^3]$ |
| $x^\alpha$ | Mole fraction of phase $\alpha$ $[-]$ |
| $x^\beta$ | Mole fraction of phase $\beta$ $[-]$ |
| $x_i$ | Liquid phase mole fraction of species $i$ $[-]$ |
| $y_i$ | Vapor phase mole fraction of species $i$ $[-]$ |
| $Z$ | Coordination factor $[-]$ |